USGS
science for a changing world

Water Availability and Use Science Program

Documentation of a Groundwater Flow Model Developed To Assess Groundwater Availability in the Northern Atlantic Coastal Plain Aquifer System From Long Island, New York, to North Carolina

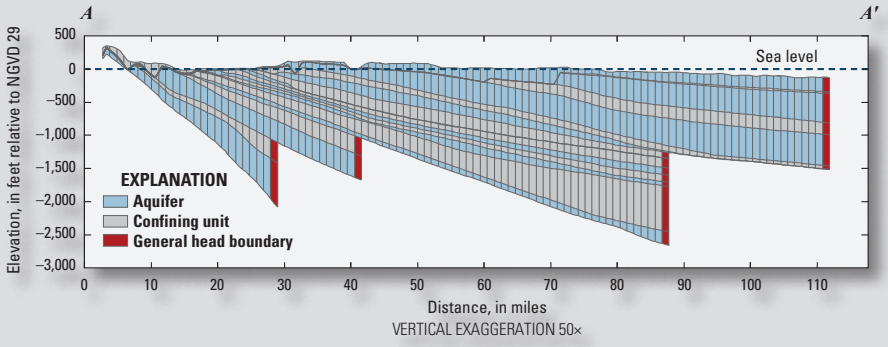

Scientific Investigations Report 2016–5076
Version 1.1, December 2016

U.S. Department of the Interior
U.S. Geological Survey

Cover.

In the background: Location and extent of the Northern Atlantic Coastal Plain aquifer system.

In the foreground: Cross section showing the vertical geometry along column 275 of the model used in the groundwater assessment for the Northern Atlantic Coastal Plain aquifer system.

Documentation of a Groundwater Flow Model Developed To Assess Groundwater Availability in the Northern Atlantic Coastal Plain Aquifer System From Long Island, New York, to North Carolina

By John P. Masterson, Jason P. Pope, Michael N. Fienen, Jack Monti, Jr., Mark R. Nardi, and Jason S. Finkelstein

Water Availability and Use Science Program

Scientific Investigations Report 2016–5076
Version 1.1, December 2016

U.S. Department of the Interior
U.S. Geological Survey

U.S. Department of the Interior
SALLY JEWELL, Secretary

U.S. Geological Survey
Suzette M. Kimball, Director

U.S. Geological Survey, Reston, Virginia: 2016
First release: 2016
Revised: December 2016 (ver. 1.1)

Suggested citation:
Masterson, J.P., Pope, J.P., Fienen, M.N., Monti, Jack, Jr., Nardi, M.R., and Finkelstein, J.S., 2016, Documentation of a groundwater flow model developed to assess groundwater availability in the Northern Atlantic Coastal Plain aquifer system from Long Island, New York, to North Carolina (ver. 1.1, December 2016): U.S. Geological Survey Scientific Investigations Report 2016–5076, 70 p., https://doi.org/10.3133/sir20165076.

ISSN 2328-0328 (online)

Contents

Figures

Tables

Conversion Factors

U.S. customary units to International System of Units

Multiply	By	To obtain
	Length	
foot (ft)	0.3048	meter (m)
mile (mi)	1.609	kilometer (km)
	Area	
square mile (mi^2)	2.590	square kilometer (km^2)
	Flow rate	
cubic foot per second (ft^3/s)	0.02832	cubic meter per second (m^3/s)
gallon per day (gal/d)	0.003785	cubic meter per day (m^3/d)
million gallons per day (Mgal/d)	0.04381	cubic meter per second (m^3/s)

Datum

Vertical coordinate information is referenced to the National Geodetic Vertical Datum of 1929 (NGVD 29).

Horizontal coordinate information is referenced to the North American Datum of 1983 (NAD 83).

Elevation, as used in this report, refers to distance above or below the vertical datum.

Abbreviations

GHB	General-Head Boundary package for MODFLOW
MODFLOW	Modular Three-Dimensional Finite-Difference Ground-Water Flow model
NACP	Northern Atlantic Coastal Plain
NWIS	National Water Information System
NWUIP	National Water-Use Information Program
PEST	inverse-modeling parameter estimation method
RCH	Recharge package for MODFLOW
RIV	River package for MODFLOW
SACP	Southern Atlantic Coastal Plain
SFR2	Streamflow-Routing package for MODFLOW
SVD	singular-value decomposition
SWB	soil-water balance
SWI	Seawater Intrusion package for MODFLOW
USGS	U.S. Geological Survey

Documentation of a Groundwater Flow Model Developed To Assess Groundwater Availability in the Northern Atlantic Coastal Plain Aquifer System From Long Island, New York, to North Carolina

By John P. Masterson, Jason P. Pope, Michael N. Fienen, Jack Monti, Jr., Mark R. Nardi, and Jason S. Finkelstein

Abstract

The U.S. Geological Survey developed a groundwater flow model for the Northern Atlantic Coastal Plain aquifer system from Long Island, New York, to northeastern North Carolina as part of a detailed assessment of the groundwater availability of the area and included an evaluation of how these resources have changed over time from stresses related to human uses and climate trends. The assessment was necessary because of the substantial dependency on groundwater for agricultural, industrial, and municipal needs in this area.

The three-dimensional, groundwater flow model developed for this investigation used the numerical code MODFLOW–NWT to represent changes in groundwater pumping and aquifer recharge from predevelopment (before 1900) to future conditions, from 1900 to 2058. The model was constructed using existing hydrogeologic and geospatial information to represent the aquifer system geometry, boundaries, and hydraulic properties of the 19 separate regional aquifers and confining units within the Northern Atlantic Coastal Plain aquifer system and was calibrated using an inverse modeling parameter-estimation (PEST) technique.

The parameter estimation process was achieved through history matching, using observations of heads and flows for both steady-state and transient conditions. A total of 8,868 annual water-level observations from 644 wells from 1986 to 2008 were combined into 29 water-level observation groups that were chosen to focus the history matching on specific hydrogeologic units in geographic areas in which distinct geologic and hydrologic conditions were observed. In addition to absolute water-level elevations, the water-level differences between individual measurements were also included in the parameter estimation process to remove the systematic bias caused by missing hydrologic stresses prior to 1986. The total average residual of –1.7 feet was normally distributed for all head groups, indicating minimal bias. The average absolute residual value of 12.3 feet is about 3 percent of the total observed water-level range throughout the aquifer system.

Streamflow observation data of base flow conditions were derived for 153 sites from the U.S. Geological Survey National Hydrography Dataset Plus and National Water Information System. An average residual of about –8 cubic feet per second and an average absolute residual of about 21 cubic feet per second for a range of computed base flows of about 417 cubic feet per second were calculated for the 122 sites from the National Hydrography Dataset Plus. An average residual of about 10 cubic feet per second and an average absolute residual of about 34 cubic feet per second were calculated for the 568 flow measurements in the 31 sites obtained from the National Water Information System for a range in computed base flows of about 1,141 cubic feet per second.

The numerical representation of the hydrogeologic information used in the development of this regional flow model was dependent upon how the aquifer system and simulated hydrologic stresses were discretized in space and time. Lumping hydraulic parameters in space and hydrologic stresses and time-varying observational data in time can limit the capabilities of this tool to simulate how the groundwater flow system responds to changes in hydrologic stresses, particularly at the local scale.

Introduction

The U.S. Geological Survey (USGS) began a multi-year regional assessment of groundwater availability in the Northern Atlantic Coastal Plain (NACP) aquifer system in 2010 as part of its ongoing regional assessments of groundwater availability of the principal aquifers of the Nation (Alley and others, 2013). The goals of this national assessment are to document effects of human activities on water levels and groundwater storage, explore climate variability effects on the regional water budget, and provide consistent and integrated information that is useful to those who use and manage the groundwater resource. As part of this nationwide assessment, the USGS evaluated available groundwater resources within

the NACP aquifer system from Long Island, New York, to northeastern North Carolina.

The NACP aquifer system consists of nine confined aquifers and nine confining units capped by an unconfined surficial aquifer. The NACP is bounded laterally on the western side by the contact between Coastal Plain sediments and the upland Piedmont bedrock and extends eastward to the limit of the Continental Shelf. However, the boundary between fresh and saline groundwater is much closer to the shoreline and varies vertically by aquifer. Detailed descriptions of the depositional history and hydrogeologic framework are provided in Masterson and others (2013) and Pope and others (2016).

The purpose of this report is to document the construction and calibration of the three-dimensional (3D), groundwater flow model that was developed for the NACP aquifer system to advance the understanding of groundwater budgets and components including recharge, discharge, and aquifer storage for the entire system and for each of the statewide systems; compute historical and recent system response and project future system response to development at a scale relevant to basinwide water-management decisions; and evaluate options for hydrologic monitoring of system changes. The results of this modeling analysis are documented in Masterson and others (2016a).

Model Design

Numerical models provide a means to synthesize existing hydrogeologic information into an internally consistent mathematical representation of a real system or process, and thus, are useful tools for testing and improving conceptual models or hypotheses of groundwater flow systems (Konikow and Reilly, 1998). A finite-difference groundwater flow model of the study area was developed by use of MODFLOW–NWT (Niswonger and others, 2011); MODFLOW–NWT was developed by modifying MODFLOW–2005 (Harbaugh, 2005) to solve the 3D groundwater flow equation using the Newton method.

The model area is approximately 27,000 square miles (mi^2) and extends from the Fall Zone (fig. 1), which is the transition from the igneous and metamorphic rocks of the upland Piedmont physiographic province to the sedimentary environment of the Coastal Plain physiographic province, east to the boundary between fresh and saline groundwater (not shown). The model area extends vertically from the water table to bedrock and includes 19 separate regional aquifers and confining units. The finite-difference grid developed for the modeled area was aligned approximately parallel with the Fall Zone.

The model simulation time was discretized into predevelopment and postdevelopment periods. The postdevelopment time period consists of 44 model stress periods and extends from January 1, 1900, to December 31, 2058. The postdevelopment model stress periods were preceded by an initial steady state stress period used to represent predevelopment (before 1900) conditions.

Parameters for the model were estimated by history matching between modeled and measured groundwater levels and streamflows using the inverse-modeling parameter estimation (PEST) software suite (Doherty, 2010), based on observation data from 1986 to 2008. A detailed description of the model parameter estimation process is presented in the "Parameter Estimation" section of this report.

The model archive for the numerical model (Masterson and others, 2016b) developed for this investigation contains the input and output files and the executable file needed to run the model. The archive also contains georeferenced files that can be used to display the 3D groundwater flow model finite-difference grid as well as the hydrologic data—water levels and streamflow sites—used in calibration of the 3D groundwater flow model.

Model Discretization and Boundaries

The finite-difference model grid consists of a series of square model cells in which user-specified hydraulic parameters, model stresses, and boundary conditions are varied spatially. The conceptualization of how and where water enters, moves through, and leaves the aquifer system is critical to the development of an accurate flow model (Reilly, 2001). Boundary conditions are applied at some model cells to simulate hydrologic features, including streams and coastal waters. A detailed discussion of grid discretization, boundary conditions, and the use of finite-difference equations to simulate groundwater flow is presented in McDonald and Harbaugh (1988).

Spatial Discretization

The lateral extent of the active onshore and offshore modeled area of the NACP aquifer system is about 51,000 mi^2 (fig. 1). The finite-difference grid for the numerical model consists of 250 rows and 500 columns of uniformly spaced model cells that are 1 mile (mi) on each side. The aquifer system was subdivided vertically from land surface to bedrock into 19 layers of variable thickness (table 1; fig. 2) to allow for the detail necessary to represent vertical changes in the lithology and in the seaward position of the boundary between the freshwater and saltwater. The hydrostratigraphic unit altitudes and extents that were used to represent the tops and bottoms of each layer were derived from a regional synthesis of the elevations and extents of the topmost layer of the hydrostratigraphic units developed for individual States (Pope and others, 2016). In general, each of the primary regional confined aquifers and confining units is represented as a separate layer in the model. Where a hydrogeologic unit does not extend across a given layer, a zone with a minimum thickness of 1-foot (ft) was created and the hydraulic properties of the overlying unit were applied in order to make the layer continuous across the entire model.

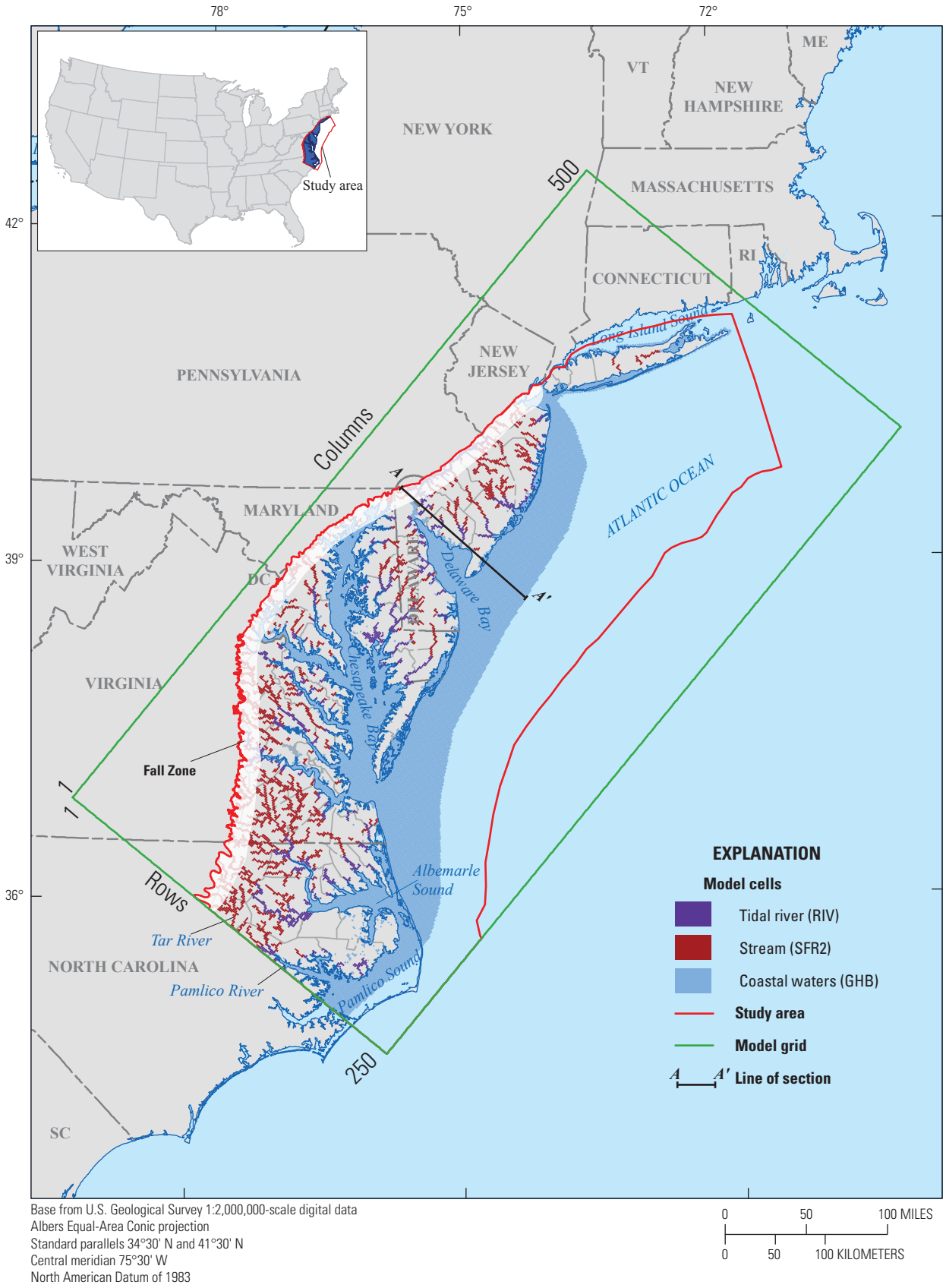

Figure 1. Extent of model grid, active model area, and boundaries used to develop a three-dimensional model for the groundwater assessment of the Northern Atlantic Coastal Plain aquifer system.

Table 1. Thickness and hydraulic properties of regional hydrogeologic units in the Northern Atlantic Coastal Plain aquifer system.

[ft, foot; ft/d, foot per day; K_x, horizontal hydraulic conductivity; K_z, vertical hydraulic conductivity; S_s, specific storage; S_y, specific yield; E[-x], $\times 10^{[-x]}$]

Layer	Hydrogeologic unit name	Thickness (ft)			Number of parameters	Model-estimated hydraulic properties			
						K_x (ft/d)			
		Minimum	Mean	Maximum		Minimum	Mean	Median	Maximum
1	Surficial aquifer	1	82	857	35	123.17	435.78	442.83	1,050.00
2	Upper Chesapeake confining unit	1	39	250	22	1.302E-8	3.888E-2	1.273E-4	1.506E-1
3	Upper Chesapeake aquifer	1	170	468	15	6.71	271.09	175.92	500.00
4	Lower Chesapeake confining unit	1	165	477	26	3.827E-2	1.318E-1	1.131E-1	3.117E-1
5	Lower Chesapeake aquifer	1	213	698	19	6.14	191.63	139.20	479.84
6	Calvert confining unit	1	88	421	48	2.503E-7	3.260E+0	8.339E-3	1.561E+2
7	Piney Point aquifer	1	102	473	20	4.10	35.15	20.87	107.84
8	Nanjemoy-Marlboro confining unit	1	156	806	41	1.325E-6	4.817E-2	1.574E-3	8.002E-1
9	Aquia aquifer	1	83	380	17	7.68	66.92	24.40	300.00
10	Monmouth-Mount Laurel confining unit	1	87	537	23	4.032E-7	4.728E-2	2.699E-6	2.338E-1
11	Monmouth-Mount Laurel aquifer	1	90	288	14	6.07	58.19	32.08	160.19
12	Matawan confining unit	1	54	230	22	6.709E-7	7.822E-5	6.876E-5	3.121E-4
13	Matawan aquifer	1	47	204	11	13.00	50.28	51.29	92.92
14	Magothy confining unit	1	152	750	31	4.227E-7	1.216E-6	1.075E-6	2.872E-6
15	Magothy aquifer	1	104	1,055	30	11.00	94.98	60.00	585.48
16	Potomac confining unit	1	119	700	48	3.922E-7	1.697E-4	1.310E-6	2.519E-3
17	Potomac-Patapsco aquifer	1	480	1,615	35	1.17	23.54	20.57	182.11
18	Potomac-Patuxent confining unit	1	199	941	12	5.945E-7	1.388E-4	2.174E-6	8.811E-4
19	Potomac-Patuxent aquifer	1	445	1,883	7	13.14	91.95	57.26	194.82

Model-estimated hydraulic properties—Continued								
K_z (ft/d)				S_s (1/ft)				S_y (1/ft)
Minimum	Mean	Median	Maximum	Minimum	Mean	Median	Maximum	
0.06	18.13	2.25	210.13	3.834E-7	1.073E-6	1.000E-6	2.888E-6	0.20
2.815E-7	2.255E-2	2.747E-4	1.389E-1	4.182E-7	9.737E-5	9.522E-5	2.122E-4	0.20
2.39	15.44	11.36	49.49	4.153E-7	1.045E-6	1.094E-6	1.731E-6	0.20
1.552E-8	1.041E-1	8.752E-2	4.370E-1	3.383E-5	1.086E-4	1.083E-4	2.498E-4	0.20
0.00	16.95	9.40	115.78	5.414E-7	1.037E-6	9.957E-7	1.907E-6	0.20
7.927E-9	7.997E-1	4.715E-4	1.700E+1	4.569E-5	1.105E-4	1.006E-4	2.774E-4	0.20
0.10	25.51	11.64	82.67	6.768E-7	1.666E-6	1.148E-6	9.937E-6	0.20
5.715E-9	4.862E-2	1.442E-4	1.700E+0	2.495E-6	7.969E-5	7.574E-5	2.206E-4	0.20
1.16	8.95	5.58	44.30	4.517E-7	1.098E-6	1.114E-6	1.830E-6	0.20
2.461E-9	2.465E-2	1.851E-6	1.760E-1	4.010E-6	1.151E-5	1.076E-5	3.534E-5	0.20
0.13	1.04	0.48	3.52	5.477E-7	1.156E-6	9.637E-7	2.395E-6	0.20
2.199E-7	7.091E-4	3.257E-5	5.259E-3	4.535E-6	1.366E-5	1.119E-5	3.148E-5	0.20
0.28	6.22	6.25	10.02	5.240E-7	1.042E-6	7.723E-7	1.957E-6	0.20
5.302E-9	2.002E-5	5.416E-7	5.984E-4	3.102E-6	3.872E-2	1.023E-5	2.000E-1	0.20
0.95	7.29	7.48	20.73	4.248E-7	2.968E-6	9.878E-7	1.750E-5	0.20
1.031E-8	7.311E-4	2.127E-6	1.747E-2	3.456E-6	1.290E-5	9.153E-6	8.412E-5	0.20
0.01	0.60	0.29	5.55	4.634E-7	2.359E-6	1.064E-6	2.655E-5	0.20
1.808E-8	3.463E-1	1.678E-6	3.386E+0	4.467E-6	9.389E-6	7.973E-6	2.457E-5	0.20
0.15	6.57	5.80	15.71	4.964E-7	1.071E-6	7.951E-7	1.984E-6	0.20

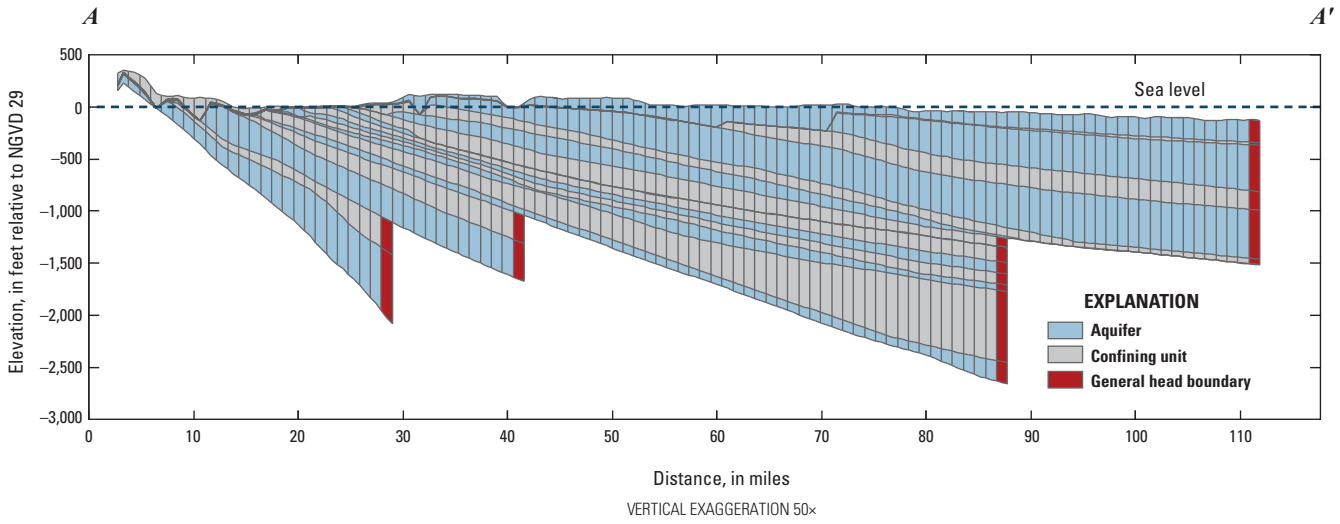

Figure 2. The vertical geometry along column 275 of the model used in the groundwater assessment for the Northern Atlantic Coastal Plain aquifer system. The location of the cross section is shown in figure 1. Each cell represents 1 square mile in map view. NVGD 29, National Geodetic Vertical Datum of 1929.

Temporal Discretization

Hydrologic stresses were simulated for an initial predevelopment steady-state condition, which was followed by transient conditions after the start of substantial groundwater withdrawal (postdevelopment). In these simulations, postdevelopment time is subdivided or discretized into stress periods and time steps from 1900 to 2058. Stress periods refer to periods of time in which specified model stresses, such as pumping and recharge, are constant; changing stresses over time are simulated by using sequential stress periods. Stress periods are further divided into time steps, which are units of time for which water levels and flows are calculated in the numerical model.

A total of 45 stress periods were simulated for this analysis. The first stress period was specified as steady state, representing predevelopment conditions, followed by 44 stress periods of variable duration to represent the postdevelopment stresses from 1900 to 2058 (table 2). Each postdevelopment stress period was subdivided into multiple time steps to increase model stability.

Stress periods 1 to 12 (before 1900 to 1985) are referred to in Masterson and others (2016a) as the historical period. The time discretization of the first 10 postdevelopment stress periods (2 to 11) were the same as those of the previous regional modeling analysis for the NACP aquifer system (Leahy and Martin, 1993) so that the pumping stresses developed for that analysis would be consistent in this report. These stress periods varied in length from 21 years for stress period 2 (1900 to 1921) to 3 years for stress period 11 (1978 to 1980; table 2), with earlier, longer stress periods representing relatively less specific information regarding earlier hydrologic conditions.

The 5-year stress period 12 from 1981 to 1985 was used as a transition period from the stresses derived from the analysis of Leahy and Martin (1993) to those derived for this report. The pumping stresses simulated for this period were the annual pumping rates for 1985 because the information on pumping rates and well locations is incomplete for the study area before 1985.

The next 24 stress periods (13–36) represent the modern period from 1986 to 2013, which is to referred to in Masterson and others (2016a) as the period of emphasis. Stress periods 13 to 35 (1986–2008) are 1 year in length and include average annual pumping and recharge rates for each of these years. Stress period 36 is 5 years in length (2009–2013) and includes the 2008 annual withdrawal rate and the average recharge for 1980 to 2008. This 5-year period is referred to as current [2013] conditions in Masterson and others (2016a). The pumping stress in 2008 was used in stress period 36 because complete reported groundwater withdrawal rates were not available after 2008 at the time the model was constructed. Stress periods 37 to 45 (2014–2058) are each 5 years in length and are continuations of the stresses simulated in stress period 36 for 45 years into the future. These stress periods together are referred to as the future period in Masterson and others (2016a).

Hydrologic Boundaries

The hydrologic boundaries in the groundwater flow model are defined as the areas from which and the method by which all the waters entering and leaving the numerical model are specified. The NACP aquifer system is bounded below and along the western boundary by bedrock and to the east

Table 2. Time discretization for model used in the groundwater assessment of the Northern Atlantic Coastal Plain aquifer system.

[--, not applicable]

Period	Stress period	Duration (days)	Duration (years)	Years (inclusive)	Start date	End date
Historical period	1[a]	Steady state	Steady state	--	--	--
	2	7,670	21	1900–1920	1/1/1900	12/31/1920
	3	6,940	19	1921–1939	1/1/1921	12/31/1939
	4	2,191	6	1940–1945	1/1/1940	12/31/1945
	5	2,557	7	1946–1952	1/1/1946	12/31/1952
	6	1,826	5	1953–1957	1/1/1953	12/31/1957
	7	2,557	7	1958–1964	1/1/1958	12/31/1964
	8	1,096	3	1965–1967	1/1/1965	12/31/1967
	9	1,826	5	1968–1972	1/1/1968	12/31/1972
	10	1,826	5	1973–1977	1/1/1973	12/31/1977
	11	1,096	3	1978–1980	1/1/1978	12/31/1980
	12[b]	1,826	5	1981–1985	1/1/1981	12/31/1985
Period of emphasis	13	365	1	1986	1/1/1986	12/31/1986
	14	365	1	1987	1/1/1987	12/31/1987
	15	366	1	1988	1/1/1988	12/31/1988
	16	365	1	1989	1/1/1989	12/31/1989
	17	365	1	1990	1/1/1990	12/31/1990
	18	365	1	1991	1/1/1991	12/31/1991
	19	366	1	1992	1/1/1992	12/31/1992
	20	365	1	1993	1/1/1993	12/31/1993
	21	365	1	1994	1/1/1994	12/31/1994
	22	365	1	1995	1/1/1995	12/31/1995
	23	366	1	1996	1/1/1996	12/31/1996
	24	365	1	1997	1/1/1997	12/31/1997
	25	365	1	1998	1/1/1998	12/31/1998
	26	365	1	1999	1/1/1999	12/31/1999
	27	366	1	2000	1/1/2000	12/31/2000
	28	365	1	2001	1/1/2001	12/31/2001
	29	365	1	2002	1/1/2002	12/31/2002
	30	365	1	2003	1/1/2003	12/31/2003
	31	366	1	2004	1/1/2004	12/31/2004
	32	365	1	2005	1/1/2005	12/31/2005
	33	365	1	2006	1/1/2006	12/31/2006
	34	365	1	2007	1/1/2007	12/31/2007
	35	366	1	2008	1/1/2008	12/31/2008
	36[c]	1,825	5	2009–2013	1/1/2009	12/31/2013
Future period	37	1,825	5	2014–2018	1/1/2014	12/31/2018
	38	1,825	5	2019–2023	1/1/2019	12/31/2023
	39	1,825	5	2024–2028	1/1/2024	12/30/2028
	40	1,825	5	2029–2033	1/1/2029	12/31/2033
	41	1,825	5	2034–2038	1/1/2034	12/31/2038
	42	1,825	5	2039–2043	1/1/2039	12/31/2043
	43	1,825	5	2044–2048	1/1/2044	12/30/2048
	44	1,825	5	2049–2053	1/1/2049	12/31/2053
	45	1,825	5	2054–2058	1/1/2054	12/31/2058

[a]Stress period 1 is before 1900.

[b]Stress period 12 is a transitional period.

[c]Stress period 36 is the current conditions period.

and north by the interface between fresh and saline groundwater (that is, the freshwater/saltwater interface). The southern boundary is aligned approximately with the Tar River and Pamlico Sound in North Carolina (fig. 1).

The upper boundary of the emergent part of the active modeled area is the water table, which is a free-surface boundary that receives spatially variable recharge from precipitation. The Recharge (RCH) package of the USGS 3D finite-difference groundwater model MODFLOW (McDonald and Harbaugh, 1988) was used to spatially distribute recharge across the water table. The General-Head Boundary (GHB) package (McDonald and Harbaugh, 1988) was used to simulate the offshore part of the upper boundary (fig. 1, coastal waters [GHB] cells), which is represented by a head-dependent flux boundary in the model. This boundary condition was specified along the seabed, and the head assigned to the cells for this boundary were calculated as equivalent freshwater heads to account for the height of the overlying saltwater column.

Tidal rivers also were represented as head-dependent flux boundaries within the upper boundary. The River (RIV) package (McDonald and Harbaugh, 1988) was used to represent the tidal parts of the rivers where these areas were assumed to be a large enough to behave as constant sources of water if influenced by pumping. Farther inland in the nontidal parts of the rivers, the Streamflow-Routing (SFR2) package (Niswonger and Prudic, 2005) was used to simulate flow in streams and the interaction of streams with the aquifer system. Unlike the RIV package, the SFR2 package does not allow streams influenced by pumping to serve as an infinite source of water to the underlying aquifer. The contribution of induced infiltration from rivers to the underlying aquifer is controlled by the assigned streambed geometry and hydraulic properties, as well as hydrologic conditions in the rivers. The locations of river (RIV), stream (SFR2), and coastal water (GHB) cells are shown in figure 1.

Streams simulated in the model were selected from the surface-water hydrology of NHDPlus (Bondelid and others, 2010; Dewald and others, 2012), a comprehensive geospatial dataset developed by the U.S. Environmental Protection Agency and the USGS. The NHDPlus dataset provides extensive attribute information about stream physical characteristics and flow statistics along with stream channel locations, which make up a linked, ordered (upstream-to-downstream) stream network. Streams chosen for inclusion in the groundwater model included those with a Strahler stream order of three or greater (Pierson and others, 2008), because NHDPlus (Bondelid and others, 2010) data indicated that these streams made up about 99 percent of the average flow through the stream network. A few additional small streams were individually selected and added to the model for Long Island to represent more completely the unique surface-water hydrology resulting from the very permeable glacial geology in that area.

The model is bounded to the west and below by the contact between the unconsolidated Coastal Plain deposits and bedrock that underlies the entire study area. This boundary was represented numerically as a no-flow boundary condition. The elevation of the bedrock surface ranges from about 400 ft above the National Geodetic Vertical Datum of 1929 (NGVD 29) along the Fall Zone to more than 10,000 ft below NGVD 29 along the Continental Shelf (Masterson and others, 2013; Pope and others, 2016). Although inflow of water may occur along the Fall Zone between the subsurface fractured rock and the coastal plain sediments (Heywood and Pope, 2009), the amount of flow across this contact is unquantifiable and assumed to be negligible compared with the total inflow from precipitation into the system (Masterson and others, 2013) and, therefore, is not considered in this report.

The northern and eastern boundaries also were represented as head-dependent boundaries using the GHB package as described in the development of the upper boundary condition (layer 1). In layers 2 through 19, the northern and eastern boundaries are defined by the interface between fresh and saline groundwater, represented with general-head boundary (GHB) cells. These locations of these boundaries were based on the 10,000 milligrams per liter isochlor delineations estimated for each aquifer in the NACP aquifer system (Charles, 2016). The heads assigned to these GHB cells were estimated from a preliminary version of the flow model used to calculate heads for those cells without a GHB cell under nonpumping conditions. These heads were then assigned to the GHB cells and held constant throughout the final model parameter estimation. This method of calculating and assigning heads in the GHB cells can provide a qualitative measure of the effects of pumping on the freshwater/saltwater interface position. Although the interface position is static in the model, the areas of the changes in flow to or from the GHB cells when pumping stresses are imposed may indicate areas where the interface position may be moving in the real system, but the amount of actual movement cannot be quantified with this modeling approach.

The southern extent of the model was represented as a no-flow boundary that roughly aligned with the Tar River and Pamlico River in North Carolina (fig. 1) and the general groundwater flow direction determined in the analysis of the Southern Atlantic Coastal Plain (SACP) aquifer system (Campbell and Coes, 2010). This boundary does not represent a natural flow boundary in this aquifer system, but was located far enough south of the area of interest so that the flows and head conditions in this area would not substantively influence the simulation results in southern Virginia. The northern part of the Coastal Plain physiographic province in North Carolina is included in the active model area to buffer the effects of the southern no-flow boundary.

The previous analysis of the SACP aquifer system (Campbell and Coes, 2010) included the North Carolina area in its regional groundwater availability study and, therefore, that model was used to determine what influence, if any, the no-flow boundary selected for the NACP aquifer system model may have on the results from the simulation. Simulated heads from the SACP aquifer system model for 2000 were

selected and assigned as a specified-head boundary in the corresponding layers in the NACP aquifer system model. Simulation results were compared between the NACP aquifer system model with a no-flow boundary condition along model column 1 and a simulation in which heads along model column 1 were specified at conditions in 2000 from the SACP aquifer system model (fig. 3*A*). This comparison indicates that there is as much as a 5-ft difference in heads in layer 17, representing the Potomac-Patapsco aquifer along the Virginia-North Carolina State line, suggesting that the no-flow boundary condition may contribute an additional 5 ft of drawdown more than would be calculated if heads along column 1 were held constant at pumping conditions in 2000. The average observed drawdown of approximately 120 ft from predevelopment conditions in this area suggests that the model may overpredict drawdowns in this area by as much as 5 percent (fig. 3*A*).

An additional simulation was made for the NACP aquifer system model that continued the pumping rates in 2000 for 50 years to determine how this boundary condition could affect future predictions of water-level change. Heads generated from a simulation of the SACP aquifer system model into 2050 were then assigned along column 1 in the NACP aquifer system model, which in turn was used to simulate pumping conditions in 2000 for an additional 50 years with and without the specified-head boundary to assess the additional influence of the boundary. These results indicated that water levels continued to decrease with each boundary condition (no-flow and specified-head), but there was an additional 3 ft of drawdown calculated at the State line with the no-flow boundary compared with that in the specified-head boundary simulation, indicating an additional effect of this boundary condition as pumping is continued in time for an additional 50 years. In total, the influence of the southern boundary appears to be less than 6 percent of the total head change in the system (fig. 3*B*). Therefore, any use or interpretation of model results that include the northeasternmost part of North Carolina should consider the potential effects of this boundary condition on these results.

Hydraulic Properties

A substantial amount of data exists on the hydrologic properties of the aquifers and confining units within the NACP aquifer system. Hundreds of measurements of transmissivity, hydraulic conductivity (most commonly horizontal for aquifers and vertical for confining units), and specific storage from aquifer tests and laboratory permeameter samples are available throughout the study area. Even so, data are relatively sparse for the apparent heterogeneity of the hydrogeologic units; the spatial distribution of measurements is extremely uneven and focused primarily around major pumping centers. Consequently, measurements of hydraulic properties are more readily available in areas of large groundwater use and for those particular aquifer units receiving the most use.

Similarly, many more data are available for the hydraulic properties of aquifers than of confining units, although the hydraulic properties of confining units are very important for determining how water moves through the system. For example, hundreds of measurements of hydraulic conductivity or transmissivity are available for the Potomac-Patapsco aquifer, but data on other, less commonly used aquifers are much more limited, and for a few of the confining units, only a handful of measurements may be available throughout the entire study area. A more detailed description of the hydraulic properties of the NACP aquifer system can be found in Masterson and others (2013).

The hydraulic properties for the model initially were grouped together as zones over blocks of model cells that were assumed to have similar properties and assigned a single parameter value that could be adjusted during the parameter estimation process. In some cases, these adjustments were made uniformly across a given zone, but in most cases, parameter values were interpolated between points assigned throughout a given zone. These points are referred to as pilot points and are described in detail in the "Parameter Estimation" section of this report. The parameters represented in the flow model include the hydraulic properties of horizontal and vertical hydraulic conductivity, specific yield, and specific storage. Hydraulic conductance, which controls the ease in which water flows into or out of a head-dependent boundary, also was simulated as a hydraulic parameter that was adjusted during the parameter estimation process.

The simulated discharge at the head-dependent boundaries is a function of the hydraulic conductance, which represents resistance to flow across the streambed or seabed from fine-grained sediments. The hydraulic conductance was calculated externally and specified for each model cell containing a RIV or GHB cell as:

$$C = \frac{(K)(W)(L)}{(M)}, \tag{1}$$

where

C is hydraulic conductance of the stream or seabed, in square feet per day;
K is vertical hydraulic conductivity of stream or seabed deposits, in feet per day;
W is the width of the stream or seabed within the model cell, in feet;
L is the length of the stream or seabed within the model cell, in feet; and
M is the thickness of the stream or seabed, in feet.

The hydraulic conductance values developed for the SFR2 boundary cells were calculated internally from stream length per cell, streambed top elevation, streambed thickness, and streambed vertical hydraulic conductivity. Stream width was estimated by using the "arbolate sum" attribute from NHDPlus version 2 (Dewald and others, 2012), and a

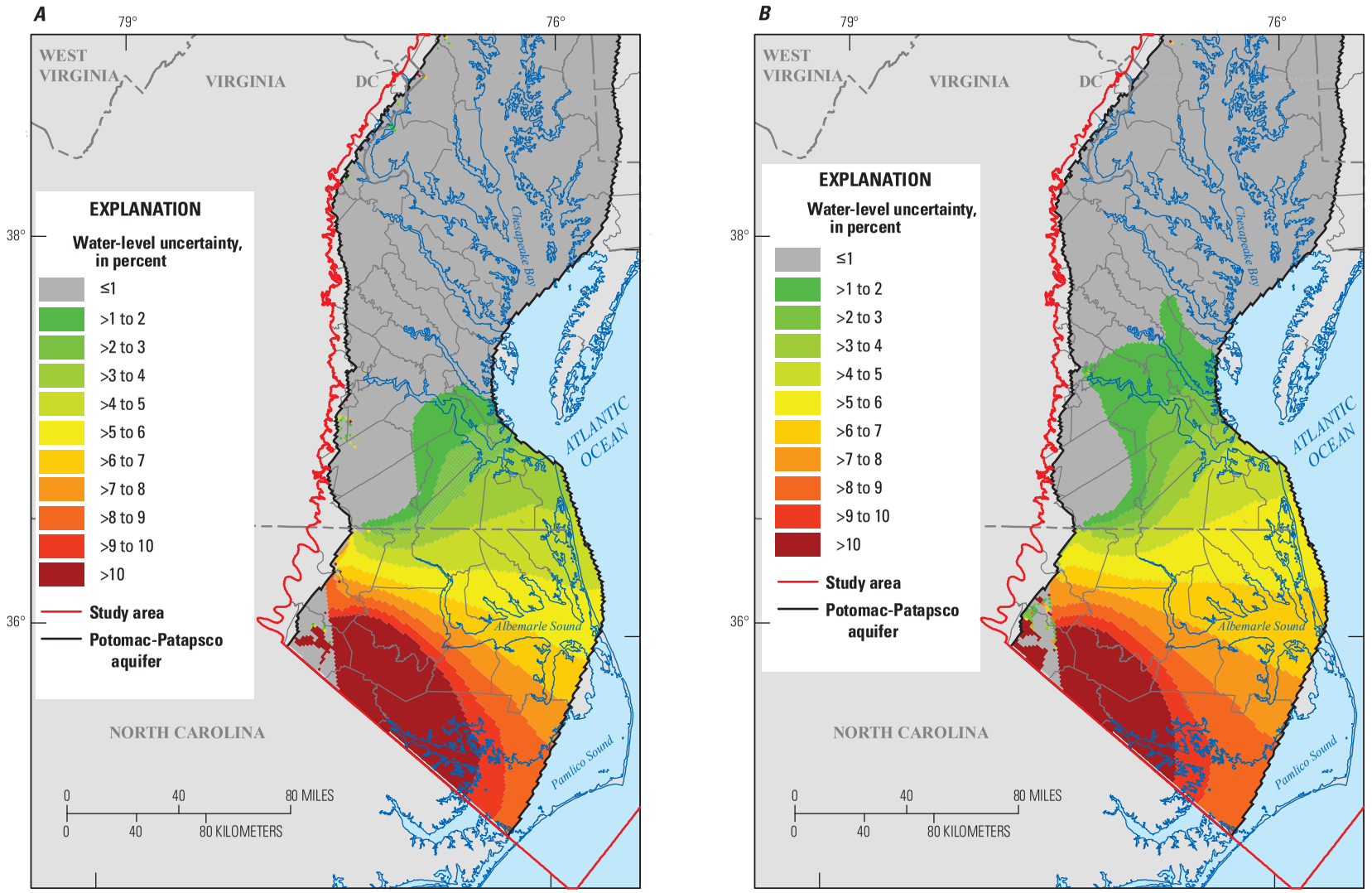

Figure 3. The percentage uncertainty of water-level change in the Potomac-Patapsco aquifer of the Northern Atlantic Coastal Plain aquifer system when comparing no-flow and specified-head boundary conditions *A*, for 2000 and *B*, projected to 2050. ≤, less than or equal to; >, greater than.

statistical regression was developed that relates arbolate sum to stream width (Feinstein and others, 2010). Stream length was derived from the intersection of the NHDPlus version 2 line-work lengths with each model cell. The resulting streambed area within a given cell was then multiplied by a streambed vertical hydraulic conductivity of 5 feet per day and divided by a streambed thickness of 1 ft. Therefore, the conductance values calculated for the model cells in the SFR2 package varied as a function of stream size to allow for a greater conductance term for larger rivers. These conductance values range from 76 to 871,000 square feet per day and, once assigned, were held constant throughout the parameter estimation process.

In the cases where multiple streams intersect the same model cell (that is, confluences or parallel streams occupying a single cell), streambed conductance was calculated for all reaches in the cell combined and assigned to the cell with the lowest elevation or farthest downstream segment. The remaining streams within the model cell were assigned a very low hydraulic conductivity value of 1×10^{-16} to avoid circular flow within a single MODFLOW cell. In this approach, all the water is assumed to convey downstream by the largest or farthest downstream node in the cell. Because all the other SFR elements in the cell have effectively a zero conductance value, they do not interact with the aquifer, so that all the water flowing into them flows to the downstream cell.

Hydrologic Stresses

The hydrologic stresses simulated in this model are recharge and groundwater withdrawals. Recharge includes natural and waste water return flow from onsite domestic septic systems in unsewered areas throughout the northern Atlantic Coastal Plain province. Groundwater withdrawals include those for agricultural (irrigation), commercial, domestic, industrial, and public supply uses.

Recharge

Precipitation is the largest source of freshwater to the NACP aquifer system. A complete accounting of the hydrologic budget for the NACP aquifer system requires an understanding of how much precipitation reaches the underlying aquifer system as groundwater recharge. Soil-water-balance (SWB) models estimate shallow groundwater recharge by simulating the physical processes of the movement of water as it enters and moves through the soil column downward to the water table. Conditions such as the amount of precipitation and evapotranspiration and the capacity of soils to absorb and store water are important components used by the model when calculating recharge.

The SWB model used for this investigation is based on a modified Thornthwaite-Mather method (Thornthwaite and Mather, 1957) that incorporates spatially distributed landscape, soils properties, and daily metrological data and produces model output of detailed spatial and temporal variability of recharge and evapotranspiration across the study area (Westenbroek and others, 2012). The aquifer recharge calculations for the 1986 to 2008 period are described in detail in Masterson and others (2013). Recharge estimates from 1900 to 1986 and 2009 to 2058 were based on the average recharge calculation from 1986 to 2008 and were applied to the model with the RCH package. Recharge estimates were adjusted as part of the model parameter estimation process using five recharge zones that were delineated for the study area (fig. 4*A*) to allow for more spatial variability than of the initial recharge distribution calculated by the SWB model. The final recharge distribution developed for the numerical model varied spatially throughout the active model area (fig. 4*B*). A comparison of the recharge rates calculated by the SWB model and those estimated as part of the model parameter-estimation process for model stress periods 13 to 35 (1986–2008) is shown in figure 5. A discussion of how the SWB model-calculated recharge rates were used as the initial values for the parameter estimation is described in the "Parameterization" section of this report.

In addition to the recharge estimated by the SWB method, recharge of wastewater from centralized sewage treatment facilities or from onsite domestic septic systems also can be an important source of water to the NACP aquifer system, particularly in areas of relatively high population density. This wastewater can originate as fresh groundwater withdrawn from the underlying aquifer system, treated saline groundwater withdrawn from the aquifer system, surface-water sources within the northern Atlantic Coastal Plain province, or from surface waters imported into the NACP aquifer system for drinking water. Regardless of the origin of this wastewater, eventually, it all discharges to the NACP aquifer system groundwater system or nearby surface waters. Nearly all the centralized wastewater treatment facilities in the NACP aquifer system are in close proximity to surface waters, and therefore, wastewater released from these facilities most likely discharges directly to these water bodies and reaches the coast with little interaction with the groundwater system. For this reason, water released from wastewater treatment facilities was not represented in the groundwater flow model.

Recharge from wastewater return flow to the NACP aquifer system was simulated for areas without sewers where domestic septic systems are common (fig. 6). Census block groups from 1990 (National Historical Geographic Information System, undated a,b) were used to identify areas where additional return-flow recharge was estimated and added to SWB-derived recharge rates, because the 1990 census was the last census to include survey information on the frequency of household septic systems and the frequency of domestic wells for household water supply. A threshold was established for this analysis such that each block group with 50 percent or more of households connected to public sewers according to the census survey was considered to be sewered, and therefore no additional return flow of wastewater was assumed or simulated for these block groups. The remaining block groups were then considered to be areas of onsite domestic septic systems

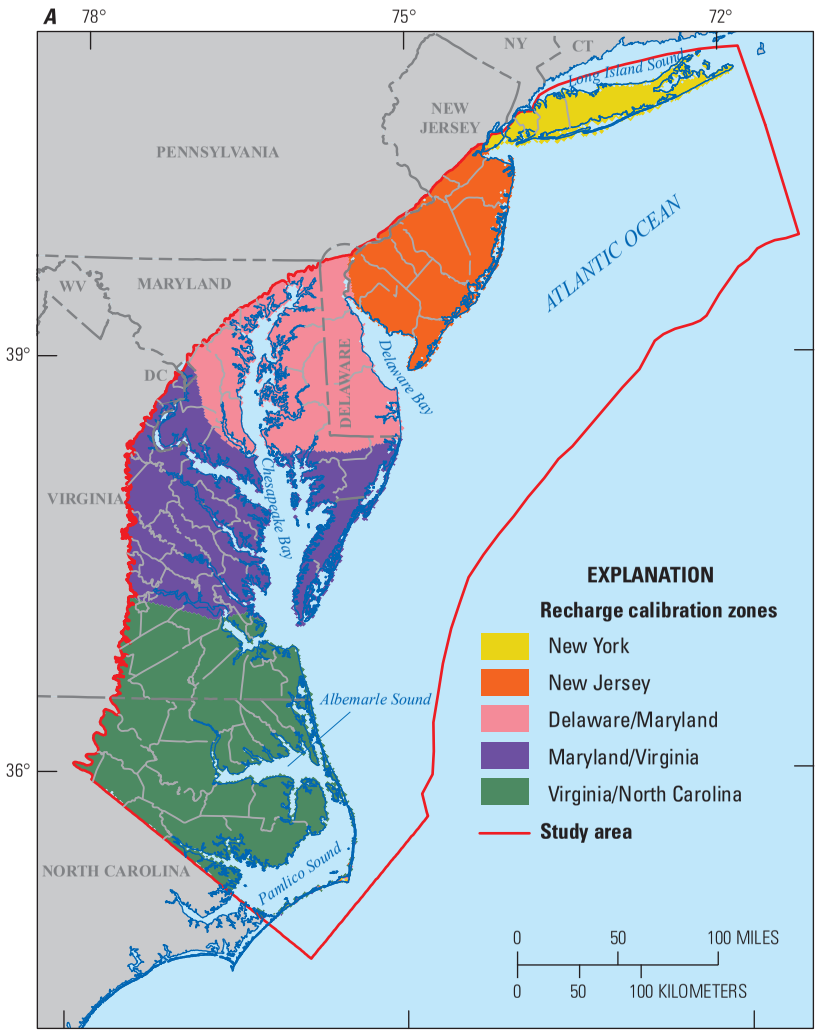

Base from U.S. Geological Survey 1:2,000,000-scale digital data
Albers Equal-Area Conic projection
Standard parallels 34°30' N and 41°30' N
Central meridian 75°30' W
North American Datum of 1983

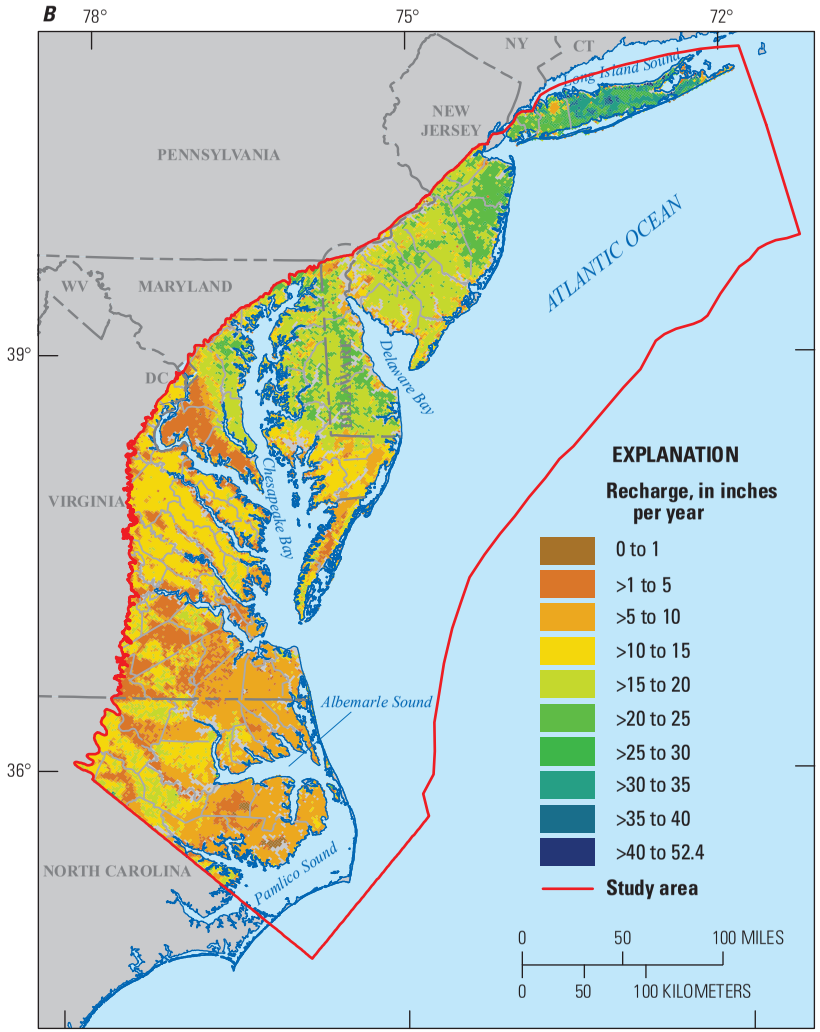

Base from U.S. Geological Survey 1:2,000,000-scale digital data
Albers Equal-Area Conic projection
Standard parallels 34°30' N and 41°30' N
Central meridian 75°30' W
North American Datum of 1983

Figure 4. Distribution of *A*, recharge zones for model calibration and *B*, average recharge rate calculated by a parameter-estimation method for model stress periods 13 through 35 (1986–2008) across the Northern Atlantic Coastal Plain aquifer system. >, greater than.

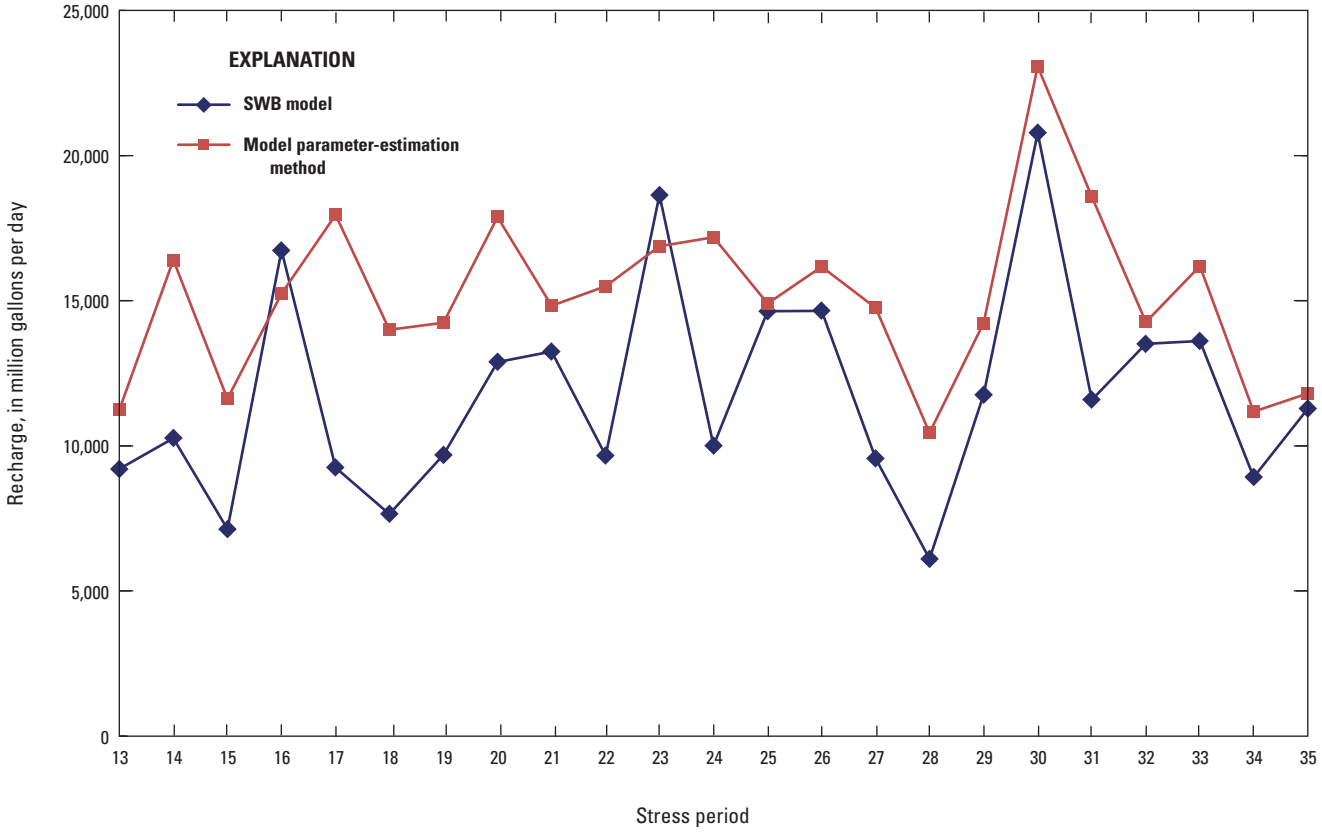

Figure 5. Comparison of recharge in the Northern Atlantic Coastal Plain aquifer system as calculated by the Soil-Water-Balance (SWB) model (Westenbroek and others, 2012) and refined by the parameter-estimation process for model stress periods 13 through 35 (1986–2008). Stress periods are listed in table 2.

for the purpose of estimating additional recharge in the model. The rate of return flow was estimated from the population within each nonsewered block group, which was further apportioned among the model grid cells intersecting each block group. The population apportioned to each nonsewered model cell was then multiplied by 60 gallons per day (gal/d), a coefficient derived from the estimate that 80 percent of the per capita domestic water use of 75 gal/d is discharged to septic systems (Shaffer and Runkle, 2007).

The total estimated wastewater return flow added as additional recharge with the RCH package was about 230 million gallons per day (Mgal/d). This rate was assumed to be constant for the 1986 to 2013 period because relatively minor changes in population during that time would yield little change to a return flow estimate; the wastewater return flow represented only a small (less than 2 percent) part of the total recharge added to the flow system. The rate of return flow for stress periods 13 to 36 (1986–2013) was also used for stress periods 37 to 45 (2014–2058) in the absence of projected information on the future distribution and use of septic systems.

Wastewater return flow rates also were estimated for each decade of the historical period by using population estimates from decadal census data at the county scale, apportioned to the block groups and model cells for which domestic wastewater return flow was estimated for the 1986 to 2008 period. These decadal estimates of rates of return flow from the 1900s to the 1980s ranged approximately from 48 to 184 Mgal/d. Return flow in New York is about 37 percent of the overall total for any period because of the large size of the population on Long Island not served by public sewers.

Groundwater Withdrawals

The locations and rates of groundwater withdrawals simulated in the flow model of the NACP aquifer system can be grouped into four categories: reported from 1986 to 2008; historical data from 1900 to 1985; domestic; and agricultural. The reported data are the most complete and well documented whereas the historical, domestic, and agricultural well locations and rates were estimated by the methods described in the following sections.

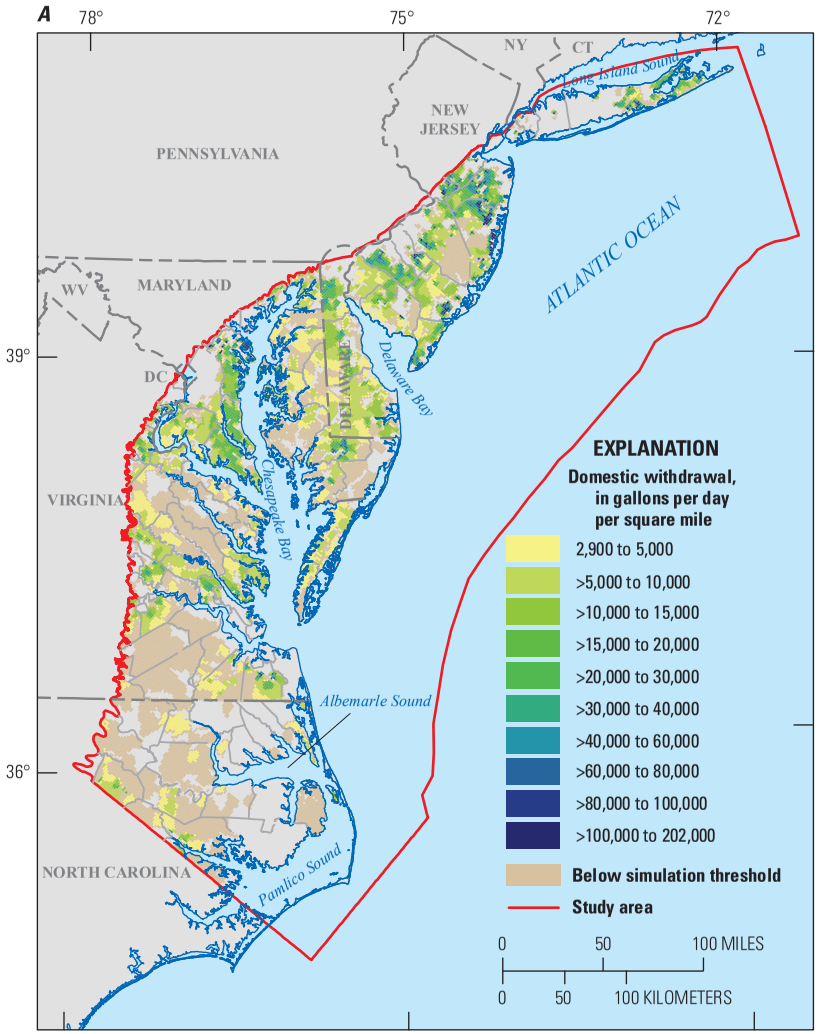

Base from U.S. Geological Survey 1:2,000,000-scale digital data
Albers Equal-Area Conic projection
Standard parallels 34°30' N and 41°30' N
Central meridian 75°30' W
North American Datum of 1983

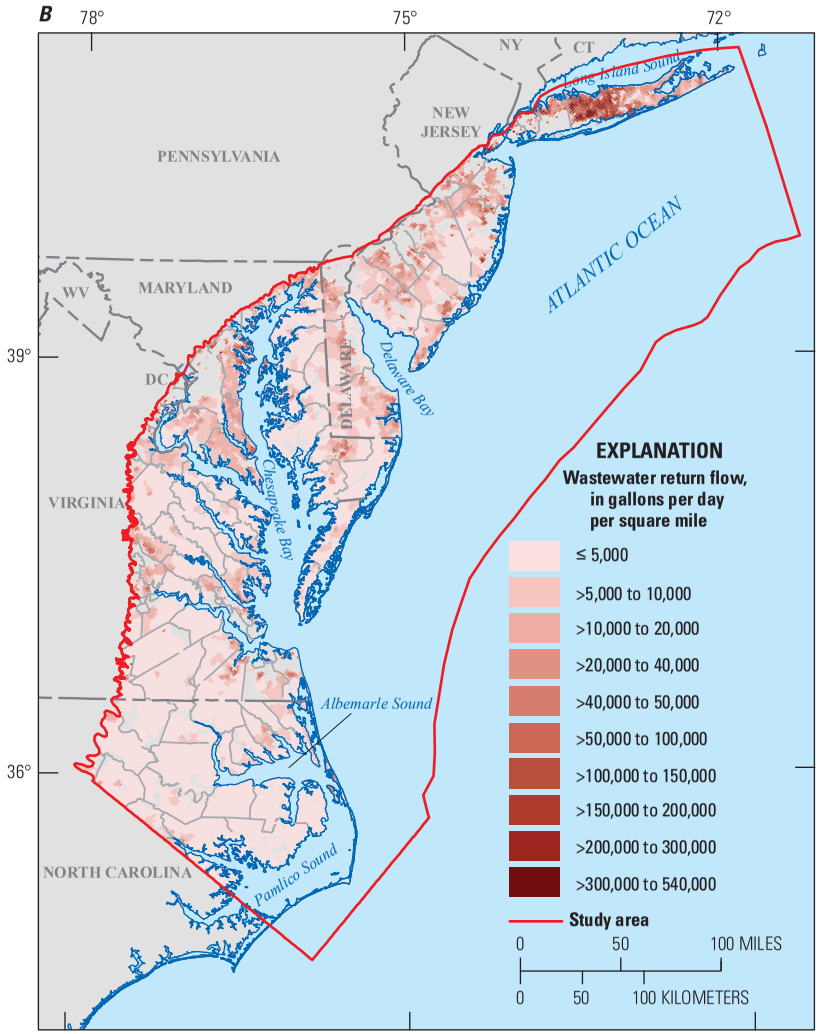

Base from U.S. Geological Survey 1:2,000,000-scale digital data
Albers Equal-Area Conic projection
Standard parallels 34°30' N and 41°30' N
Central meridian 75°30' W
North American Datum of 1983

Figure 6. Distribution of rates of *A*, groundwater withdrawal by domestic wells and *B*, wastewater return flow recharge across the Northern Atlantic Coastal Plain aquifer system for conditions in 2005. ≤, less than or equal to; >, greater than.

Reported Groundwater Withdrawals After 1985

The reported withdrawal data were obtained from the water-use programs of each of the USGS water science centers in the study area, which in turn regularly obtain the information from various State and local agencies. In most instances, the withdrawal data include only withdrawals at rates greater than a minimum threshold ranging from 10,000 to 50,000 gal/d and often only include data since the early 1980s, a time when regular collection and reporting of the data began across the study area. Reported withdrawals, including annual and sometimes monthly data, were combined into annual rates for each of the model stress periods from 1986 to 2008 (stress periods 13 to 35). The pumping rates in 1985 were used to represent the 5-year period from 1981 to 1985 (stress period 12) in order to provide a transition from the historical period through the first year [1985] of complete data on reported withdrawals across the study area. The pumping rates in 2008 were used to represent the 5-year period from 2009 to 2013 (stress period 36), which is defined as current [2013] conditions in Masterson and others (2016a).

Model layer assignments for withdrawal wells were based primarily on local aquifer designations reported with well construction information, matched to the equivalent regional aquifers. Available well screen elevation intervals for wells without reported aquifer designations were cross-referenced with hydrogeologic unit elevations (Pope and others, 2016) to determine the appropriate aquifer and model layer assignments. The well-construction data available for the reported withdrawal wells provided the necessary information for the determination of aquifers and model layers for almost all these wells. The quality of available data and confidence in the aquifer and layer determinations typically increase with the magnitude of the withdrawal rate because construction details for large municipal or industrial withdrawal wells usually have been thoroughly documented. The total reported rates of groundwater withdrawals for the entire study area range from a low of 873 Mgal/d in 1989 to a high of 1,045 Mgal/d in 2004 with an average of 957 Mgal/d from 1985 to 2013.

Historical Groundwater Withdrawals

Groundwater withdrawal locations and rates for the historical period were obtained from the regional model of the NACP aquifer system in Leahy and Martin (1993) by approximating the location of the pumping center in the 7-mi×7-mi-grid cells in the Leahy and Martin (1993) model within the 1-mi×1-mi grid used in this report. The total withdrawal rates in the 7-mi×7-mi grid of the Leahy and Martin (1993) model were apportioned to model cells in the model in this report based on the known or estimated location of pumping wells in 1985 to ensure that the total pumping stress in the Leahy and Martin (1993) model is represented in the model in this report for the historical period. The layer assignments in both models are based on the regional aquifers in the system so the vertical discretization of pumping also was comparable between the two models.

Self-Supplied Domestic Groundwater Withdrawals

Self-supplied domestic withdrawals from private wells compose a substantial part of groundwater withdrawals in many parts of the study area, but are typically not reported like the large-capacity withdrawal sites (Maupin and others, 2014). Depending on local hydrogeologic conditions and other variables, these domestic withdrawals may be taken from wells in several of the confined aquifers in addition to the unconfined surficial aquifer (Pope and others, 2008). For this study, self-supplied domestic withdrawals of groundwater were estimated using the 1990 census block group data (National Historical Geographic Information System, undated b) on household water supply, combined with information from the USGS National Water-Use Information Program (NWUIP; Solley and others, 1993).

The percentage of housing units served by public supply in each block group for each county within the study area was ranked in descending order and the respective populations of those counties were summed until the total population approached the public-supply population estimates for 1990 in Solley and others (1993). When the public-supply population data from Solley and others (1993) closely matched the summation of the U.S. Census Bureau block group data, the respective percentage of housing units served by public supply was set as a cutoff value for each county. This analysis showed a correlation between housing density and the frequency of public supply, with higher housing density associated with greater public supply as the primary source of water. Any block group with a percentage of housing units served by public supply above the cutoff value was considered to be served entirely by public supply, whereas all percentages of housing units less than the cutoff value were considered to be self-supplied (domestic wells). The self-supplied domestic block groups and the populations for these block groups were further apportioned to the groundwater model cells intersecting each block group estimated to be self-supplied by domestic groundwater withdrawals. A domestic use per capita coefficient of 75 gal/d was applied to the model cell population to calculate the annual withdrawal rate.

The methodology developed for the available water-use information obtained from the 1990 census was then used for subsequent decadal census surveys for which this detailed information was not collected. Domestic withdrawals estimated by this approach used the 1990 population data to calculate pumping for 1986 to 1995, the 2000 population data for 1996 to 2005, and the 2010 population data for 1996 to 2013. As with reported withdrawals, estimated self-supplied domestic withdrawals for stress periods 37 to 45 (2014–2058) were based on those used for 2008.

Domestic withdrawals were represented as virtual wells in the model; however, not all of these virtual domestic withdrawal wells were included in the analysis. A virtual well assigned in every groundwater model cell with any estimated self-supplied population would have meant adding more than 22,500 wells to the model, some with very small withdrawal

rates in areas of low population density. However, 90 percent of the estimated domestic withdrawals were accounted for with about 10,000 virtual wells distributed in less than 50 percent of the model cells, which simplified the spatial distribution and focused the task of managing the well data on the areas where domestic withdrawals were likely to have the greatest influence. Specific information on actual domestic wells in the study area is limited because the domestic withdrawals estimates were based only on population distribution; consequently, aquifer and layer assignments for the estimated self-supplied withdrawal wells were derived from the reported aquifer designations for nearby public-supply wells.

Groundwater Withdrawals for Irrigation

Groundwater withdrawals for agricultural irrigation have been reported and recorded in water-use databases by State agencies throughout the northern Atlantic Coastal Plain region since the early 1980s, along with other large commercial and industrial withdrawals. However, groundwater withdrawals for irrigation were found to be widely underreported by comparison with agricultural irrigation estimates found in the U.S. Department of Agriculture Farm and Ranch Irrigation Survey (U.S. Department of Agriculture, National Agricultural Statistics Service, 2014) and from conversations with water management officials at State agencies throughout the study area. In particular, irrigation withdrawals reported for row crops, such as corn and soybeans, on the Delmarva Peninsula are known to be substantially less than the amounts actually withdrawn. Consequently, reported groundwater withdrawals for agricultural irrigation were found to be inadequate for representing groundwater withdrawals for irrigation over much of the study area. More comprehensive analysis was needed to better estimate irrigation of row crops, improve estimates of total groundwater withdrawals for agricultural irrigation, and accurately represent the effect of these withdrawals on the flow system.

Reported groundwater withdrawals for agricultural irrigation in the study area for Delaware, Maryland, New Jersey, New York, and Virginia totaled 125.9 Mgal/d for 2008 (table 3) and ranged from 15.2 Mgal/d in 1989 to a maximum of 147.3 Mgal/d in 2007 (table 4). Information on irrigation withdrawals for the North Carolina part of the study area was not available for the analysis documented in this report.

Irrigation withdrawals are reported to have increased since the early 1980s, but it was apparent from examination of the data that much of the large difference in reported withdrawals over time (table 4) was the result of inconsistent data collection in earlier years. More consistent reporting of withdrawals since the 2000s suggests that greater confidence can be given to withdrawal values for irrigation withdrawals reported more recently than those reported before 2000.

During analysis of agricultural irrigation in the study area, examination of aerial photography revealed extensive areas of irrigated crop land—particularly on the Delmarva Peninsula—with no corresponding entries in the database for reported irrigation withdrawals. Subsequently, a dataset was created to inventory the total acreage of center-pivot irrigation areas across the northern Atlantic Coastal Plain province (Finklestein and Nardi, 2015). This irrigation dataset identifies about 272,000 acres operated primarily with center-pivot irrigation in 57 counties. Manual digitizing was performed against aerial imagery, with observable center-pivot irrigation characteristics—such as irrigation arms, concentric wheel paths through cropped areas, and differential colors—used to identify and map irrigated areas. In some instances (such as in Suffolk County, N.Y.) rectangular irrigation fields were observed and digitized as well. Estimated irrigation rates in the irrigated areas were computed by the SWB model (Westenbroek and others, 2012) based on crop-water demand that exceeded the amount provided by precipitation in a given year. Estimated irrigation totals computed with this method are listed in tables 3 and 4.

The reported irrigation withdrawals typically had aquifer and well screen information available with the well withdrawal rates in the reported withdrawal data supplied by individual States. However, aquifer assignments for irrigation withdrawals estimated as part of this analysis were made based on the aquifer of the reported irrigation well in closest proximity to the locations of estimated irrigation withdrawal sites. For estimated withdrawals in areas without nearby reported irrigation wells, aquifer information was taken from the nearest reported municipal or industrial well.

The Delmarva Peninsula accounts for about 75 percent of the total estimated irrigated acreage in the study area. Center-pivot irrigation is the method used in this area for the predominant crop types of corn and soybeans. Other irrigation methods include subsurface drip and flood irrigation, which are commonly used on vegetable crops such as peppers and tomatoes and some fruit and nursery stock crops. Drip irrigation is especially prevalent in New Jersey where truck crops are more common. Drip and flood irrigation methods were not accounted for in the dataset of estimated withdrawals developed for this investigation, which partly explains why reported irrigation is greater than estimated irrigation in New Jersey and New York (table 3).

Digitized crop acreage totals compared favorably with the county irrigation estimates provided by the U.S. Department of Agriculture Farm and Ranch Irrigation Survey (U.S. Department of Agriculture, National Agricultural Statistics Service, 2014), which is the most comprehensive source of information on irrigation water use. Furthermore, in areas where irrigation estimates coincided with reported withdrawals, estimated and reported withdrawal rates were generally in approximate agreement. However, because neither the reported nor estimated irrigation withdrawals provided a complete dataset of withdrawals, the reported and estimated withdrawals were combined to produce a spatial and temporal representation of all withdrawals of groundwater for irrigation across the study area. The total rates of irrigation withdrawals used in the groundwater model are listed in table 4. The total

Table 3. Withdrawals of groundwater for irrigation in 2008 in the Northern Atlantic Coastal Plain aquifer system.

[Mgal/d, million gallons per day]

State	Reported (Mgal/d)	Estimated (Mgal/d)	Total simulated[1] (Mgal/d)	Reported as a percentage of total simulated (percent)	Percentage of estimated total for study area
New York	3.6	2.5	5.7	63.4	2.5
New Jersey	49.8	7.2	44.6	[2]111.0	19.5
Delaware	26.2	83.8	84.8	31.0	37.1
Maryland	42.2	46.5	52.8	79.9	23.1
Virginia	4.1	13.2	15.8	25.7	6.9
North Carolina	0.0	25.0	25.0	0.0	10.9
Total	125.9	178.1	228.7	55.0	100.0

[1]Total simulated withdrawal is less than the sum of reported and estimated withdrawals because of overlap between reported and estimated withdrawals.

[2]Total simulated withdrawal in New Jersey is less than the reported amount because of uncertainty in estimation methods.

Table 4. Withdrawals of groundwater for irrigation from 1981 to 2008 in the Northern Atlantic Coastal Plain aquifer system.

[Mgal/d, million gallons per day]

Year	Model stress period	Reported[1] (Mgal/d)	Estimated[2] (Mgal/d)	Simulated[2,3] (Mgal/d)	Reported as percentage of total
1981–1985	12	18.8	152.0	167.5	11.2
1986	13	19.6	177.1	193.3	10.2
1987	14	20.0	202.4	214.8	9.3
1988	15	22.0	194.6	207.6	10.6
1989	16	15.2	128.0	135.9	11.2
1990	17	32.2	151.0	168.7	19.1
1991	18	46.1	176.3	203.7	22.6
1992	19	42.7	155.2	175.5	24.3
1993	20	56.4	178.0	204.9	27.5
1994	21	49.7	157.2	184.5	27.0
1995	22	66.9	179.2	213.5	31.3
1996	23	45.5	136.2	157.9	28.8
1997	24	70.6	192.0	225.2	31.3
1998	25	67.5	185.9	224.1	30.1
1999	26	65.5	191.1	219.2	29.9
2000	27	46.5	115.5	142.5	32.6
2001	28	85.8	133.5	183.6	46.7
2002	29	120.7	217.9	273.9	44.1
2003	30	48.3	107.4	138.0	35.0
2004	31	110.5	139.6	183.0	60.4
2005	32	79.2	156.8	202.1	39.2
2006	33	91.7	174.6	218.6	42.0
2007	34	147.3	195.4	251.4	58.6
2008	35	125.9	178.1	228.7	55.0

[1]As reported by State agencies in Delaware, Maryland, New York, New Jersey, and Virginia.

[2]From the model detailed in this report.

[3]Total simulated withdrawal is less than the sum of reported and estimated withdrawals because of overlap between reported and estimated withdrawals.

simulated irrigation withdrawal in table 4 is not a sum of the reported and estimated irrigation withdrawals because of areas of overlap between reported and estimated withdrawals; in such areas, the more consistent estimated withdrawals were generally applied.

Total agricultural irrigation aggregated for 1986 to 2008 from reported and estimated data ranged from 135.9 Mgal/d in 1989 to 273.9 Mgal/d in 2002 (table 4). Based on data for 2008, about 37 percent of agricultural irrigation withdrawals were in Delaware; about 23 percent were in Maryland, mostly on the Eastern Shore; and more than 19 percent were in New Jersey; the remaining 20 percent were in New York, North Carolina, and Virginia combined (table 3). Across the study area, about 55 percent of the total estimated withdrawals in 2008 were reported, though the amount reported varies substantially by State (table 3). The percentage of total estimated withdrawals reported for the study area has generally increased with time (table 4), which reflects more comprehensive reporting in addition to probable increases in irrigation.

Parameter Estimation

The parameter estimation process used for the NACP aquifer system flow model was performed in multiple steps. These steps, outlined broadly, were as follows:

- assembling available data,
- assigning weights to data,
- defining hydraulic parameterization (discretization and zonation),
- conducting manual trial-and-error history matching to determine initial parameter values,
- conducting sensitivity analysis,
- iteratively exchanging parameter values between parameter estimation steps, and
- revising the conceptual model and observation weights.

These steps do not necessarily follow in sequence from one to the other because feedbacks throughout the process identify shortcomings and indicate changes that cascade throughout the process. Because the final model is based on the results at each step, each step is described in this section. First, the parameter estimation algorithm is described to provide context for the steps outlined.

Parameter Estimation Algorithm

The parameter estimation process was achieved through history matching, using observations of both steady-state and transient conditions, as described below, and using the Gauss-Levenberg-Marquardt algorithm implemented in the PEST software suite (Doherty, 2010, 2014; Doherty and Hunt, 2010) and the singular-value decomposition (SVD)-based parameter estimation methodology (SVD-assist) of PEST (Tonkin and Doherty, 2005). The Gauss-Levenberg-Marquardt method is a gradient-based search algorithm that adjusts parameters in detecting the minimum value of an objective function. The objective function is the weighted sum of squared errors comparing field observations with simulated values at the same time and place made by the model. The objective function is referred to as:

$$\Phi = \left(y - g\left(p\right)\right)^T Q^{-1}\left(y - g\left(p\right)\right), \qquad (2)$$

where

Φ is the objective function;
y is a vector of observations;
$g(p)$ is a vector of modeled values collocated in time and space with the observations, evaluated at parameter values p;
T indicates a vector transpose;
Q is a matrix of observation weights (in this work, Q is a diagonal matrix indicating no correlation among observation errors is assumed); and
-1 indicates a matrix inversion.

The term "$y - g(p)$" is the vector of residuals—also called errors—comparing measured and modeled results.

The observation weights assigned to the data play important roles both in enforcing an appropriate level of fit (correspondence between observed and modeled results) and in balancing Φ such that observations of various types all contribute to the objective function. These two roles are an acknowledgement that a perfect match between modeled and observed values is unattainable and, in fact, undesirable. The many reasons for imperfect match include errors in the observations, the necessary fact that the model is a simplification of the true physical system, and the smoothing of time signals by the model among others. The flexibility that the use of these observation weights imparts, however, is underscored by the fact that many (in fact, infinite) arrangements of parameters can result in the same value of Φ. This nonuniqueness motivates the need to incorporate expert knowledge to arrive at a set of parameters that both satisfies the desired level of fit and conforms to expert understanding of reasonable values for the parameters.

The introduction of previously collected data that have undergone expert qualitative analysis is made through several avenues including enforcing the level of fit desired through the assignment of weights, normalizing observation group weight contributions through weight adjustment, inclusion of a penalty to the objective function for parameters deviating from a preferred condition through regularization, and the SVD algorithm. Decisions made regarding all these aspects of previously collected information are inherently subjective. However, using qualitatively analyzed data is an

important way for human understanding of the groundwater flow system to play a role in the process beyond blind trust of the algorithm, leading to more meaningful results than those obtained from depending entirely upon algorithms (for example, Fienen, 2013).

The assignment and normalization of observation weights are discussed in the context of the history matching targets. A penalty to the objective function Φ is assigned as a form of Tikhonov regularization (Tikhonov, 1963a, b) through an additional term in the objective function that penalizes deviation from a preferred condition—in this case, preferred values of parameters:

$$\Phi = \left(y - g\left(p\right)\right)^T Q^{-1}\left(y - g\left(p\right)\right) + \frac{1}{\Phi_{MLIM}}\left(p - p_0\right)^T\left(p - p_0\right), \quad (3)$$

where

Φ_{MLIM} controls the strength of regularization (Doherty, 2003; Fienen and others, 2009), and

p_0 is a vector of preferred parameter values.

The variable Φ_{MLIM} was set to a value the same order of magnitude as the number of observations, as suggested by Fienen and others (2009), to balance the level of fit with the importance of the qualitatively analyzed information.

The SVD method was also used to enhance solution stability and provide a secondary level of regularization. In SVD-based parameter estimation, the sensitivity of observations to parameters is transformed to align with principal orientations of maximum information. This transformed space can then be divided into the calibration space and the null space. The calibration space is the region in which information from observations is meaningfully projected onto parameters, whereas the null space represents a space where variability in parameters has little or no effect on model outputs of interest. This division between solution and null space is controlled by the stability of the sensitivity matrix, and the settings recommended by Doherty and Hunt (2010) was adopted. Finally, to make the history-matching process more computationally tractable, SVD-assist (Tonkin and Doherty, 2005; Doherty, 2014) was used with 250 superparameters.

History matching was first performed using a steady-state version of the model. The steady-state model is much faster to run and provides important information about hydraulic conductivity, GHB conductance, and spatial patterns in recharge. Using the steady-state results as a starting point, history matching was then performed on the transient-condition model.

Parameterization

Parameters representing model properties are adjusted in the history matching process to tune the model in response to the correspondence between observations and collocated model outputs. Five types of parameters were adjusted and estimated in the history matching process: GHB conductance, horizontal (K_x) and vertical (K_z) hydraulic conductivity, recharge (*RM*), specific yield (S_y), and specific storage (S_s), resulting in a total of 2,260 separate parameters. The distribution of the pilot points and parameter zones are presented by model layer as a map in figure 7 (in back of report).

A series of zones also was assigned for GHB conductances to simulate the seawater boundary for the model (fig. 7, in back of report). The conductance in the GHB cells was estimated with one value assigned to each zone. The GHB zones were subdivided into four groups: seabed, subsurface regional, subsurface Long Island, and subsurface impact crater distributed throughout the 19 layers. These subdivisions were assigned to allow for more flexibility in estimating the GHB conductance parameter to account for the suspected variations in hydraulic conductivity throughout the region.

Hydraulic conductivity values were assigned in two ways: through homogeneous zones and by using pilot points. Hydraulic conductivity zones were first assigned based on lithology and assumptions of similar values throughout each zone. An example of the zonation used in the model includes the use of a single zone value (41) in a layer 1 (fig. 7*A*, in back of report) to represent the streambed sediments in the simulated stream cells. A zone value of 40 was used in layers 2 to 19 for the hydraulic connection between the streams and the underlying incised aquifer and confining unit sediments (figs. 7*B–S*, in back of report). Additional examples of zonation changes within a layer include zones 16 and 86 in layer 16 (fig. 7*P*, in back of report). In this instance, zone 86 was added along western edge of the active model area to allow for changes in hydraulic properties in the Fall Zone.

In certain subsets of the zones assigned throughout the model domain, a single homogeneous value would not be sufficient to represent the variability of the property in the zone. In these cases, pilot points were employed following the guidelines in Doherty and others (2010) throughout these zones, now referred to as heterogeneous zones. It is important that pilot points are used not only where variability is important, but also where observation data can inform parameter values through history matching. The maps presented in figure 7 (in back of report) show, for each layer, the locations of pilot points within the heterogeneous zones, homogeneous zones (without pilot points), and areas where the primary aquifer or confining unit is not present (secondary zones). The zonation of the model layer and the associated parameter value for the secondary zones is assigned from the first overlying layer where a primary aquifer or confining unit is present at that location.

Interpolation for the pilot point values to fill in the entire zone of model cells is accomplished through a Kriging process regression using an exponential variogram. At each pilot point, a value was estimated for horizontal (K_x) and vertical (K_z) hydraulic conductivity and for specific storage (S_s), and those values were interpolated to all model cells using the same variogram parameters. The same zones and pilot points, including the same variogram parameters, were used for both

specific yield and specific storage. The combination of zones and pilot points results in values for all these parameters being estimated for each model cell. The final values of each of the 2,260 hydraulic parameters are listed in the parameter estimation files in the model archive (Masterson and others, 2016b).

The final hydraulic parameters derived from the parameter estimation process are consistent with the hydraulic properties summarized in Masterson and others (2013) for the hydrogeologic units throughout the NACP aquifer system. The range of hydraulic parameters (K_x, K_z, S_s, S_y) by model layer and corresponding hydrogeologic unit is given in table 1.

Recharge initially was estimated using the SWB model as described in the "Hydrologic Stresses" section of this report. The SWB results were subdivided geographically into five recharge zones (fig. 4*A*) and, in the steady-state analysis, a multiplier was assigned to each of these zones to allow for subregional adjustments of the SWB results to provide greater flexibility for history matching to the observation data than could have been achieved with the initial SWB results for the entire model area. These adjustments were then applied to each initial array for transient-condition recharge, which then received new adjustment multipliers at the entire array scale for recharge—one for each stress period during the parameter estimation process for the transient-condition model. The final recharge rates estimated from the parameter estimation process (fig. 4*B*) were on average about 29 percent greater than the recharge computed by the SWB model for the 1986 to 2008 period. This difference varies both temporally and spatially; however, over the entire model area, the annual recharge initially calculated by the SWB model and the final model-estimated recharge compared reasonably well for stress periods representing years with higher recharge compared with those stress periods with lower recharge (fig. 5).

History Matching of Water-Level and Streamflow Observations

History matching for calibration of the NACP aquifer system model was based on water-level (head) and streamflow measurements (observations) from the National Water Information System (NWIS) database from 1986 to 2008 (U.S. Geological Survey, 2011). The observations were selected to provide a reasonable spatial and temporal distribution of observations to supply an adequate measure of how well the model simulates observed hydrologic conditions throughout the NACP aquifer system. Consideration was given to both the number and the quality of observations available.

Head Observations

Abundant water-level observations were available for potential history matching targets for the NACP aquifer system groundwater model. From about 11,400 observation wells within the study area, 3,252 wells were selected for consideration as targets for history matching based on the lengths of their water-level records. For these wells, 40,450 annual average water levels from 1900 to 2008 were computed from 246,804 available water-level measurements. Available data from NWIS, such as screen and aquifer information, were used to place observation wells in the correct model layers.

The water-level observations initially selected were not evenly distributed in space and time, and the distribution was particularly uneven for some individual aquifers. As a result, giving the same weight in the history-matching process to all observations tends to push the overall history matching toward the specific areas and hydrogeologic units with the higher observation density, thus limiting the regional predictive capabilities of this model. Therefore, in order to develop a regional groundwater model representative across all areas and hydrogeologic units, wells were selected within individual aquifers to provide a generally even distribution of observations and eliminate multiple observations in close proximity to each other. This process resulted in the final selection of 644 observation wells, which were then combined in 29 observation groups within the regional aquifers.

The distribution of selected observation locations for each aquifer is shown in figure 8 (in back of report), and the number of wells for each group is listed in table 5. The head observation mean residuals on figure 8 (in back of report) are the means of the differences between observed water levels for a given well and the model-calculated water levels values for each stress period. A negative value indicates the mean observed water levels are lower than the mean model-calculated water levels.

Wells that were selected as history-matching targets had available water-level observations throughout the simulated period, from 1900 to 2008. The 1986 to 2008 period for this report corresponds to the highest level of data quality used in the model construction. For example, the reported and estimated withdrawal data assembled for the 1986 to 2008 period provide much more detail than the data assembled for the historical time period. As a result, water levels for stress periods 2 to 12 (before 1986) were retained in the analysis for visual comparison but were given zero weight in the history matching process, thereby removing them from the objective function calculation. The 644 selected wells displayed by aquifer and group in figure 8 (in back of report) are the locations of 8,868 annual average water-level observations selected for history matching in the model. Observations before 1986 for selected wells are shown only for comparison in time-series graphs but were not given any weight in the parameter estimation, and therefore, simulation results for the period before 1986 should take into account this limitation in the parameter estimation process.

In addition to absolute water-level elevations, the water-level differences between individual measurements were also included in the parameter estimation process for the 8,868 selected observations at 644 selected wells. These water-level differences provide information on the dynamic response to storage (both specific yield and specific storage) over time. By taking the difference between consecutive measurements rather than always referencing back to the original value (as

drawdown targets are often defined), useful information for the parameter estimation process is provided by these water-level difference values even if a systematic bias is observed between sequential absolute water elevations.

Examples of how the differences provide additional information to overcome a systematic bias are presented for the Piney Point (fig. 9) and Potomac-Patapsco (fig. 10) regional aquifers. In the example of the Piney Point aquifer, this analysis of the differences rather than the absolute water levels allows for a more accurate comparison of how well the model matches water levels after 1990 by removing the systematic bias from the underpredicted water levels before 1990 (fig. 9*B*).

Water levels before 1987 appear to have been underpredicted in the model for the Potomac-Patapsco aquifer, but the total magnitude of the simulated water-level decrease from 1987 to 2008 appears to be consistent with the observed data (fig. 10*A*). Therefore, creating history-matching targets that also include the differences (fig. 10*B*) in water levels rather than the absolute elevation, removes the systematic bias caused by missing stresses in the early stress periods.

The 29 water-level observation groups were chosen to focus the history matching on specific hydrogeologic units in geographic areas in which distinct geologic and hydrologic conditions were observed. In the history-matching process, the weights of the observation groups were adjusted to guide the process and normalize the contribution of each observation group to the objective function to correct the fit between measured and modeled results from specific units and areas. In many cases, this grouped approach was very effective in guiding the history matching toward lower errors than would have resulted without the use of groups. In a few cases, however, the group approach not only isolated problem areas where the model was less effective at simulating water levels but also had little overall effect on the overall fit of the model. Grouping water-level observations and weighting them by group enabled control of the history-matching process by allowing the influence of observation measurements in certain units to be adjusted independently of the number of observations. Giving the same weight to each observation would have focused too much of the history matching on a few important units with a large number of observations while giving almost no weight to some areas or aquifers where measurements were sparse but where a greater understanding of the flow system was desired.

The final observation weights illustrate that relatively important aquifers like the Potomac-Patapsco received a proportionally large weight in the parameter estimation process, but individual measurements in Potomac-Patapsco groups received less weight because there were more observations available for those observation groups and aquifers (tables 5 and 6). The weights given to individual observations tended to be highest for observation groups and aquifers for which few wells and observations were available.

The parameter estimation process was guided by adjusting relative weights of observation groups with attention to the average residual of each observation group in the model output as well as the overall average residual and average absolute residual for all observations. The parameter estimation process uses the sum of squared errors to minimize the objective function while adjusting parameters. Residuals here are defined as the difference between observed and modeled value. The summaries of observation residuals listed by group provide one way of evaluating the quality of the history matching as a whole and for individual groups and aquifers (table 7).

The total average residual and the average absolute residual were both used to provide information on how well the simulated observations matched the measured ones. The total average residual of –1.7 ft is close to zero, indicating minimal bias. Also, the residuals are also normally distributed (based on the Shapiro-Wilk test [Shapiro and Wilk, 1965]) for all head groups, further indicating low bias in the residuals. The average absolute residual value of 12.3 ft provides a better measure of the differences between simulated and observed water levels that have been averaged by group than the total average residual because it eliminates the potential for large positive and negative residual values from negating one another.

The mean residual and root mean square error by group are presented in table 7 to provide the information necessary to evaluate how well the model matched the observations throughout each layer across the model domain. The maps presented in figure 8 (in back of report) show the residuals for every well location for each group and provide a spatial illustration of the residuals by calibration group listed in table 7. These maps show overall patterns in the model fit at individual wells for the various groups and aquifers and allow for the assessment of any bias in history matching throughout the model domain. For example, one high residual among many low residuals may represent a local anomaly, but a group of high residuals probably indicates an area where the model does a relatively poor job of simulating conditions overall. Specific examples of simulated and observed hydrographs are shown to illustrate examples of both good and bad model fit for selected observation groups (fig. 8, in back of report).

The quality of the overall history matching is illustrated in hexbin (fig. 11) and histogram (fig. 12) plots that illustrate the point density rather than the individual points themselves. Both of these plot types highlight the generally good agreement and lack of bias with respect to head and base flow residuals as well as show where outliers are found. As an iterative part of the parameter estimation process, head and base flow residuals were evaluated and outliers were investigated closely to consider data quality and potential structural errors in the model. Outliers and potential structural errors both were encountered, resulting in revision of the structure of the model in some cases, adjustment of stresses or observations where appropriate, and relegation of observation values to zero weight where water-level data anomalies could not be resolved.

Table 5. Water-level and base flow flux observation weights by observation group for the model used in the groundwater assessment of the Northern Atlantic Coastal Plain aquifer system.

[--, not applicable]

Observation group	Model layer	Aquifer	Number of wells	Number of observations	Single observation weight	Sum of weights	Proportional group weight, in percent	Minimum well weight	Average well weight	Maximum well weight	Percentage of total observation weight
A. Observations of water level, in feet											
sf1a	1	Surficial	55	1,195	0.137	163.88	11.97	2.19	2.98	4.25	3.05
sf1b	1	Surficial	36	137	0.178	24.40	1.78	0.18	0.68	3.92	0.45
sf1c	1	Surficial	45	548	0.106	58.34	4.26	0.32	1.3	2.34	1.08
sf1d	1	Surficial	21	310	0.120	37.25	2.72	0.24	1.77	2.64	0.69
uc3a	3	Upper Chesapeake	1	22	0.963	21.19	1.55	21.19	21.19	21.19	0.39
uc3b	3	Upper Chesapeake	13	278	0.183	50.78	3.71	3.29	3.91	4.02	0.94
uc3c	3	Upper Chesapeake	12	222	0.110	24.49	1.79	0.99	2.04	2.43	0.46
lc5a	5	Lower Chesapeake	32	359	0.075	27.01	1.97	0.08	0.84	1.66	0.50
lc5b	5	Lower Chesapeake	5	64	0.216	13.83	1.01	0.65	2.77	4.76	0.26
pp7a	7	Piney Point	9	163	0.115	18.82	1.38	0.69	2.09	2.54	0.35
pp7b	7	Piney Point	13	239	0.067	16.04	1.17	0.13	1.23	1.48	0.30
pp7c	7	Piney Point	13	198	0.382	75.67	5.53	2.29	5.82	8.41	1.41
aq9a	9	Aquia	14	49	0.267	13.09	0.96	0.27	0.93	3.74	0.24
aq9b	9	Aquia	49	773	0.077	59.68	4.36	0.08	1.22	1.7	1.11
aq9c	9	Aquia	15	154	0.165	25.45	1.86	0.17	1.7	3.64	0.47
ml11a	11	Monmouth-Mount Laurel	26	220	0.057	12.64	0.92	0.06	0.49	1.26	0.23
ml11b	11	Monmouth-Mount Laurel	2	42	2.581	108.40	7.92	51.62	54.2	56.78	2.02
mw13a	13	Matawan	8	83	0.034	2.84	0.21	0.03	0.35	0.75	0.05
mw13b	13	Matawan	13	112	0.098	10.93	0.80	0.2	0.84	2.15	0.20
mw13c	13	Matawan	2	5	0.478	2.39	0.17	0.96	1.19	1.43	0.04
m15a	15	Magothy	22	379	0.360	136.54	9.98	1.44	6.21	10.45	2.54
m15b	15	Magothy	29	305	0.143	43.52	3.18	0.14	1.5	3.14	0.81
m15c	15	Magothy	27	499	0.162	80.63	5.89	0.48	2.99	3.55	1.50
pp17a	17	Potomac-Patapsco	17	257	0.474	121.94	8.91	2.37	7.17	15.18	2.27
pp17b	17	Potomac-Patapsco	29	238	0.103	24.59	1.80	0.21	0.85	2.27	0.46
pp17c	17	Potomac-Patapsco	55	842	0.053	44.31	3.24	0.21	0.81	1.16	0.82
pp17d	17	Potomac-Patapsco	52	741	0.051	37.84	2.76	0.05	0.73	1.12	0.70
pp19n	19	Potomac-Patuxent	10	116	0.747	86.62	6.33	1.49	8.66	16.43	1.61
pp19s	19	Potomac-Patuxent	19	318	0.080	25.45	1.86	0.16	1.34	1.76	0.47
Total	All	All	644	8,868		1,368.56	100.00	0.03	2.13	56.78	25.45

Table 5. Water-level and base flow flux observation weights by observation group for the model used in the groundwater assessment of the Northern Atlantic Coastal Plain aquifer system.—Continued

[--, not applicable]

Observation group	Model layer	Aquifer	Number of wells	Number of observation differences	Single difference weight	Sum of weights	Proportional group weight, in percent	Minimum well weight	Average well weight	Maximum well weight	Percentage of total observation difference weight
B. Differences in observations of water level, in feet											
sf1a_d	1	Surficial	55	1,179	0.303	356.87	26.08	4.84	6.49	9.08	18.50
sf1b_d	1	Surficial	36	117	0.461	53.93	3.94	0.46	1.50	10.14	2.80
sf1c_d	1	Surficial	45	525	0.499	261.94	19.14	1.50	5.82	10.98	13.58
sf1d_d	1	Surficial	21	303	0.264	79.87	5.84	0.26	3.80	5.80	4.14
uc3a_d	3	Upper Chesapeake	1	22	1.227	27.00	1.97	27.00	27.00	27.00	1.40
uc3b_d	3	Upper Chesapeake	13	278	1.092	303.56	22.18	19.65	23.35	24.02	15.74
uc3c_d	3	Upper Chesapeake	12	219	0.653	142.95	10.45	5.87	11.91	14.36	7.41
lc5a_d	5	Lower Chesapeake	32	348	0.227	78.94	5.77	0.23	2.47	4.99	4.09
lc5b_d	5	Lower Chesapeake	5	60	1.870	112.20	8.20	3.74	22.44	41.14	5.82
pp7a_d	7	Piney Point	9	160	1.023	163.73	11.96	6.14	18.19	22.51	8.49
pp7b_d	7	Piney Point	13	239	0.370	88.54	6.47	0.74	6.81	8.15	4.59
pp7c_d	7	Piney Point	13	194	0.689	133.73	9.77	3.45	10.29	15.17	6.93
aq9a_d	9	Aquia	14	46	0.640	29.45	2.15	0.64	2.10	8.32	1.53
aq9b_d	9	Aquia	49	759	0.222	168.25	12.29	0.22	3.43	4.88	8.72
aq9c_d	9	Aquia	15	148	1.252	185.32	13.54	1.25	12.35	27.55	9.61
ml11a_d	11	Monmouth-Mount Laurel	26	213	0.244	51.93	3.79	0.24	2.00	5.36	2.69
ml11b_d	11	Monmouth-Mount Laurel	2	41	8.966	367.62	26.86	170.36	183.81	197.26	19.06
mw13a_d	13	Matawan	8	81	0.192	15.54	1.14	0.19	1.94	4.22	0.81
mw13b_d	13	Matawan	13	109	0.473	51.58	3.77	0.95	3.97	10.41	2.67
mw13c_d	13	Matawan	2	5	0.920	4.60	0.34	1.84	2.30	2.76	0.24
m15a_d	15	Magothy	22	366	0.660	241.48	17.64	2.64	10.98	18.47	12.52
m15b_d	15	Magothy	29	298	0.235	70.04	5.12	0.24	2.42	5.17	3.63
m15c_d	15	Magothy	27	495	0.141	69.88	5.11	0.28	2.59	3.11	3.62
pp17a_d	17	Potomac-Patapsco	17	244	0.842	205.44	15.01	3.37	12.08	26.10	10.65
pp17b_d	17	Potomac-Patapsco	29	236	0.201	47.43	3.47	0.40	1.64	4.42	2.46
pp17c_d	17	Potomac-Patapsco	55	819	0.114	93.33	6.82	0.46	1.70	2.51	4.84
pp17d_d	17	Potomac-Patapsco	52	736	0.244	179.94	13.15	0.24	3.46	5.38	9.33
pp19n_d	19	Potomac-Patuxent	10	114	0.794	90.50	6.61	1.59	9.05	17.46	4.69
pp19s_d	19	Potomac-Patuxent	19	311	0.448	139.25	10.18	0.45	7.33	9.85	7.22
Total	All	All	644	8,665		3,814.86	278.75	0.19	5.92	197.26	70.95
C. Observations of base flow, in cubic feet per second											
q_nhd	--	--	122	122	0.364	44.47	23.02	0.02	0.36	2.19	0.83
q_nwis	--	--	31	568	0.260	148.74	76.98	0.37	4.80	50.40	2.76
Total	--	--	153	690	--	193.20	100.00	--	--	--	3.59

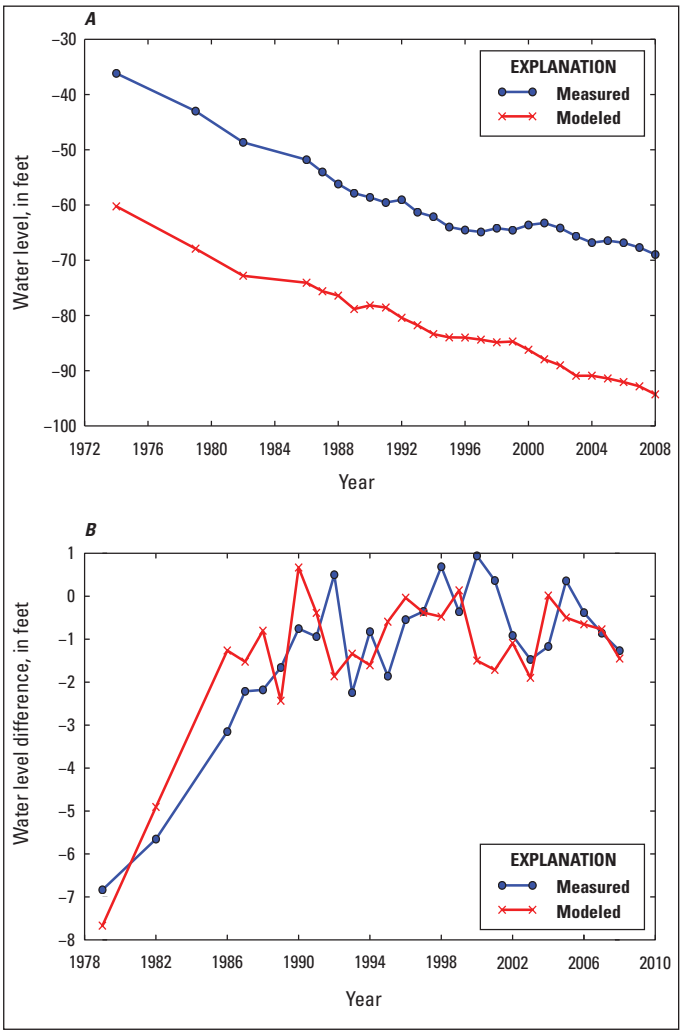

Figure 9. Comparison of *A*, measured and simulated water levels and *B*, the differences in measured and simulated water levels from 1974 to 2008 at observation well 365120076585101 in the Piney Point regional aquifer of the Northern Atlantic Coastal Plain aquifer system.

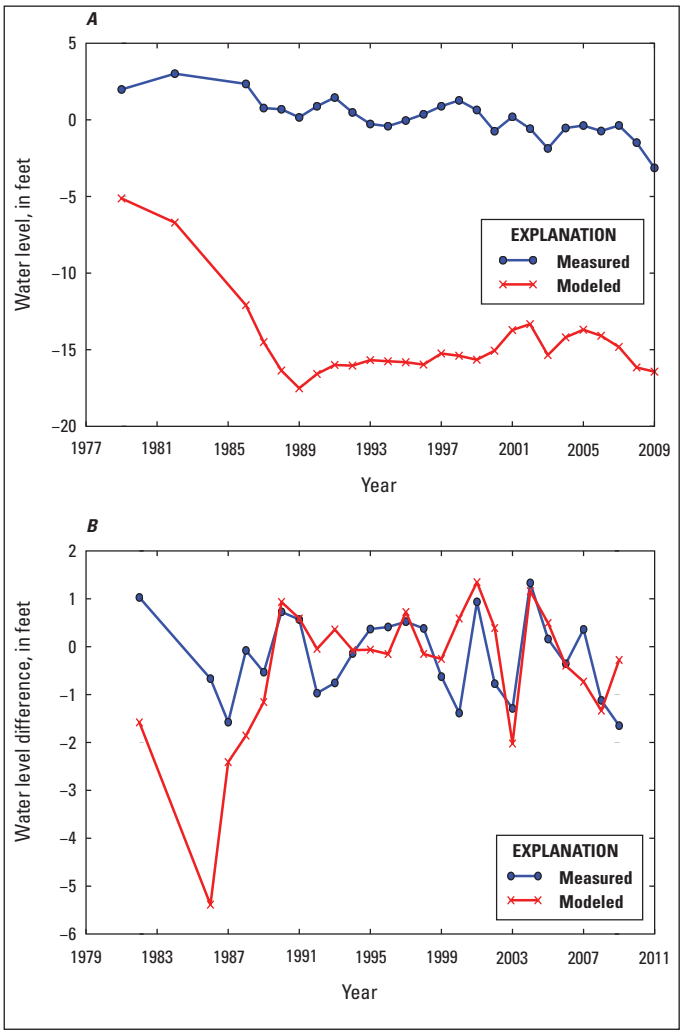

Figure 10. Comparison of *A*, measured and simulated water levels and *B*, the differences in measured and simulated water levels from 1978 to 2009 at observation well 384923076100601 in the Potomac-Patapsco regional aquifer of the Northern Atlantic Coastal Plain aquifer system.

Table 6. Final weights of water-level observations used in the model for the groundwater assessment of the Northern Atlantic Coastal Plain aquifer system.

Model layer	Aquifer	Number of wells	Number of observations	Sum of weights	Proportional aquifer weight	Minimum well weight	Average well weight	Maximum well weight	Average observation weight
1	Surficial	157	2,190	283.9	0.207	0.178	1.808	4.251	0.130
3	Upper Chesapeake	26	522	96.5	0.070	0.993	3.710	21.194	0.185
5	Lower Chesapeake	37	423	40.8	0.030	0.075	1.104	4.755	0.097
7	Piney Point	35	600	110.5	0.081	0.134	3.158	8.408	0.184
9	Aquia	78	976	98.2	0.072	0.077	1.259	3.739	0.101
11	Monmouth-Mount Laurel	28	262	121.0	0.088	0.057	4.323	56.783	0.462
13	Matawan	23	200	16.2	0.012	0.034	0.703	2.147	0.081
15	Magothy	78	1,183	260.7	0.190	0.143	3.342	10.447	0.220
17	Potomac-Patapsco	153	2,078	228.7	0.167	0.051	1.495	15.183	0.110
19	Potomac-Patuxent	29	434	112.1	0.082	0.160	3.864	16.427	0.258
Total		**644**	**8,868**	**1,368.6**	**1.000**				

Streamflow Observations

Streamflow (base flow) observations were divided into two sets of observation data, NHDPlus and NWIS. Both sets of observations represent calculated base flow conditions. Base flows were calculated using the USGS Groundwater Toolbox for hydrograph separation (Barlow and others, 2014) for each individual NWIS site, whereas baseflow indices available as attribute values in NHDPlus were applied to the NHDPlus sites to adjust average computed streamflows to base flows.

Average Base Flow From NHDPlus Streamflow Estimates

Average historical streamflow estimates from NHDPlus Version 1 (Bondelid and others, 2010) were used to generate base flow targets for model streams near discharge locations to coastal waters. The locations of the measurements were determined by identifying the approximate locations of high tide along the stream segments for each of the major watersheds (Titus and Wang, 2008). A flow estimate (average annual flow for the period of record) was taken from the selected downstream terminal stream segment for each of the major watersheds; flow into each watershed from outside the Coastal Plain region (beyond the active model area) was calculated as the sum of all upstream segments crossing the Fall Zone from outside the active model area. Subtracting Coastal Plain inflow from outflow for each of the stream networks yielded average annual streamflow generated within the Coastal Plain. Application of the NHDPlus base flow index for each stream resulted in an average annual base flow for the period of record for each of the terminal segments of the stream network at the point of discharge into coastal waters. These average values then were compared with the model-calculated average values from 1986 to 2008.

The published estimated base flow indices for selected NHDPlus streams average about 48 percent and range from a low value of 29 percent in Virginia to a high of more than 85 percent on Long Island. The calculated base flows are approximately equivalent to the total groundwater discharge to streams within each watershed. From 129 initial base flow targets at stream outflows, 7 measurements were given zero weight, leaving 122 measurements for use in history matching (fig. 13*A*). The removal of the seven sites was based on information about artificial structures and dams that have altered flow in these areas making them less suitable for simulation in the groundwater model. The initial weights assigned to the base flow targets were based on an assumed coefficient of variation of 10 percent. The weights employed in PEST corresponded to the inverse of standard deviation (Doherty, 2010). Coefficient of variation is expressed as:

$$cv = \frac{\sigma}{\overline{x}}, \tag{4}$$

where

σ is the standard deviation, and

$\overline{x}$ is the mean value (in this case, the flow).

For cv = 10 percent = 0.1:

$$\sigma = cv \times \overline{x} = 0.1 \times \overline{x} = \frac{\overline{x}}{10}. \tag{5}$$

The weight is as follows:

$$\frac{1}{\sigma} = \frac{1}{\frac{\overline{x}}{10}} = \frac{10}{\overline{x}}. \tag{6}$$

These weights were subjected to adjustment in the same way as the head groups to balance the objective function contributions.

The match of simulated to computed base flows for the NHDPlus average flows is generally good, with an average residual of about –8 cubic feet per second (ft^3/s) and an average absolute residual of about 21 ft^3/s. The minimum and maximum computed base flows for the NHDPlus average flows are about 3 and 422 ft^3/s, respectively. This match between model-simulated and computed base flows for the NHDPlus average flows can be displayed graphically to illustrate the distribution of the residuals (defined as modeled-calculated minus estimated; fig. 13*A*) and in map view to illustrate the spatial distribution of these residuals (fig. 11*L*).

NWIS Streamflow

In addition to the average base flow targets from the NHDPlus measurements, NWIS streamgage measurements provided transient base flow targets varying in time (U.S. Geological Survey, 2011). While the NHDPlus measurement locations were selected to capture the total streamflow and groundwater discharge to streams leaving the NACP aquifer system, NWIS streamflow observation locations were selected mostly for streams originating within the entire Coastal Plain region. This approach reduced the complication of subtracting out inflow from across the Fall Zone before computing base flow from total streamflow values, though this adjustment was required for the flows at a few of the streamgages. The selected NWIS streamflow measurements enabled history matching that included matching to a broad range of transient flow conditions across a variety of selected streams within the study area.

Initially, 59 NWIS streamgages were selected as targets for evaluation of base flow for inclusion into the model to augment the locations selected for the NHDPlus base flow estimates. During model construction, 28 of the streamgages were eliminated because local streamflow effects were discovered that were not accounted for in the NACP aquifer system groundwater model. For the remaining 31 streamgages selected for history matching (fig. 13*B*), in total, 568 flow measurements used were based on annual mean streamflow values reported by NWIS. As with head observations, flow measurements were given zero weight for years before 1986.

Table 7. Observation group residuals in the model used in the groundwater assessment of the Northern Atlantic Coastal Plain aquifer system.

[MAE, mean absolute error; RMSE, root mean square error; RMSE/range, root mean square error divided by range of residuals; --, not applicable; Y, Yes; N, No]

Observation group	Regional aquifer	Number of observations	Number of wells	Residuals				Standard deviation	MAE	RMSE	RMSE/range	Normally distributed
				Range	Minimum	Mean	Maximum					
A. Head observation residuals, in feet												
sf1a	Surficial	1,195	55	64.30	–28.16	1.44	36.14	10.93	7.72	11.02	0.17	Y
sf1b	Surficial	137	36	95.58	–74.61	–1.58	20.96	14.26	10.69	14.30	0.15	Y
sf1c	Surficial	548	45	61.70	–24.07	3.75	37.63	12.57	9.49	13.10	0.21	Y
sf1d	Surficial	310	21	87.79	–48.86	–0.45	38.93	16.15	12.10	16.13	0.18	Y
uc3a	Upper Chesapeake	22	1	15.55	–12.53	–1.80	3.02	3.92	2.60	4.23	0.27	Y
uc3b	Upper Chesapeake	278	13	40.08	–6.96	2.71	33.12	9.07	4.74	9.46	0.24	Y
uc3c	Upper Chesapeake	222	12	57.12	–26.42	12.04	30.70	13.25	15.76	17.88	0.31	Y
lc5a	Lower Chesapeake	359	32	98.49	–57.65	–6.36	40.84	20.02	17.10	20.98	0.21	Y
lc5b	Lower Chesapeake	64	5	33.56	–13.62	–0.09	19.94	9.59	8.13	9.51	0.28	Y
pp7a	Piney Point	163	9	69.96	–42.04	–2.98	27.92	16.02	12.35	16.24	0.23	Y
pp7b	Piney Point	239	13	139.80	–86.27	4.80	53.52	24.68	19.63	25.10	0.18	Y
pp7c	Piney Point	198	13	47.25	–35.19	–0.52	12.06	9.61	5.93	9.60	0.20	Y
aq9a	Aquia	49	14	43.57	–31.91	–14.08	11.66	10.10	16.14	17.26	0.40	Y
aq9b	Aquia	773	49	88.29	–54.86	–4.05	33.43	14.30	11.20	14.85	0.17	Y
aq9c	Aquia	154	15	43.26	–29.19	–2.68	14.07	7.52	6.02	7.96	0.18	Y
ml11a	Monmouth-Mount Laurel	220	26	170.99	–124.12	–2.31	46.87	32.11	23.00	32.12	0.19	Y
ml11b	Monmouth-Mount Laurel	42	2	6.32	–2.69	1.07	3.63	1.92	1.86	2.17	0.34	Y
mw13a	Matawan	83	8	142.62	–135.46	–44.13	7.17	36.07	45.08	56.85	0.40	Y
mw13b	Matawan	112	13	46.58	–3.27	15.65	43.31	14.36	16.02	21.20	0.46	Y
mw13c	Matawan	5	2	19.50	–17.17	–8.75	2.33	10.01	10.46	12.52	0.64	Y
m15a	Magothy	379	22	45.63	–17.61	0.57	28.02	7.00	4.85	7.01	0.15	Y
m15b	Magothy	305	29	71.30	–43.15	–5.98	28.15	15.07	12.75	16.19	0.23	Y
m15c	Magothy	499	27	42.46	–23.14	0.24	19.32	7.28	5.63	7.28	0.17	Y
pp17a	Potomac-Patapsco	257	17	45.74	–33.19	0.83	12.55	5.98	4.30	6.02	0.13	Y
pp17b	Potomac-Patapsco	238	29	107.57	–58.89	–10.59	48.68	15.68	15.03	18.89	0.18	Y
pp17c	Potomac-Patapsco	842	55	190.99	–157.16	–16.92	33.84	30.87	22.57	35.19	0.18	Y
pp17d	Potomac-Patapsco	741	52	189.62	–88.07	7.86	101.55	23.88	18.33	25.13	0.13	Y
pp19n	Potomac-Patuxent	116	10	31.37	–23.20	–0.07	8.17	4.74	3.10	4.72	0.15	Y
pp19s	Potomac-Patuxent	318	19	74.30	–49.84	–2.77	24.46	13.38	9.87	13.64	0.18	Y

Table 7. Observation group residuals in the model used in the groundwater assessment of the Northern Atlantic Coastal Plain aquifer system.—Continued

[MAE, mean absolute error; RMSE, root mean square error; RMSE/range, root mean square error divided by range of residuals; --, not applicable; Y, Yes; N, No]

Observation group	Regional aquifer	Number of observations	Number of wells	Residuals				Standard deviation	MAE	RMSE	RMSE/range	Normally distributed
				Range	Minimum	Mean	Maximum					
B. Difference of head observation residuals, in feet												
sf1a_d	Surficial	1,179	55	18.18	–5.91	0.19	12.27	1.70	1.30	1.71	0.09	Y
sf1b_d	Surficial	117	36	33.09	–16.45	–0.10	16.64	3.97	2.31	3.95	0.12	Y
sf1c_d	Surficial	525	45	18.94	–7.75	0.06	11.19	1.83	1.30	1.83	0.10	Y
sf1d_d	Surficial	303	21	42.40	–21.13	0.00	21.27	3.82	2.22	3.81	0.09	Y
uc3a_d	Upper Chesapeake	22	1	22.95	–13.55	0.23	9.40	4.32	3.01	4.23	0.18	Y
uc3b_d	Upper Chesapeake	278	13	9.49	–6.83	–0.04	2.66	1.02	0.70	1.02	0.11	Y
uc3c_d	Upper Chesapeake	219	12	17.02	–9.68	–0.08	7.34	2.26	1.45	2.25	0.13	Y
lc5a_d	Lower Chesapeake	348	32	39.71	–21.67	–0.11	18.05	2.87	1.64	2.87	0.07	Y
lc5b_d	Lower Chesapeake	60	5	9.73	–4.10	–0.02	5.63	1.60	0.97	1.59	0.16	Y
pp7a_d	Piney Point	160	9	14.90	–11.79	–0.29	3.11	1.94	1.09	1.96	0.13	Y
pp7b_d	Piney Point	239	13	61.54	–51.22	–0.75	10.33	4.64	2.24	4.69	0.08	Y
pp7c_d	Piney Point	194	13	40.88	–22.68	–0.22	18.21	2.88	1.27	2.88	0.07	Y
aq9a_d	Aquia	46	14	26.98	–9.90	–0.47	17.08	4.68	3.32	4.65	0.17	Y
aq9b_d	Aquia	759	49	87.50	–43.19	–0.45	44.31	4.22	2.13	4.24	0.05	Y
aq9c_d	Aquia	148	15	15.45	–5.68	–0.06	9.77	1.61	1.00	1.61	0.10	Y
ml11a_d	Monmouth-Mount Laurel	213	26	48.83	–12.04	0.88	36.79	5.73	3.24	5.78	0.12	Y
ml11b_d	Monmouth-Mount Laurel	41	2	1.48	–1.02	–0.20	0.45	0.32	0.28	0.37	0.25	N
mw13a_d	Matawan	81	8	100.31	–43.98	3.74	56.33	10.00	5.63	10.62	0.11	Y
mw13b_d	Matawan	109	13	15.83	–8.08	–0.09	7.75	2.77	1.90	2.76	0.17	Y
mw13c_d	Matawan	5	2	3.24	–2.86	–1.62	0.38	1.50	1.77	2.10	0.65	N
m15a_d	Magothy	366	22	16.28	–8.67	0.24	7.60	1.79	1.26	1.80	0.11	Y
m15b_d	Magothy	298	29	22.89	–9.81	0.29	13.08	2.84	1.82	2.85	0.12	Y
m15c_d	Magothy	495	27	38.73	–20.37	0.01	18.36	3.17	1.97	3.17	0.08	Y
pp17a_d	Potomac-Patapsco	244	17	20.05	–10.71	0.06	9.34	1.95	1.26	1.95	0.10	Y
pp17b_d	Potomac-Patapsco	236	29	83.59	–30.53	1.07	53.05	7.68	3.91	7.74	0.09	Y
pp17c_d	Potomac-Patapsco	819	55	122.89	–78.10	–0.57	44.79	6.22	2.78	6.24	0.05	Y
pp17d_d	Potomac-Patapsco	736	52	113.50	–30.97	0.54	82.53	4.55	1.98	4.58	0.04	Y
pp19n_d	Potomac-Patuxent	114	10	38.06	–21.87	0.51	16.19	3.85	2.08	3.87	0.10	Y
pp19s_d	Potomac-Patuxent	311	19	62.68	–33.88	–0.16	28.80	4.36	2.01	4.35	0.07	Y
C. Base flow observation residuals, in cubic feet per second												
q_nhd	--	122	122	421.93	–249.68	–7.72	172.26	40.01	21.41	40.59	0.10	Y
q_nwis	--	248	31	1,002.37	–157.45	9.83	844.92	70.99	34.05	71.60	0.07	Y

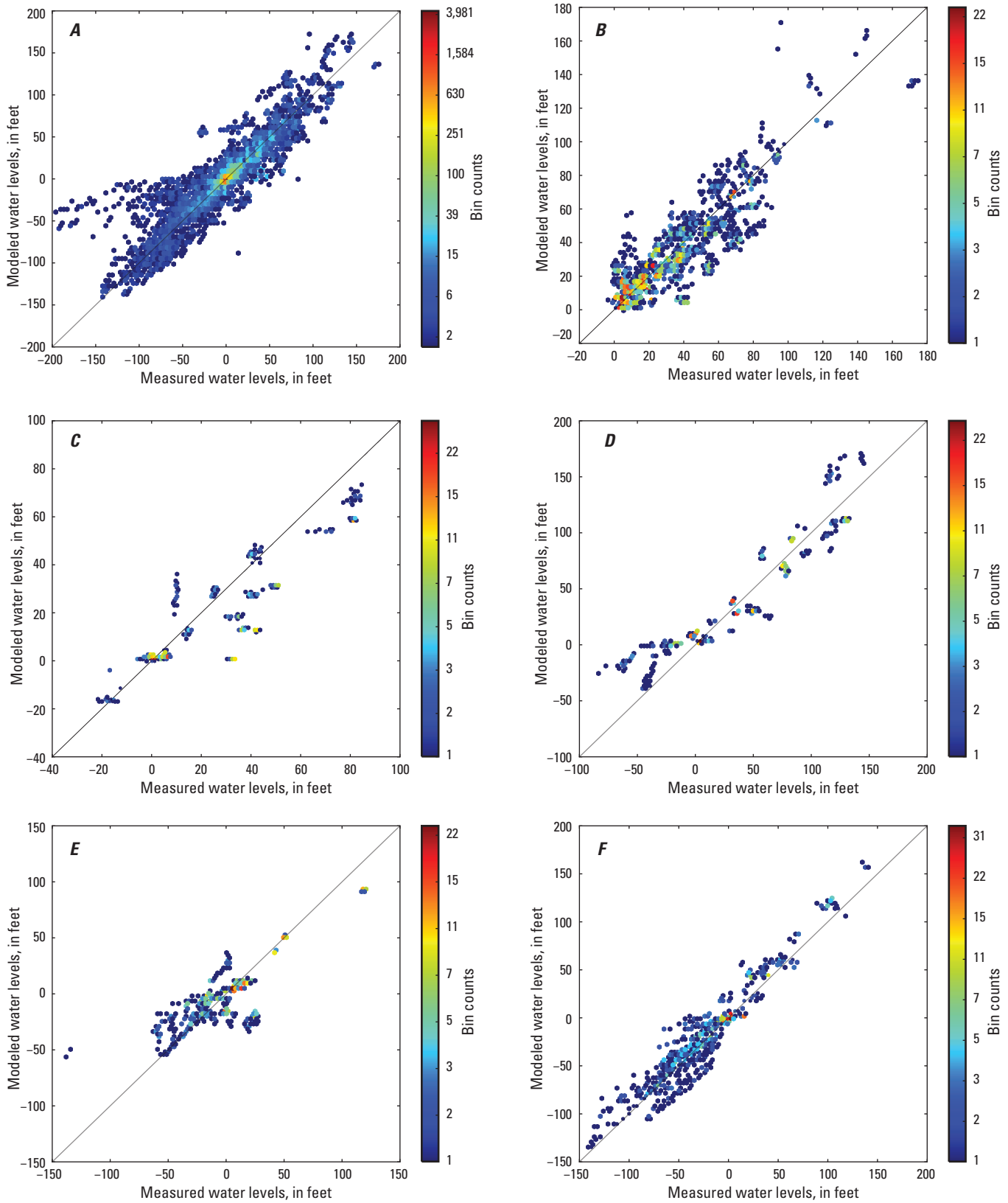

Figure 11. Hexbin plots of goodness of fit of measured and model-calculated water levels for *A*, the Northern Atlantic Coastal Plain aquifer system by aquifer and the *B*, surficial, *C*, Upper Chesapeake, *D*, Lower Chesapeake, *E*, Piney Point, *F*, Aquia, *G*, Monmouth-Mount Laurel, *H*, Matawan, *I*, Magothy, *J*, Potomac-Patapsco, and *K*, Potomac-Patuxent regional aquifers and for model-calculated base flows and base flow computations based on data from *L*, NHDPlus and *M*, the U.S. Geological Survey National Water Information System. All water levels are in units of feet relative to NGVD 29.

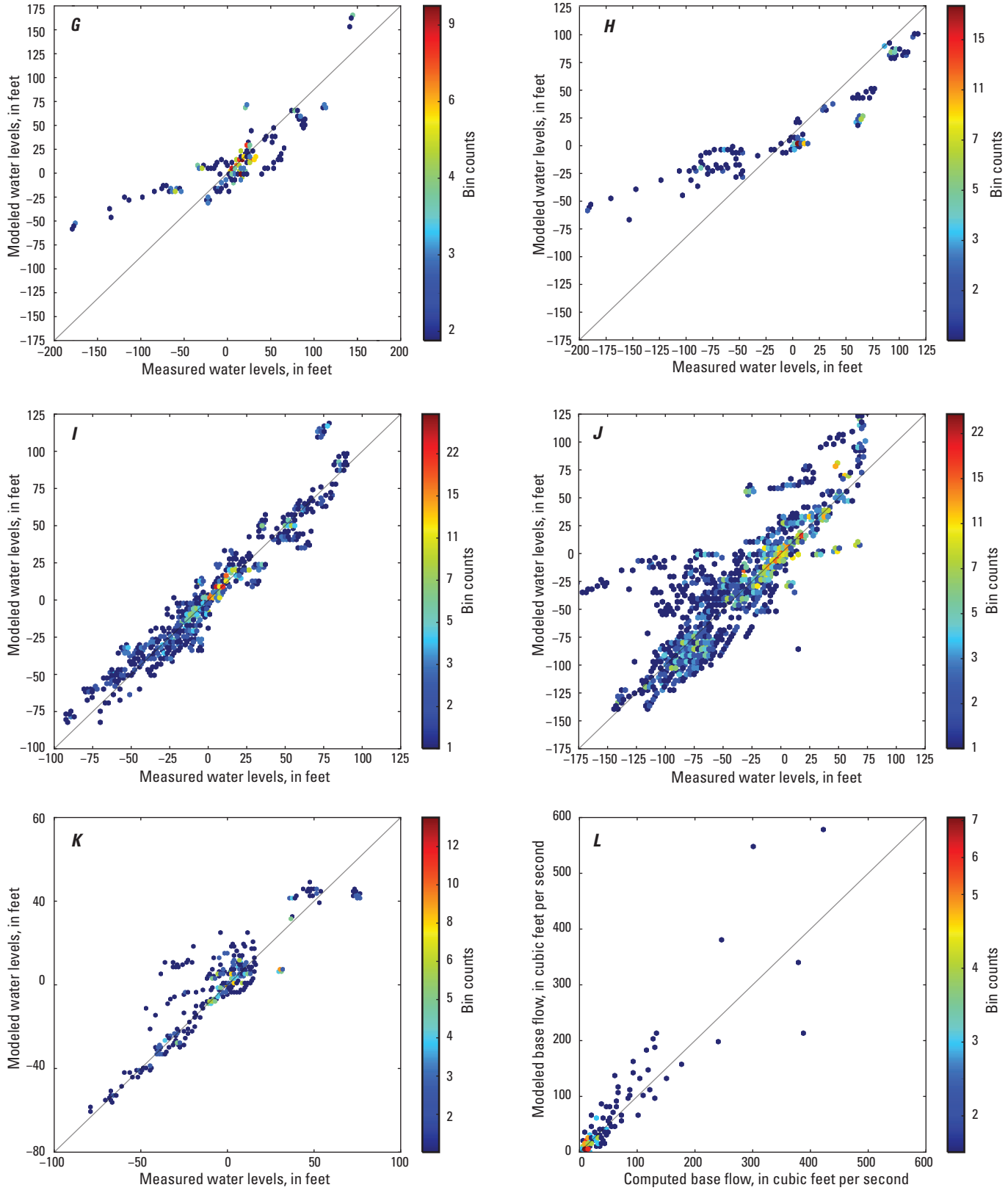

Figure 11. Hexbin plots of goodness of fit of measured and model-calculated water levels for *A*, the Northern Atlantic Coastal Plain aquifer system by aquifer and the *B*, surficial, *C*, Upper Chesapeake, *D*, Lower Chesapeake, *E*, Piney Point, *F*, Aquia, *G*, Monmouth-Mount Laurel, *H*, Matawan, *I*, Magothy, *J*, Potomac-Patapsco, and *K*, Potomac-Patuxent regional aquifers and for model-calculated base flows and base flow computations based on data from *L*, NHDPlus and *M*, the U.S. Geological Survey National Water Information System. All water levels are in units of feet relative to NGVD 29.—Continued

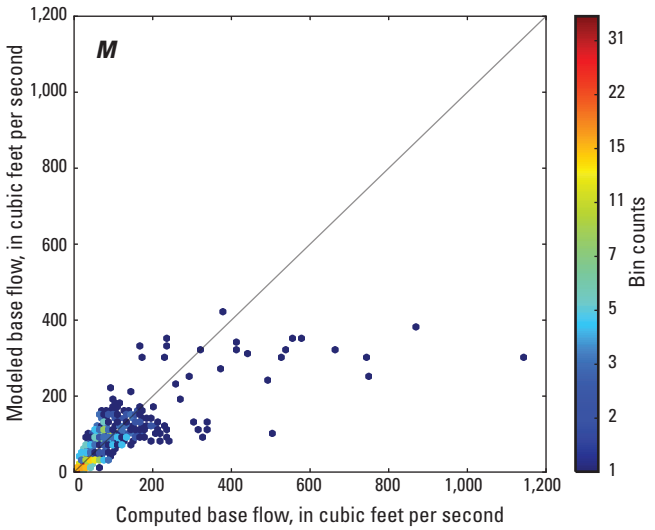

Figure 11. Hexbin plots of goodness of fit of measured and model-calculated water levels for *A*, the Northern Atlantic Coastal Plain aquifer system by aquifer and the *B*, surficial, *C*, Upper Chesapeake, *D*, Lower Chesapeake, *E*, Piney Point, *F*, Aquia, *G*, Monmouth-Mount Laurel, *H*, Matawan, *I*, Magothy, *J*, Potomac-Patapsco, and *K*, Potomac-Patuxent regional aquifers and for model-calculated base flows and base flow computations based on data from *L*, NHDPlus and *M*, the U.S. Geological Survey National Water Information System. All water levels are in units of feet relative to NGVD 29.—Continued

Base flow estimates for direct comparison with the model were computed from flow measurements with the use of the USGS Groundwater Toolbox for hydrograph separation (Barlow and others, 2014). Calculated mean base flow indices for selected NWIS streamgages average about 69 percent and range from a minimum of about 23 percent for a streamgage in Virginia to a maximum of about 95 percent for a streamgage on Long Island. The same weighting strategy that was used for the NHDPlus flow observations was applied to the NWIS observations.

The match of simulated to computed base flows is satisfactory for the NWIS time-series flows (fig. 11*M*), with an average residual of about 10 ft^3/s and an average absolute residual of about 34 ft^3/s. The minimum and maximum NWIS computed base flows are about 2 and 1,143 ft^3/s, respectively. This graphic accounting of the residuals illustrates the poor fit of the simulated flows to very high observed values. This may be because in periods of high flows, computed base flow indices for streams may no longer be valid, and application of base flow indices to the annual average flow values may produce anomalously high measured flow values that cannot be matched by simulated base flow. About 10 percent of the streamgages accounted for the largest residuals expressed as undersimulated flow. However, on balance, the overall match to observed flux targets appears to adequately constrain the water balance for the purposes of a regional modeling analysis.

Sensitivity and Identifiability

In the parameter estimation process, the gradient of observation values due to changes in parameters is used to define the magnitude and directions of changes in candidate parameter values from iteration to iteration. The Jacobian matrix is a matrix of sensitivity values relating each observation to each parameter. Sensitivity is defined as:

$$\frac{\partial y_i}{\partial p_j} \cong \frac{g\left(p_j + \Delta p\right) - g\left(p_j\right)}{\Delta p}, \tag{7}$$

where

i is a dummy variable in n number of observations (1, 2, …, n),

j is a dummy variable in n number of parameters (1, 2, …, n}, and

Δp is a small increment in parameter value.

The result of evaluating this equation for all combinations of parameters and observations is the Jacobian matrix X of number of observations by number of parameters. Beyond use in the parameter estimation algorithm, sensitivity can provide insight into which parameters have the greatest effect on forecasts made by the model. In fact, this can be considered as one metric of parameter importance. A challenge is encountered in that parameters are often correlated with one another, so sensitivity can be misleading when thought of as parameter importance. Correlation is evaluated in pairs of parameters; therefore with thousands of parameters, it is impractical to deconvolve sensitivity from correlation. Identifiability addresses this issue because it is based on SVD, which splits information content among correlated parameters algorithmically.

It is also possible to calculate identifiability by using SVD for parameter estimation, (Doherty and Hunt, 2009). Identifiability is a qualitative metric that indicates how much information from the observations (taken as a whole set) is projected onto the parameters in the history-matching process. Based on a singular value cutoff, the identifiability value calculates the projection of information from observations onto the calibration space. The remaining information is projected onto the null space, meaning parameter values can change potentially by large amounts without affecting the model outputs of interest.

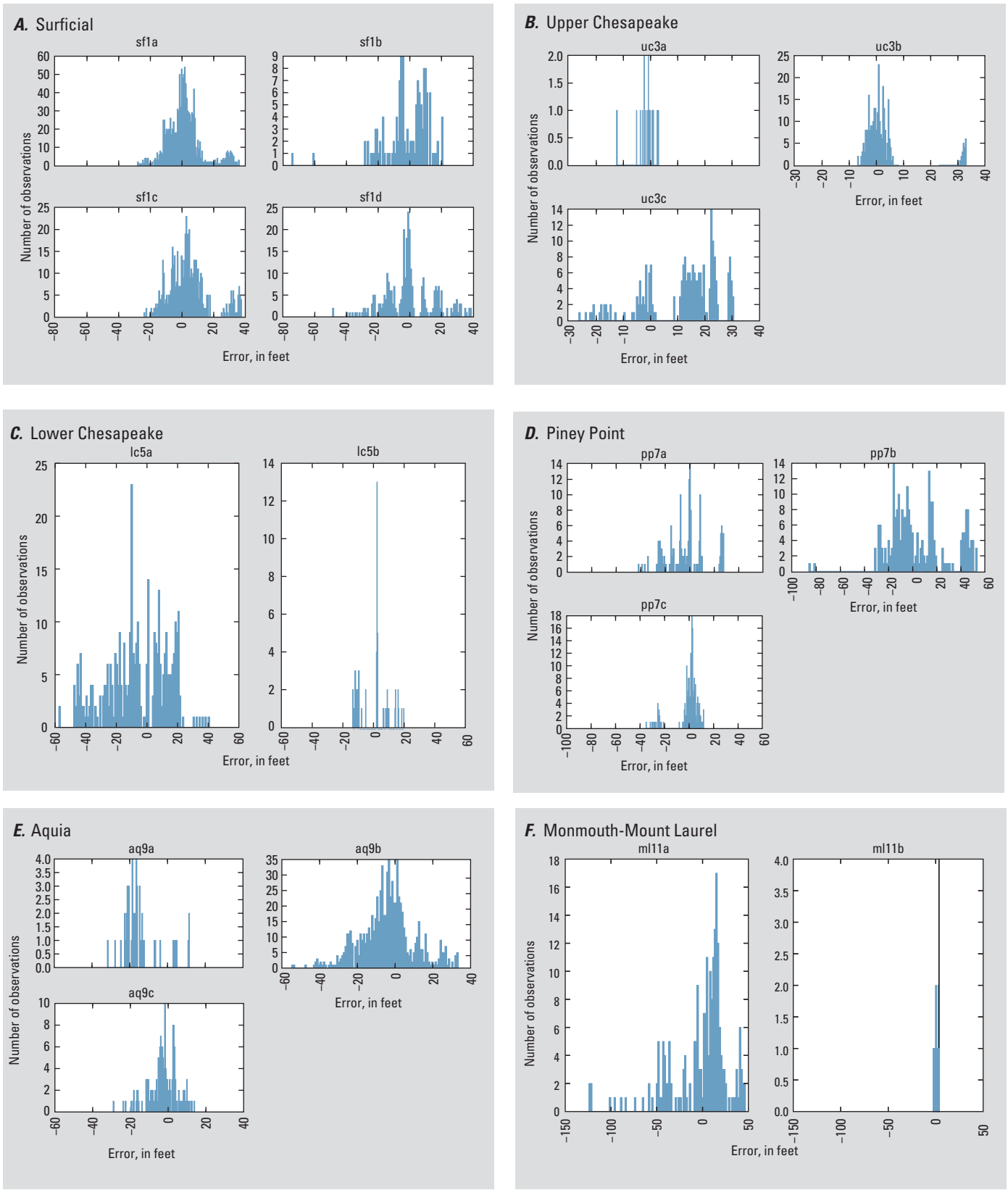

Figure 12. Histogram plots of goodness of fit of measured and model-calculated water levels for *A*, the surficial, *B*, Upper Chesapeake, *C*, Lower Chesapeake, *D*, Piney Point, *E*, Aquia, *F*, Monmouth-Mount Laurel, *G*, Matawan, *H*, Magothy, *I*, Potomac-Patapsco, and *J*, Potomac-Patuxent regional aquifers.

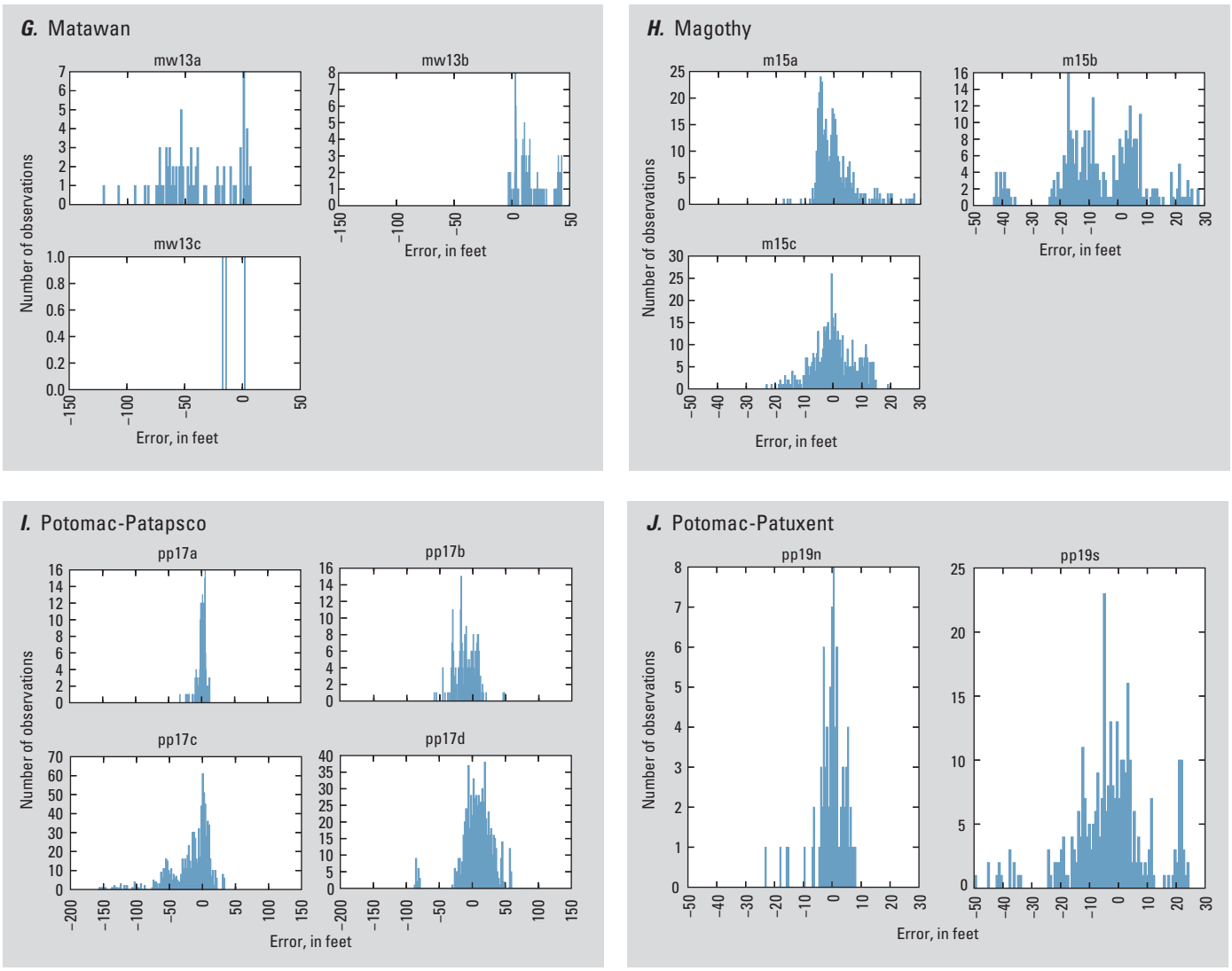

Figure 12. Histogram plots of goodness of fit of measured and model-calculated water levels for *A*, the surficial, *B*, Upper Chesapeake, *C*, Lower Chesapeake, *D*, Piney Point, *E*, Aquia, *F*, Monmouth-Mount Laurel, *G*, Matawan, *H*, Magothy, *I*, Potomac-Patapsco, and *J*, Potomac-Patuxent regional aquifers.—Continued

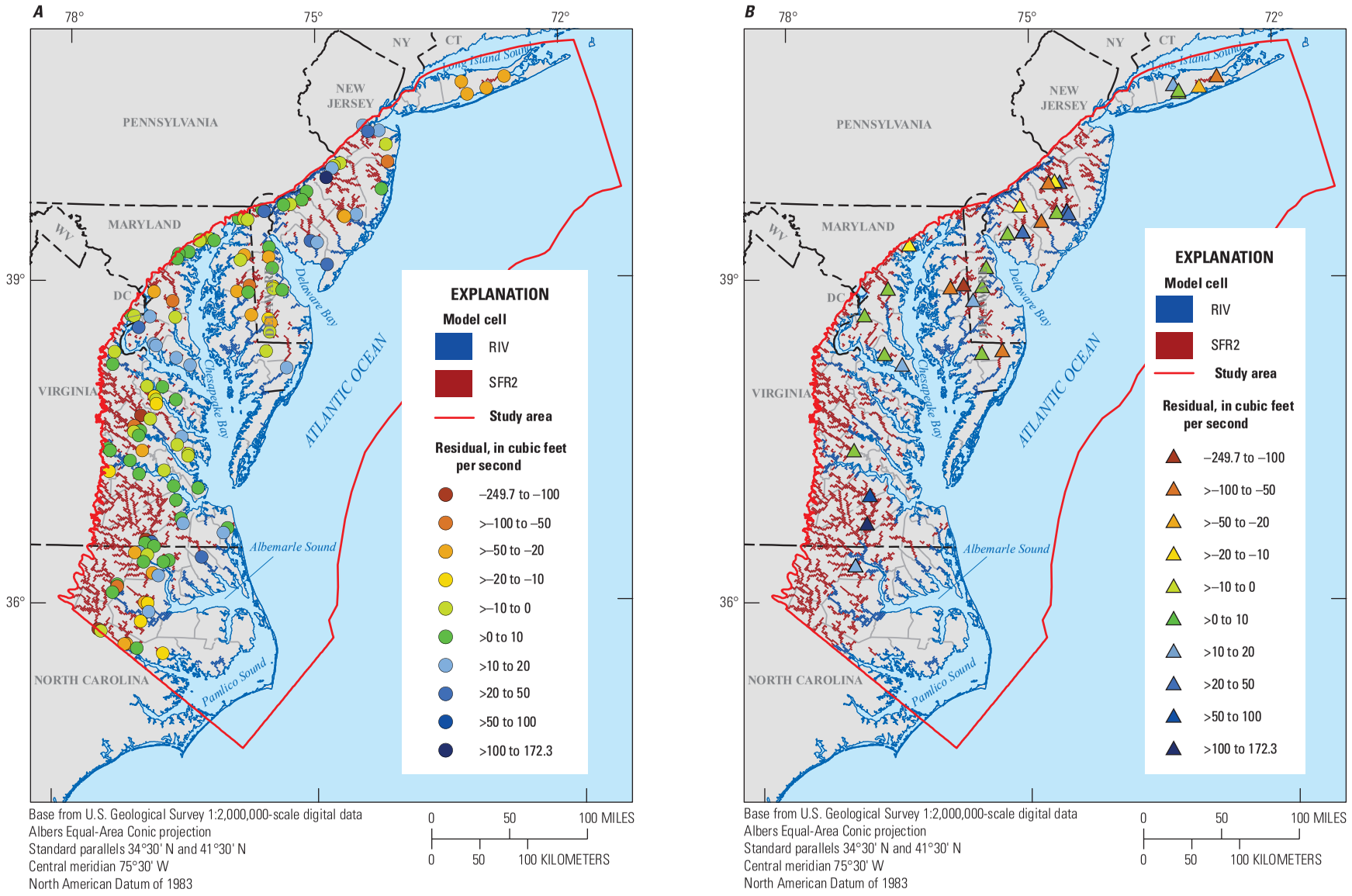

Figure 13. Base flow observation locations and residuals for *A*, NHDPlus and *B*, U.S. Geological Survey National Water Information System (NWIS) monitoring sites in the Northern Atlantic Coastal Plain aquifer system. RIV and SFR2 cells are the locations of tidal and nontidal rivers simulated in model. >, greater than.

Parameters with high identifiability are interpreted to be well-informed by the observations, whereas parameters with low identifiability are interpreted to be ill-informed by the observations and are generally held relatively constant in the history-matching process. Identifiability values are normalized to a maximum value of 1.0. The overall height of each bar indicates its identifiability on a normalized scale between 0.0 (parameter is not informed by the observations) and 1.0 (parameter is fully informed by the observations). For the purposes of this report, only the parameters with identifiability values greater than 0.7 are considered (fig. 14).

By definition, if all singular values are considered, all identifiability values will be equal to 1.0. The identifiability value quantifies the projection of observation information onto the solution space of the parameters as defined by an SVD cutoff. As more singular values are considered to be part of the solution space, fewer are in the null space, and the amount of projection onto solution space increases. The SVD cutoff is 250, which is the number of SVD analysis superparameters used in this model. In addition to the 250 singular value cutoff, a stability criterion was used to enforce a threshold on how many of those superparameters were considered part of the solution space. On each bar of the identifiability graph (fig. 14), the contribution to identifiability due to each singular value is displayed, separated by black lines. Areas shaded in colors on the warm end of the color spectrum (hot colors) indicate identifiability attributable to most informative singular values (for example, 1, 2, and so on), whereas areas shaded in colors on the cool end of the color spectrum (cool colors) indicate identifiability attributable to the least informative singular values (for example, 248, 249, and 250). This spectrum is displayed to highlight that no particular singular value cutoff is the perfect definition of separating the solution space from the null space, but bars that are made up almost entirely of hot colors can be qualitatively interpreted to have overall higher identifiability than those containing cool colors.

Identifiability is only a qualitative metric and should not be overinterpreted, but it can provide some insight into important model behavior. In a qualitative sense, parameters with high identifiability can be interpreted as important controls on model behavior. The two parameters with the highest identifiability are ghbcond32 and sspss18_8 (fig. 14).

Parameter ghbcond32 controls the lateral exchange of water at the boundary between freshwater and saltwater in model layer 3 in the vicinity of the impact crater in southern Virginia (fig. 7*C*, in back of report). The high identifiability value assigned to this parameter indicates that the effect of the impact crater on groundwater flow along this boundary is an important process in the model.

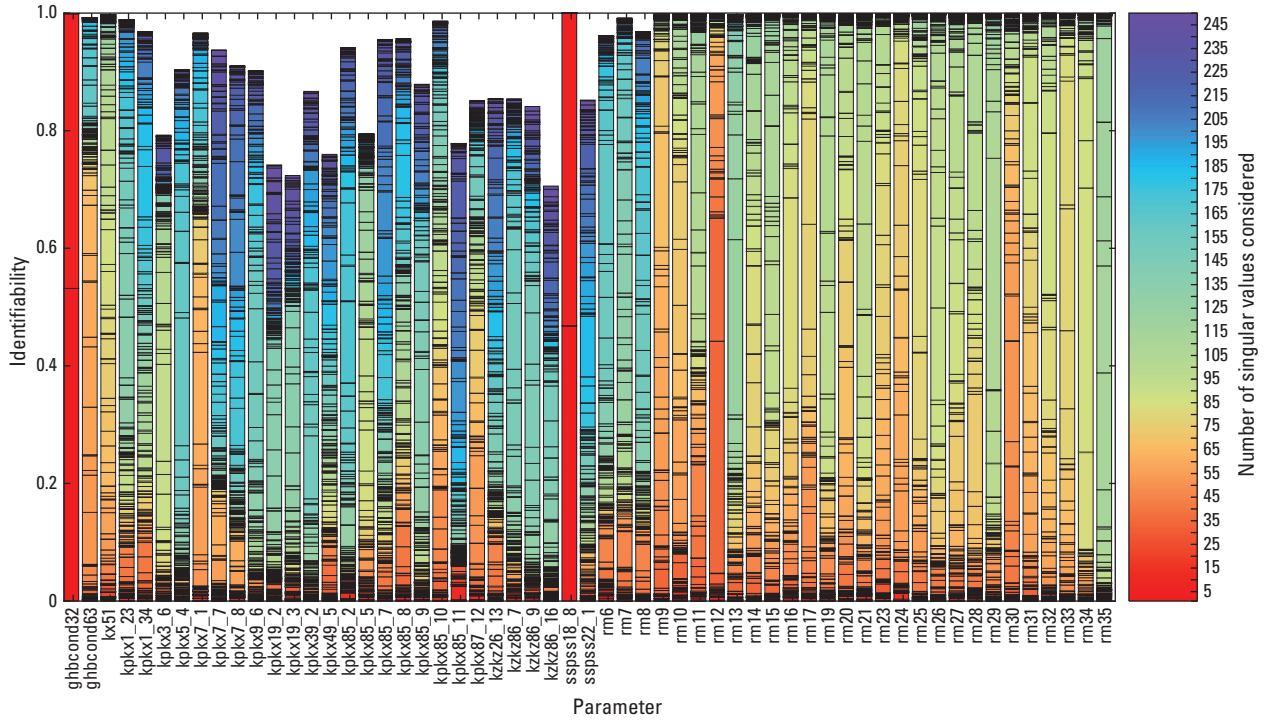

Figure 14. Identifiability of all parameters with values greater than 0.7 used in the assessment of groundwater in the Northern Atlantic Coastal Plain aquifer system.

Parameter sspss18_8 is a specific storage pilot point in the confining unit represented by layer 18. This storage value affects whether the confining unit behaves as such or allows more water to convey between the aquifers above and below it. The pilot point sspss18_8 is near the Fall Zone in an area where this confining unit may be less continuous than in others along the Fall Zone (fig. 7*R*, in back of report) and, therefore, have more variability in hydraulic properties over short distances than farther downdip toward the coast. Several additional hydraulic conductivity pilot points (both horizontal and vertical) also have high identifiability, in particular in zones along the Fall Zone, which controls the entry of water into the system through all layers and is an important control on the water balance; parameter sspss18_8 has the highest identifiability among the pilot points.

The horizontal hydraulic conductivity in the zone represented by parameter kx51 also has relatively high identifiability (fig. 14). This zone (zone 51) encompasses a large area between the Fall Zone and the sea in layer 1 (fig. 7*A*, in back of report) and, therefore, may influence the ocean boundary condition in the upper layers of the model.

Finally, all recharge multipliers on stress periods that were not held constant show relatively high identifiability (fig. 14, parameters with prefix "rm" followed by the number of the stress period). Recharge is a vital component to the water balance and is expected to be an important process in the model. In particular, parameter rm12—the recharge multiplier for stress period 12—shows high identifiability. Stress period 12 (the last in the historical period, table 2) represents a transition between long stress periods in the historical period and short stress periods from 1986 to 2008; the stresses represented in this stress period are averages of the subsequent periods (stress periods 13 to 35) and not representative of the actual conditions for stress period 12 (1981–1985). As a result, the recharge multiplier is important both in accommodating the uncertainty of the water balance in that time and in setting up conditions for the later in the simulations. Parameter rm30 also stands out as more identifiable and, in this case, is due to the corresponding year (2003) experiencing high recharge. Adjustment to that extreme condition can continue to influence results in subsequent stress periods.

Model Limitations

The use of numerical models to simulate regional groundwater flow systems such as the NACP aquifer system has inherent limitations; however, a proper model design to address scale-appropriate questions can help minimize these limitations. Assumptions made regarding model-boundary conditions can affect model results, and therefore, an understanding of these assumptions and their potential influence on model results should be considered.

Structural error is associated with issues in model design that can contribute to differences between simulated and actual hydrologic conditions. One component of structural error relates to model discretization. Models represent a hydrologic system as a series of discrete spatial units, throughout each of which intrinsic properties and stresses are uniform. The use of a discretized model to represent a hydrologic system introduces some limitations, especially if model discretization is much larger than the hydrologic features being simulated. These limitations can be reduced by designing models with the appropriate discretization for the hydrologic system; however, in the case of regional aquifer systems such the NACP aquifer system, this will always be a limitation for local-scale analyses.

The 27,000-mi^2 NACP aquifer system was subdivided in this analysis into 125,000 cells of 1-mi×1-mi horizontal grid spacing vertically distributed over the 19 principal aquifers and confining units. Limitations associated with this model discretization scheme include vertical layering of framework, locations of pumping stresses and observation wells, time-averaging of stresses and time-varying observations, and representation of surface-water features.

The vertical layering was based on the hydrostratigraphic surfaces of the 19 principal units in the NACP aquifer system. Although, this layering scheme may be appropriate for a regional assessment, it presented challenges for matching the time histories of observation measurements in discrete vertical zones that were lumped into principal aquifers represented at the regional scale. Often times, this averaging of simulated water levels at the principal aquifer scale resulted in an underrepresenting of the water-level decreases observed in the measured data.

Additionally, the vertical discretization affected the assignment of pumping stresses throughout the flow system, resulting in the same limitation as that described for the water-level observations. Pumping from subzones within a given regional aquifer could not be accounted for when each regional aquifer and confining unit is represented as a single model layer. This limitation resulted in averaging the simulated stress over the entire model layer rather than for only the discrete zone from which the water was actually being withdrawn; the averaging of the simulated stress over the entire model allowed for more release from storage than would otherwise be available, resulting in an underprediction of the simulated response to the pumping stress. This model limitation also has a similar effect in the horizontal direction, particularly when the pumping stress is averaged over the entire 1-mi×1-mi grid spacing and the observation points used for calibration are in close proximity to the pumping well.

The discretization of time can also limit the ability of the model to adequately represent time-varying pumping and recharge stresses and the time-varying observations used in the history matching of measured and simulated water levels and flows. Transient models are discretized into a series of discrete units of time (stress periods), during each of which hydrologic stresses are constant. Therefore, if stresses or observations vary at a time-scale less than the simulated stress periods, then discretized time may introduce additional sources of model

inaccuracy; these inaccuracies are often unavoidable in the large models developed for regional-scale analyses.

In addition to these challenges, the level of model discretization required for regional-scale analyses presents an additional challenge that can limit the accuracy of model predictions: the quality and availability of basic hydrologic data in the study area. The primary hydrologic data types include water use, monitoring, and hydrogeologic information. Often, issues with these data are magnified in models used for regional studies mainly because of the scale of these efforts and the time needed to synthesize and compile the necessary information. The inability to resolve the inevitable data issues can result in limitations in model accuracy, particularly at the subregional scale.

The groundwater withdrawal information synthesized for the analysis in this report and Masterson and others (2016) was derived primarily from existing databases provided typically by State and local water resource managers throughout the study area. Often, this information is adequate to support countywide compilations, such as those conducted by the NWUIP, but the level of detail needed to adequately represent these stresses in a numerical model requires detailed information on pumping rates and the spatial and vertical location of the individual wells. When such information is incomplete, suspect, or unattainable, the accuracy of the numerical simulations of the groundwater system is affected accordingly.

Similar concerns can be raised for the monitoring or observation data of water levels and streamflows. These data are stored in the USGS NWIS database, and the accuracy of the measurements and the reported spatial and vertical locations of these observations is critical to understanding how the physical system is responding to hydrologic stresses, which is critical to determining how well the numerical representation of system matches reality. Therefore, the importance of basic water-use and monitoring data of high quality cannot be overstated for these availability studies.

Hydrogeologic information such as aquifer-test results, lithologic borings, geophysical logs, and the hydrostratigraphic surfaces that are developed from this information also are necessary to understanding the distribution and movement of groundwater flow in the subsurface. The analysis of the NACP aquifer system relied heavily on the hydrostratigraphic surfaces that were developed initially as part of the previous regional assessment and subsequently updated locally by more site-specific studies. This information is often difficult and expensive to obtain but is key to developing a conceptual understanding of the aquifer framework that is then applied to the numerical model used in groundwater availability assessments. Missing or incomplete hydrogeologic information can result in greater uncertainty in the accuracy of the study results.

The representation of the boundary condition in the model also can limit the accuracy of model predictions in areas where boundaries may exert control over the flow system response to changes in stresses. The three boundary conditions to consider in the NACP aquifer system model were surface-water features, the interface between freshwater and saltwater, and the southern no-flow boundary.

Representation of surface-water features at the regional scale can present challenges for matching flows at individual streamgages in the study area. The Strahler third-order stream network was selected for the NACP aquifer system model because it provided a reasonably well distributed coverage of surface water throughout the study area without creating an intractable problem of attempting to represent every surface-water feature in the system. The limitation to this approach is that locally simulated water levels may rise above land surface, particularly in the headwaters of the streams where the minor tributaries that route flow to the larger rivers are not accounted for in the analysis.

The interface between the freshwater and saltwater systems was represented in this analysis as a static interface not subject to natural or anthropogenic stresses. At the regional scale, this assumption may be adequate, but locally, areas such as Long Island, N.Y., Atlantic City, N.J., and Virginia Beach, Va., have experienced the effects of saltwater intrusion from overpumping near this interface. A numerical code such as SEAWAT (Guo and Langevin, 2002) or the Seawater Intrusion (SWI2) package for MODFLOW (Bakker and others, 2013) would be more appropriate to address these local-scale issues; however, such an analysis was beyond the scope of this regional analysis.

The third boundary condition issue that arose in this analysis was the no-flow boundary condition assigned along the southern boundary of the model. The southern extent of the NACP aquifer system study area was selected to be far enough to the south so as to be well beyond the area of interest (from Long Island south to Virginia) to not affect simulation results. For this analysis, a no-flow condition was used for this boundary, but a sensitivity analysis was conducted to determine how simulation results can be affected if a specified-head boundary was used instead. The difference was as much as 5 percent of the total drawdowns in southern Virginia and much greater closer to the boundary in northeastern North Carolina, indicating that the uncertainty in simulation results increases south of southern Virginia; the results of the assessment should be considered in light of this uncertainty.

Although the limitations associated with regional analyses such as the one presented in this report and Masterson and others (2016a) can greatly affect the results of simulations, it is important to understand the purposes for which the model was developed and avoid using this tool for analyses for which it was not designed. All models, whether regional or local in scale, are at best oversimplifications of complex natural systems, but can provide useful information despite their limitations.

Summary

The U.S. Geological Survey implemented a detailed assessment of the groundwater availability of the Northern Atlantic Coastal Plain aquifer system from Long Island, New York, to northeastern North Carolina because of the substantial dependency on groundwater for agricultural, industrial, and municipal needs in the area. To evaluate how water resources have changed over time, numerical modeling tools were used to assess system responses to stresses from future human uses and climate trends.

The 3D transient groundwater flow model developed for this assessment used the numerical code MODFLOW–NWT to represent changes in groundwater pumping and aquifer recharge from predevelopment (before 1900) to future conditions, from 1900 to 2058. The model was constructed using hydrogeologic and geospatial information to represent the geometry, boundaries, and hydraulic properties of the aquifer system. The finite-difference grid developed for the approximately 51,000-square-mile (mi^2) modeled area was aligned with the contact between the Piedmont Uplands and Coastal Plain physiographic provinces and extends east to the boundary between freshwater and saltwater and from the water table down to the top of the bedrock. This grid consists of 250 rows, 500 columns, and 19 layers. Each model cell is 1 mi^2 in map view with varying thickness by cell and by layer based on existing information on the hydrogeologic unit elevations and geometry of the 19 separate regional aquifers and confining units.

The model was calibrated using the inverse modeling parameter-estimation technique PEST. The parameter estimation process was achieved through history matching, using observations of both steady-state and transient conditions. Five types of parameters were adjusted and estimated in the history matching process—general head boundary conductance, horizontal and vertical hydraulic conductivity, recharge, and specific storage—resulting in a total of 2,260 separate parameters. History matching of the NACP aquifer system model was based on water level (head) observations and base flow measurements. A final selection of 644 observation wells was combined in 29 observation groups within the regional aquifers. The total average residual of –1.7 feet was normally distributed for all head groups, indicating minimal bias. The average absolute residual value of 12.3 feet is about 3 percent of the total observed water-level range throughout the aquifer system.

Base flows also were computed at 153 sites and used for comparison with model-calculated estimates of base flow in streams through the northern Atlantic Coastal Plain province. An average residual of about –8 cubic feet per second and an average absolute residual of about 21 cubic feet per second for a range of computed base flows of about 417 cubic feet per second were calculated for the 122 sites from the National Hydrography Dataset Plus. An average residual of about 10 cubic feet per second and an average absolute residual of about 34 cubic feet per second were computed for the 568 flow measurements in the 31 sites obtained from the National Water Information System for a range in computed base flows of about 1,141 cubic feet per second.

The resulting transient flow solution was used to conduct a comprehensive assessment of the groundwater availability and water resources of the NACP aquifer system given the limitations inherent of a regional modeling analysis. The numerical representation of the hydrogeologic information used in the development of this flow model was dependent upon how the hydraulic properties, system boundaries, and simulated hydrologic stresses were discretized in space and time. Lumping hydraulic parameters in space and hydrologic stresses and time-varying observational data in time can limit the capabilities of this tool to simulate how the groundwater flow system responds to changes in hydrologic stresses, particularly at the local scale.

References Cited

Alley, W.M., Evenson, E.J., Barber, N.L., Bruce, B.W., Dennehy, K.F., Freeman, M.C., Freeman, W.O., Fischer, J.M., Hughes, W.B., Kennen, J.G., Kiang, J.E., Maloney, K.O., Musgrove, MaryLynn, Ralston, Barbara, Tessler, Steven, and Verdin, J.P., 2013, Progress toward establishing a national assessment of water availability and use: U.S. Geological Survey Circular 1384, 34 p., accessed March 11, 2013, at http://pubs.usgs.gov/circ/1384.

Bakker, Mark, Schaars, Frans, Hughes, J.D., Langevin, C.D., and Dausman, A.M., 2013, Documentation of the seawater intrusion (SWI2) package for MODFLOW: U.S. Geological Survey Techniques and Methods, book 6, chap. A46, 47 p. [Also available at http://pubs.usgs.gov/tm/6a46/.]

Barlow, P.M., Cunningham, W.L., Zhai, Tong, and Gray, Mark, 2014, U.S. Geological Survey groundwater toolbox, a graphical and mapping interface for analysis of hydrologic data (version 1.0)—User guide for estimation of base flow, runoff, and groundwater recharge from streamflow data: U.S. Geological Survey Techniques and Methods, book 3, chap. B10, 27 p. [Also available at http://dx.doi.org/10.3133/tm3B10.]

Bondelid, Tim, Johnston, Craig, McKay, Cindy, Moore, Rich, and Rea, Alan, 2010, NHDPlus version 1—User guide: U.S. Environmental Protection Agency and U.S. Geological Survey, 115 p., accessed June 10, 2011, at http://www.horizon-systems.com/NHDPlus/NHDPlusV1_home.php.]

Campbell, B.G., and Coes, A.L., eds., 2010, Groundwater availability in the Atlantic coastal plain of North and South Carolina: U.S. Geological Survey Professional Paper 1773, 241 p., 7 pls., accessed March 11, 2013, at http://pubs.er.usgs.gov/publication/pp1773.

Charles, E.G., 2016, Regional chloride distribution in the Northern Atlantic Coastal Plain aquifer system from Long Island, New York, to North Carolina: U.S. Geological Survey Scientific Investigations Report 2016–5034, 37 p., accessed August 31, 2016, at http://dx.doi.org/10.3133/sir20165034.

Dewald, Tommy, McKay, Lucinda, Bondelid, Timothy, Johnston, Craig, Moore, Richard, and Rea, Alan, 2012, NHDPlus version 2—User guide: U.S. Environmental Protection Agency and U.S. Geological Survey, 181 p., accessed November 15, 2014, at http://www.horizon-systems.com/NHDPlus/NHDPlusV2_documentation.php.

Doherty, J.E., Fienen, M.N., and Hunt, R.J., 2010, Approaches to highly parameterized inversion—Pilot-point theory, guidelines, and research directions: U.S. Geological Survey Scientific Investigations Report 2010–5168, 36 p., accessed November 13, 2014, at http://pubs.er.usgs.gov/publication/sir20105168.

Doherty, J.E., and Hunt, R.J., 2010, Approaches to highly parameterized inversion—A guide to using PEST for groundwater-model calibration: U.S. Geological Survey Scientific Investigations Report 2010–5169, 59 p. [Also available at http://pubs.er.usgs.gov/publication/sir20105169.]

Doherty, John, 2003, Ground water model calibration using pilot points and regularization: Ground Water, v. 41, no. 2, p. 170–177. [Also available at http://dx.doi.org/10.1111/j.1745-6584.2003.tb02580.x.]

Doherty, John, 2010, PEST—Model-independent parameter estimation—User manual (5th ed.): Brisbane, Australia, Watermark Numerical Computing, [variously paged], accessed November 13, 2014, at http://www.pesthomepage.org/files/pestman.pdf.

Doherty, John, 2014, Addendum to the PEST manual: Brisbane, Australia, Watermark Numerical Computing, 316 p., accessed November 13, 2014, at http://www.pesthomepage.org/Downloads.php.

Doherty, John, and Hunt, R.J., 2009, Two statistics for evaluating parameter identifiability and error reduction: Journal of Hydrology, v. 366, nos. 1–4, p. 119–127. [Also available at http://dx.doi.org/10.1016/j.jhydrol.2008.12.018.]

Feinstein, D.T., Hunt, R.J., and Reeves, H.W., 2010, Regional groundwater-flow model of the Lake Michigan Basin in support of Great Lakes Basin water availability and use studies: U.S. Geological Survey Scientific Investigations Report 2010–5109, 379 p. [Also available at http://pubs.er.usgs.gov/publication/sir20105109.]

Fienen, M.N., 2013, We speak for the data: Groundwater, v. 51, no. 2, p. 157. [Also available at http://dx.doi.org/10.1111/gwat.12018.]

Fienen, M.N., Muffels, C.T., and Hunt, R.J., 2009, On constraining pilot point calibration with regularization in PEST: Groundwater, v. 47, no. 6, p. 835–844. [Also available at http://dx.doi.org/10.1111/j.1745-6584.2009.00579.x.]

Finkelstein, J.S., and Nardi, M.R., 2015, Geospatial compilation and digital map of centerpivot irrigated areas in the mid-Atlantic region, United States: U.S. Geological Survey Data Series 932, accessed May 25, 2016, at http://pubs.er.usgs.gov/publication/ds932.

Guo, Weixing, and Langevin, C.D., 2002, User's guide to SEAWAT—A computer program for simulation of three-dimensional variable-density ground-water flow: U.S. Geological Survey Techniques of Water-Resources Investigations, book 6, chap. A7, 77 p. [Also available at https://pubs.er.usgs.gov/publication/twri06A7.]

Harbaugh, A.W., 2005, MODFLOW–2005—The U.S. Geological Survey modular ground-water model—The ground-water flow process: U.S. Geological Survey Techniques and Methods, book 6, chap. A16, [variously paged]. [Also available at http://pubs.er.usgs.gov/publication/tm6A16.]

Heywood, C.E., and Pope, J.P., 2009, Simulation of groundwater flow in the coastal plain aquifer system of Virginia: U.S. Geological Survey Scientific Investigations Report 2009–5039, 115 p., accessed March 11, 2013, at http://pubs.er.usgs.gov/publication/sir20095039.

Konikow, L.F., and Reilly, T.E., 1998, Groundwater modeling, chap. 20 *of* Delleur, J.W., ed., The handbook of groundwater engineering: Boca Raton, Fla., CRC Press, p. 20–1—20–40.

Leahy, P.P., and Martin, Mary, 1993, Geohydrology and simulation of ground-water flow in the Northern Atlantic Coastal Plain aquifer system: U.S. Geological Survey Professional Paper 1404–K, 81 p., 22 pls., accessed March 11, 2013, at http://pubs.er.usgs.gov/publication/pp1404K.

Masterson, J.P., Pope, J.P., Fienen, M.N., Monti, Jack, Jr., Nardi, M.R., and Finkelstein, J.S., 2016a, Assessment of groundwater availability in the Northern Atlantic Coastal Plain aquifer system from Long Island, New York, to North Carolina: U.S. Geological Survey Professional Paper 1829, 76 p. [Also available at http://dx.doi.org/10.3133/pp1829.]

Masterson, J.P., Pope, J.P., Fienen, M.N., Monti, Jack, Jr., Nardi, M.R., and Finkelstein, J.S., 2016b, MODFLOW–NWT model used to assess groundwater availability in the Northern Atlantic Coastal Plain aquifer system from Long Island, New York, to North Carolina: U.S. Geological Survey data release, accessed August 31, 2016, at http://dx.doi.org/10.5066/F7MG7MKR.

Masterson, J.P., Pope, J.P., Monti, Jack, Jr., Nardi, M.R., Finkelstein, J.S., and McCoy, K.J., 2013, Hydrogeology and hydrologic conditions of the Northern Atlantic Coastal Plain aquifer system from Long Island, New York, to North Carolina: U.S. Geological Survey Scientific Investigations Report 2013–5133, 76 p. [Also available at http://dx.doi.org/10.3133/sir20135133.]

Maupin, M.A., Kenny, J.F., Hutson, S.S., Lovelace, J.K., Barber, N.L., and Linsey, K.S., 2014, Estimated use of water in the United States in 2010: U.S. Geological Survey Circular 1405, 56 p. [Also available at http://dx.doi.org/10.3133/cir1405.]

McDonald, M.G., and Harbaugh, A.W., 1988, A modular three-dimensional finite-difference groundwater flow model: U.S. Geological Survey Techniques of Water-Resources Investigations, book 6, chap. A1, 586 p. [Also available at http://pubs.usgs.gov/twri/twri6a1/.]

National Historical Geographic Information System, [undated]a, Total persons, 1990, table STF1 *of* Block group totals based on 1990 U.S. census: National Historical Information System database, accessed June 8, 2011, at https://www.nhgis.org/.

National Historical Geographic Information System, [undated]b, Source of water, 1990, table STF3 *of* Block group totals based on 1990 U.S. census: National Historical Information System database, accessed June 8, 2011, at https://www.nhgis.org/.

Niswonger, R.G., Panday, Sorab, and Ibaraki, Motomu, 2011, MODFLOW–NWT, A Newton formulation for MODFLOW–2005: U.S. Geological Survey Techniques and Methods, book 6, chap. A37, 44 p. [Also available at https://pubs.er.usgs.gov/publication/tm6A37.]

Niswonger, R.G., and Prudic, D.E., 2005, Documentation of the streamflow-routing (SFR2) package to include unsaturated flow beneath streams—A modification to SFR1: U.S. Geological Survey Techniques and Methods, book 6, chap. A13, 50 p. [Also available at https://pubs.er.usgs.gov/publication/tm6A13.]

Pierson, S.M., Rosenbaum, B.J., McKay, L.D., and Dewald, T.G., 2008, Strahler stream order and Strahler calculator values in NHDPlus: U.S. Environmental Protection Agency and U.S. Geological Survey, 10 p., accessed March 11, 2013, at ftp://ftp.horizon-systems.com/nhdplus/NHDPlusV1/NHDPlusExtensions/SOSC/SOSC_technical_paper.pdf.

Pope, J.P., Andreasen, D.C., McFarland, E.R., and Watt, M.K., 2016, Digital elevations and extents of regional hydrogeologic units in the Northern Atlantic Coastal Plain aquifer system from Long Island, New York, to North Carolina: U.S. Geological Survey Data Series 996, 28 p., accessed August 31, 2016, at http://dx.doi.org/10.3133/ds996.

Pope, J.P., McFarland, E.R., and Banks, R.B., 2008, Private domestic-well characteristics and the distribution of domestic withdrawals among aquifers in the Virginia Coastal Plain: U.S. Geological Survey Scientific Investigations Report 2007–5250, 47 p. [Also available at http://pubs.usgs.gov/sir/2007/5250/.]

Reilly, T.E., 2001, System and boundary conceptualization in ground-water flow simulation: U.S. Geological Survey Techniques of Water-Resources Investigations, book 3, chap. B8, 29 p. [Also available at http://pubs.er.usgs.gov/publication/twri03B8.]

Shaffer, K.H., and Runkle, D.L., 2007, Consumptive water-use coefficients for the Great Lakes basin and climatically similar areas: U.S. Geological Survey Scientific Investigations Report 2007–5197, 191 p. [Also available at http://pubs.er.usgs.gov/publication/sir20075197.]

Shapiro, S.S., and Wilk, M.B., 1965, An analysis of variance test for normality (complete samples): Biometrika, v. 52, nos. 3–4, p. 591–611.

Solley, W.B., Pierce, R.R., and Perlman, H.A., 1993, Estimated use of water in the United States in 1990: U.S. Geological Survey Circular 1081, 76 p. [Also available at http://pubs.er.usgs.gov/publication/cir1081.]

Thornthwaite, C.W., and Mather, J.R., 1957, Instructions and tables for computing potential evapotranspiration and the water balance: Centerton, N.J., Drexel Institute of Technology Laboratory of Climatology, 129 p.

Tikhonov, A.N., 1963a, Solution of incorrectly formulated problems and the regularization method: Soviet Mathematics Doklady, v. 4, p. 1035–1038.

Tikhonov, A.N., 1963b, Regularization of incorrectly posed problems: Soviet Mathematics, v. 4, p. 1624–1637.

Titus, J.G., and Wang, Jue, 2008, Maps of lands close to sea level along the middle Atlantic coast of the United States—An elevation data set to use while waiting for lidar, sec. 1.1 *of* Titus, J.G., and Strange, E.M., eds., Background documents supporting Climate Change Science Program synthesis and assessment product 4.1: U.S. Environmental Protection Agency EPA 430R07004, 44 p., accessed March 11, 2013, at http://papers.risingsea.net/federal_reports/Titus_and_Strange_EPA_section1_1_Titus_and_Wang_may2008.pdf.

Tonkin, M.J., and Doherty, John, 2005, A hybrid regularized inversion methodology for highly parameterized environmental models: Water Resources Research, v. 41, no. 10, paper W10412, 16 p., accessed June 23, 2015, at http://dx.doi.org/10.1029/2005WR003995.

U.S. Department of Agriculture, National Agricultural Statistics Service, 2014, Table 10. Irrigation—2012 and 2007, *in* State level data, chap. 2 *of* U.S. summary and state data: U.S. Department of Agriculture 2012 Census of Agriculture, v. 1, part 51, p. 332–339. [Also available at http://www.agcensus.usda.gov/Publications/2012/Full_Report/Volume_1,_Chapter_2_US_State_Level/st99_2_010_010.pdf.]

U.S. Geological Survey, 2011, USGS water data for the Nation: U.S. Geological Survey National Water Information System Web interface, accessed May 2, 2011, at http://waterdata.usgs.gov/nwis/.

Westenbroek, S.M., Kelson, V.A., Dripps, W.R., Hunt, R.J., and Bradbury, K.R., 2012, SWB—A modified Thornthwaite-Mather soil-water-balance code for estimating groundwater recharge [revised]: U.S. Geological Survey Techniques and Methods, book 6, chap. A31, 60 p., accessed March 11, 2013, at https://pubs.er.usgs.gov/publication/tm6A31.

Figures 7–8

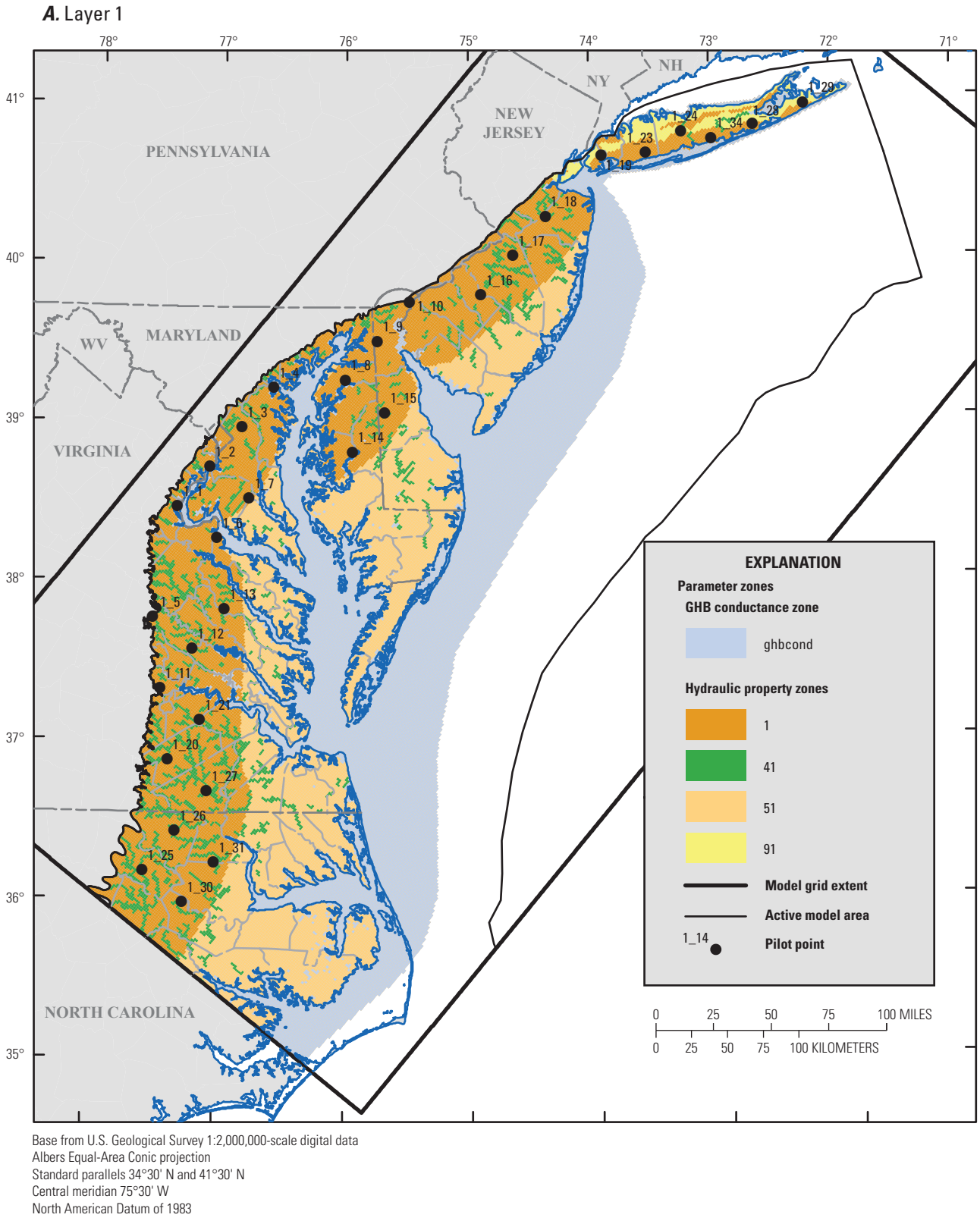

Figure 7. Distribution of pilot points and zones used to parameterize general-head boundary (GHB) conductance, hydraulic conductivity, and specific storage in the Northern Atlantic Coastal Plain aquifer system for *A*, model layer 1 through *S*, model layer 19.

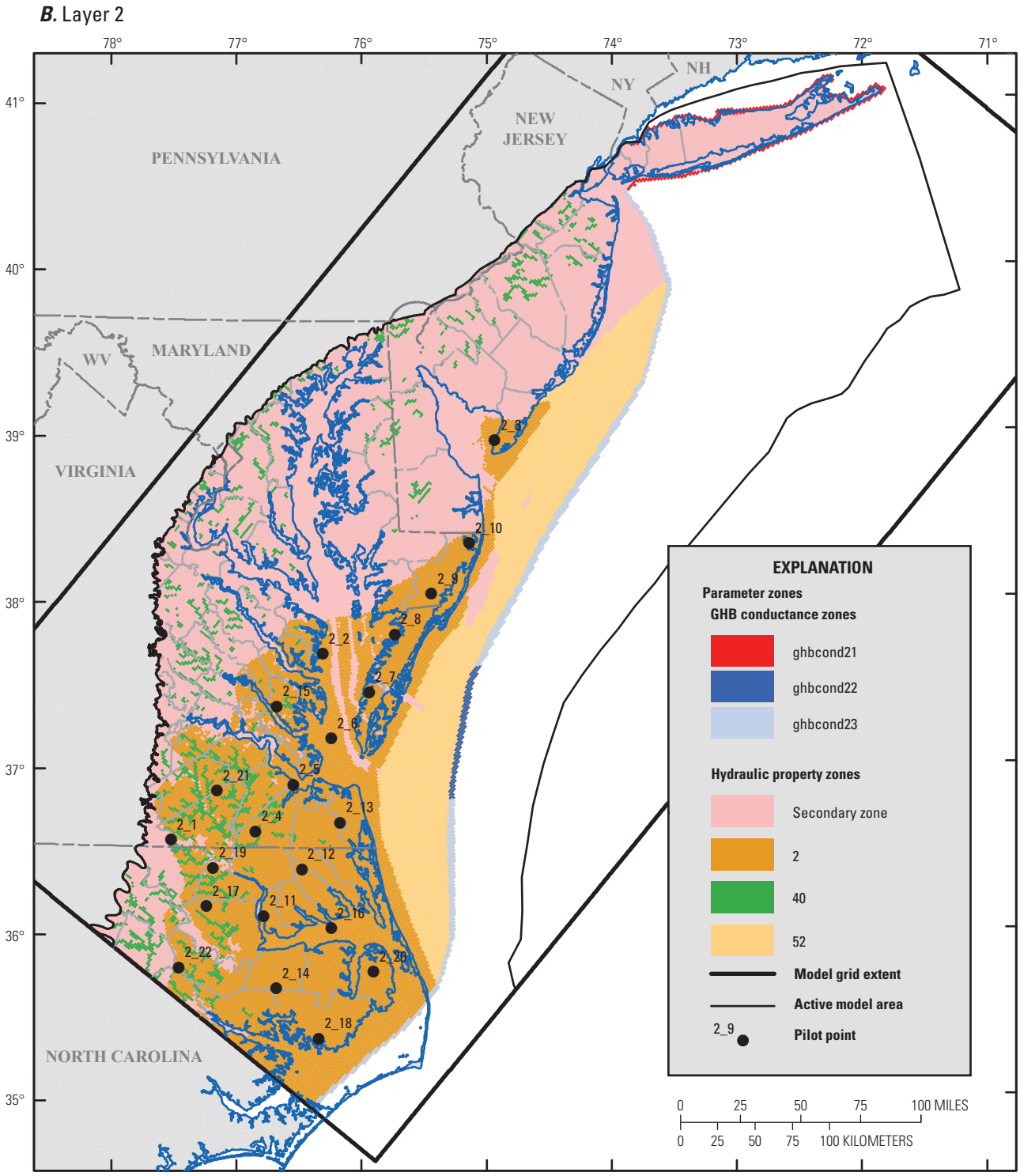

Figure 7. Distribution of pilot points and zones used to parameterize general-head boundary (GHB) conductance, hydraulic conductivity, and specific storage in the Northern Atlantic Coastal Plain aquifer system for *A*, model layer 1 through *S*, model layer 19.—Continued

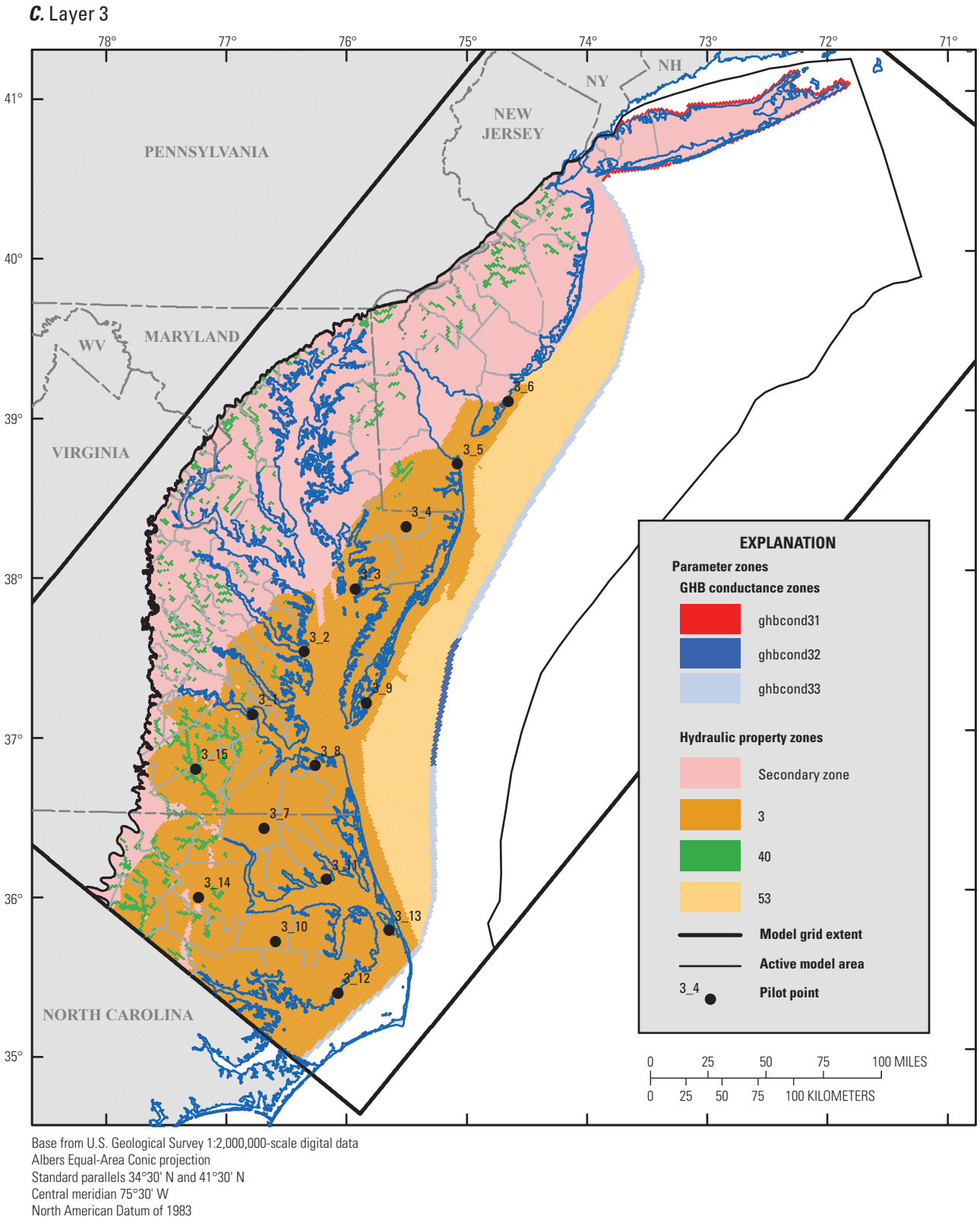

Figure 7. Distribution of pilot points and zones used to parameterize general-head boundary (GHB) conductance, hydraulic conductivity, and specific storage in the Northern Atlantic Coastal Plain aquifer system for *A*, model layer 1 through *S*, model layer 19.—Continued

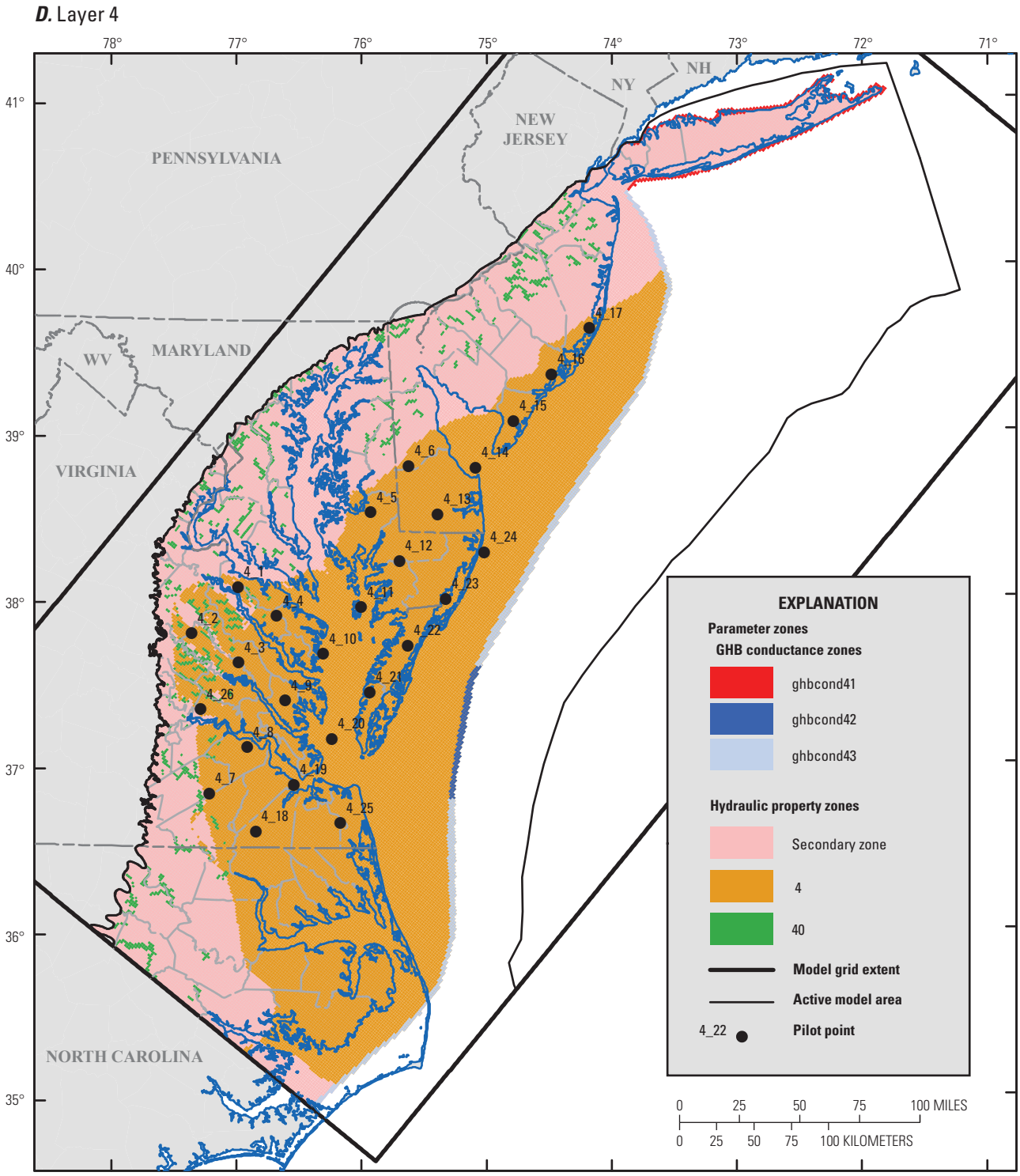

Base from U.S. Geological Survey 1:2,000,000-scale digital data
Albers Equal-Area Conic projection
Standard parallels 34°30' N and 41°30' N
Central meridian 75°30' W
North American Datum of 1983

Figure 7. Distribution of pilot points and zones used to parameterize general-head boundary (GHB) conductance, hydraulic conductivity, and specific storage in the Northern Atlantic Coastal Plain aquifer system for *A*, model layer 1 through *S*, model layer 19.—Continued

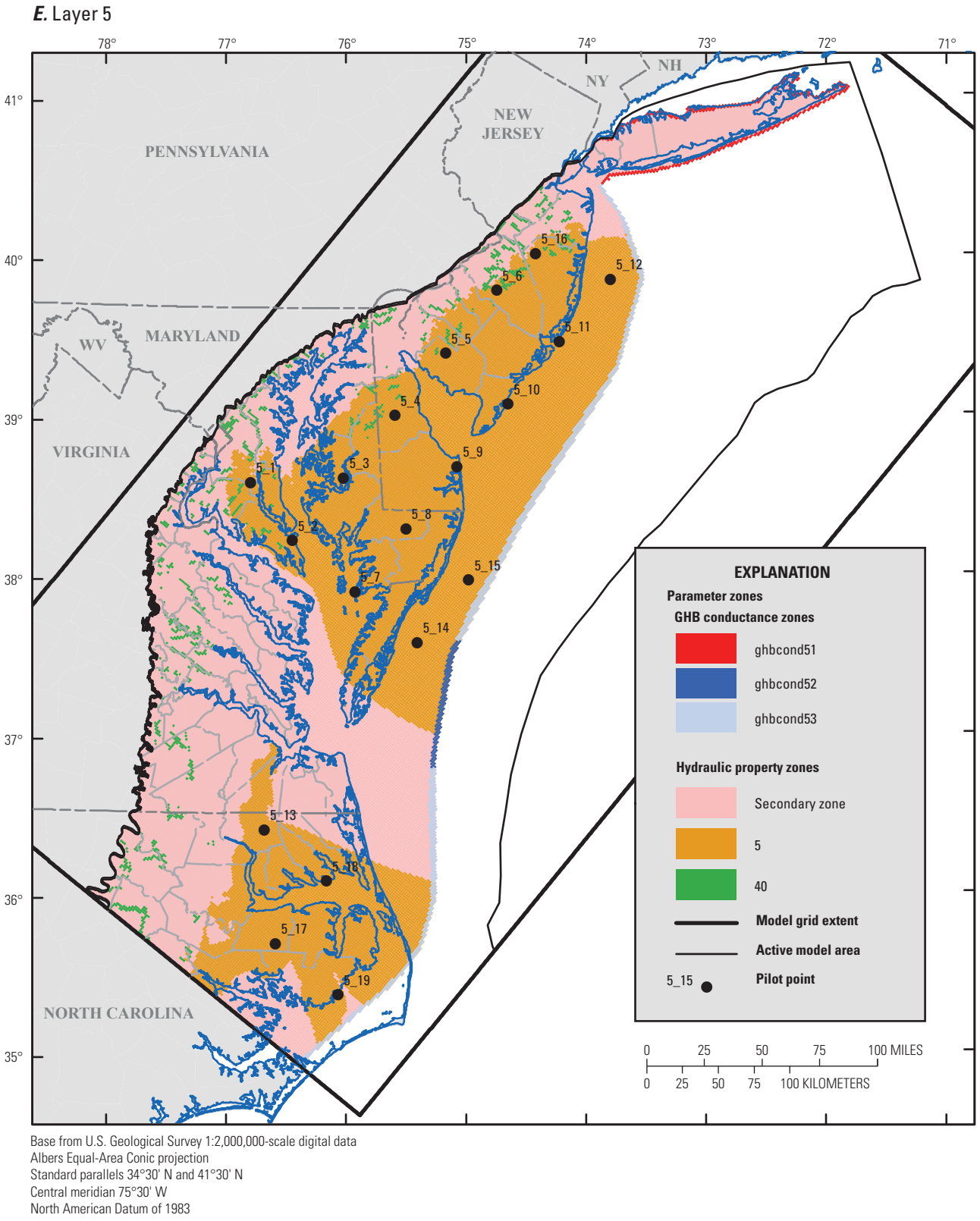

Figure 7. Distribution of pilot points and zones used to parameterize general-head boundary (GHB) conductance, hydraulic conductivity, and specific storage in the Northern Atlantic Coastal Plain aquifer system for *A*, model layer 1 through *S*, model layer 19.—Continued

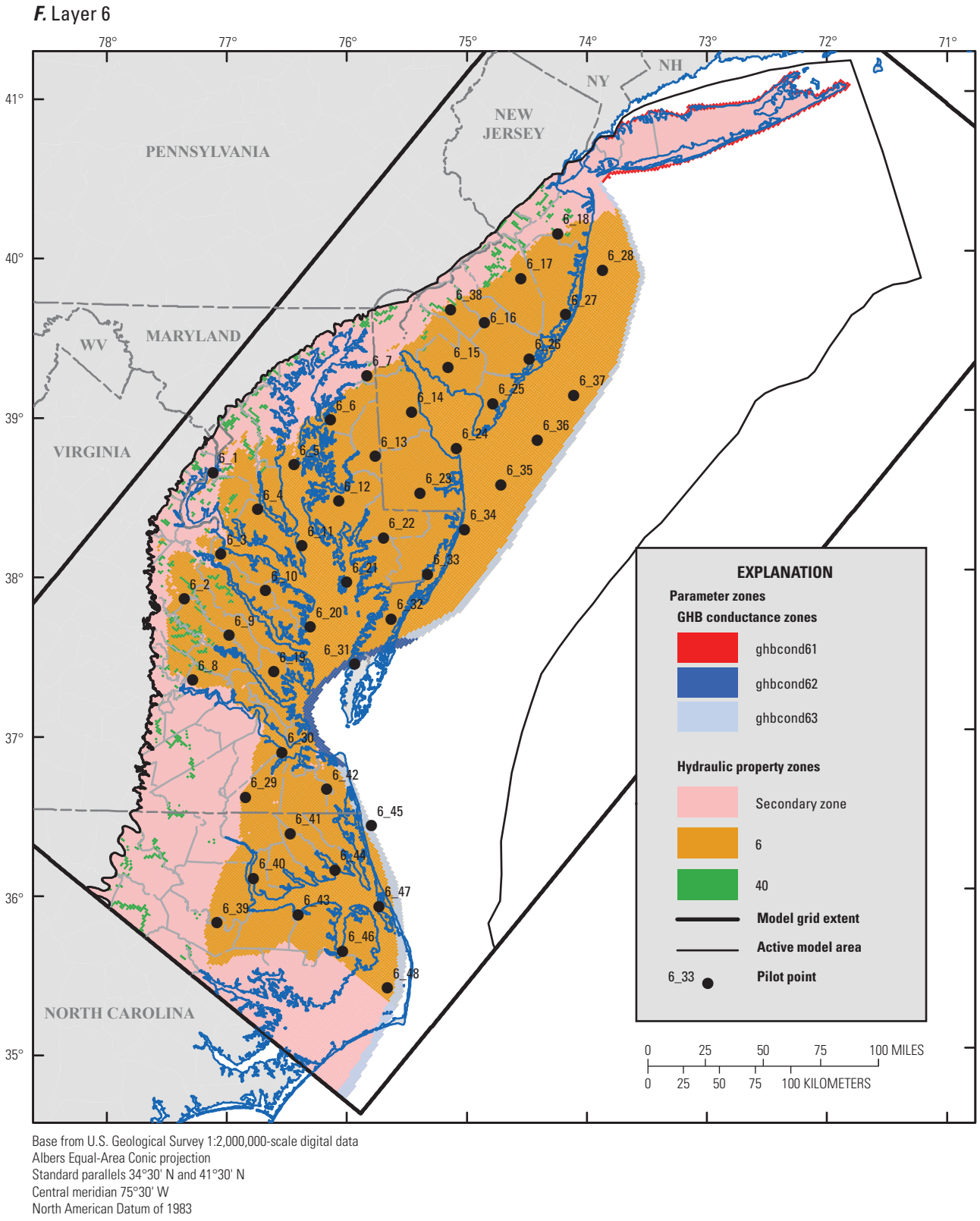

Base from U.S. Geological Survey 1:2,000,000-scale digital data
Albers Equal-Area Conic projection
Standard parallels 34°30' N and 41°30' N
Central meridian 75°30' W
North American Datum of 1983

Figure 7. Distribution of pilot points and zones used to parameterize general-head boundary (GHB) conductance, hydraulic conductivity, and specific storage in the Northern Atlantic Coastal Plain aquifer system for *A*, model layer 1 through *S*, model layer 19.—Continued

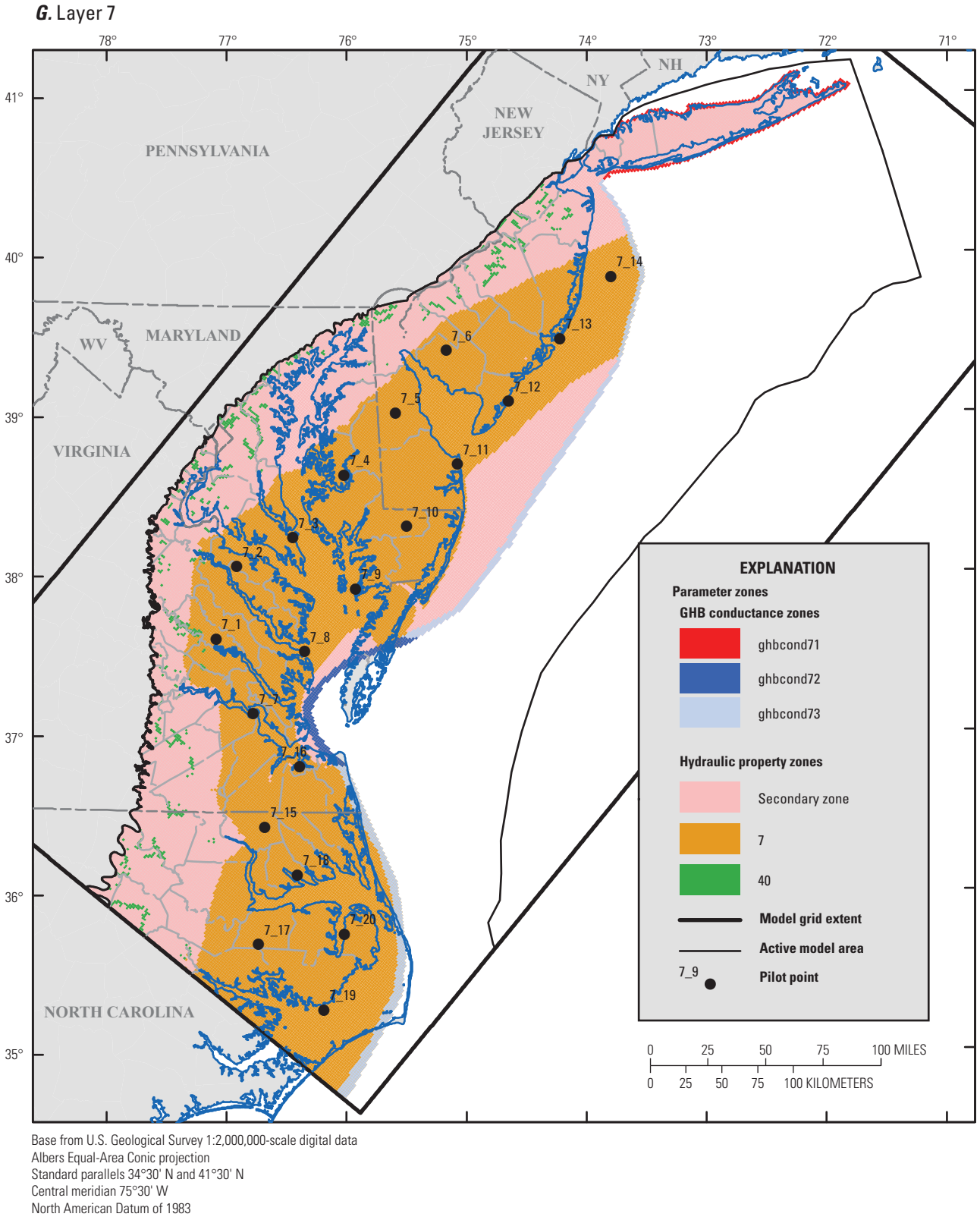

Figure 7. Distribution of pilot points and zones used to parameterize general-head boundary (GHB) conductance, hydraulic conductivity, and specific storage in the Northern Atlantic Coastal Plain aquifer system for *A*, model layer 1 through *S*, model layer 19.—Continued

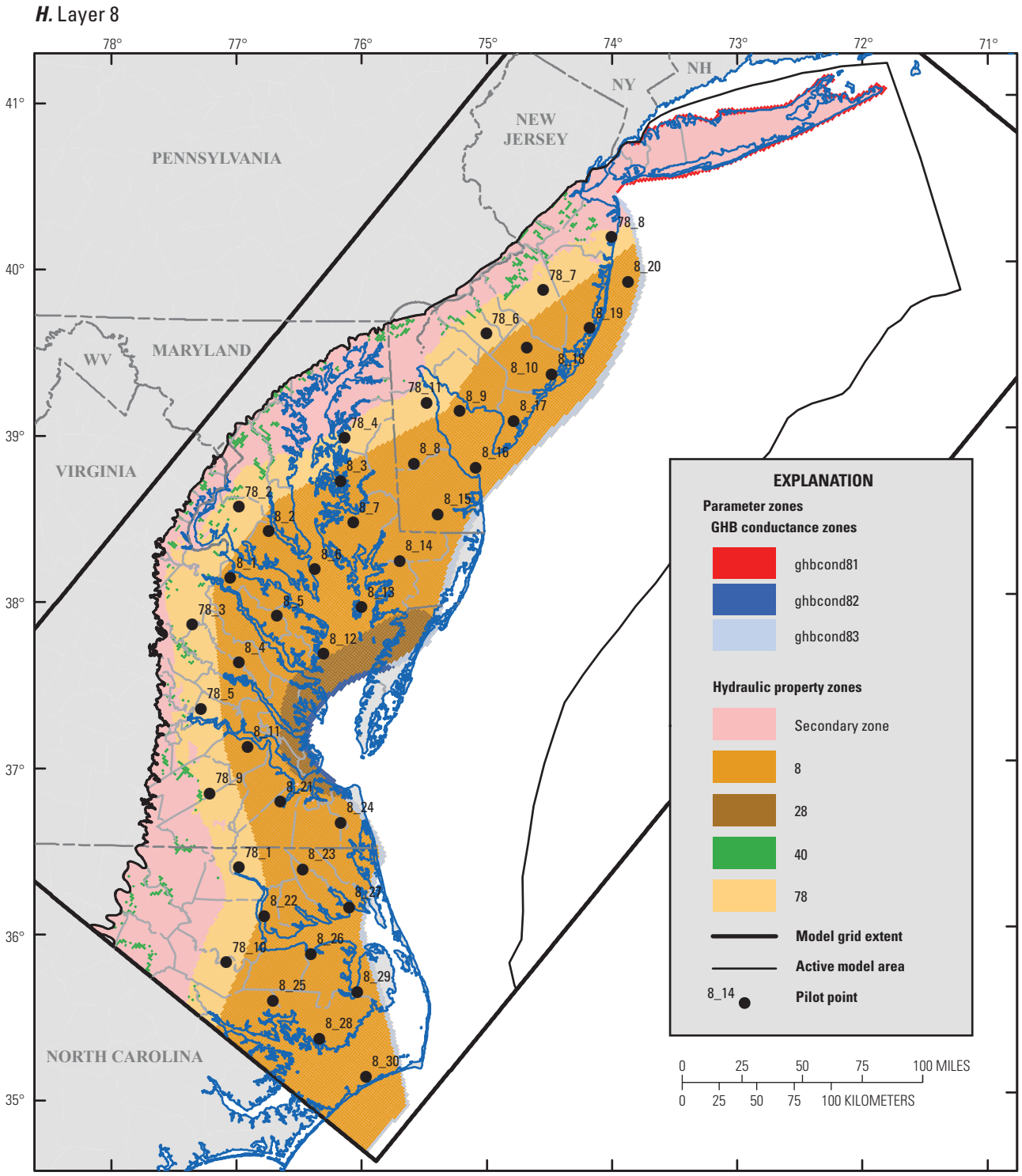

Figure 7. Distribution of pilot points and zones used to parameterize general-head boundary (GHB) conductance, hydraulic conductivity, and specific storage in the Northern Atlantic Coastal Plain aquifer system for *A*, model layer 1 through *S*, model layer 19.—Continued

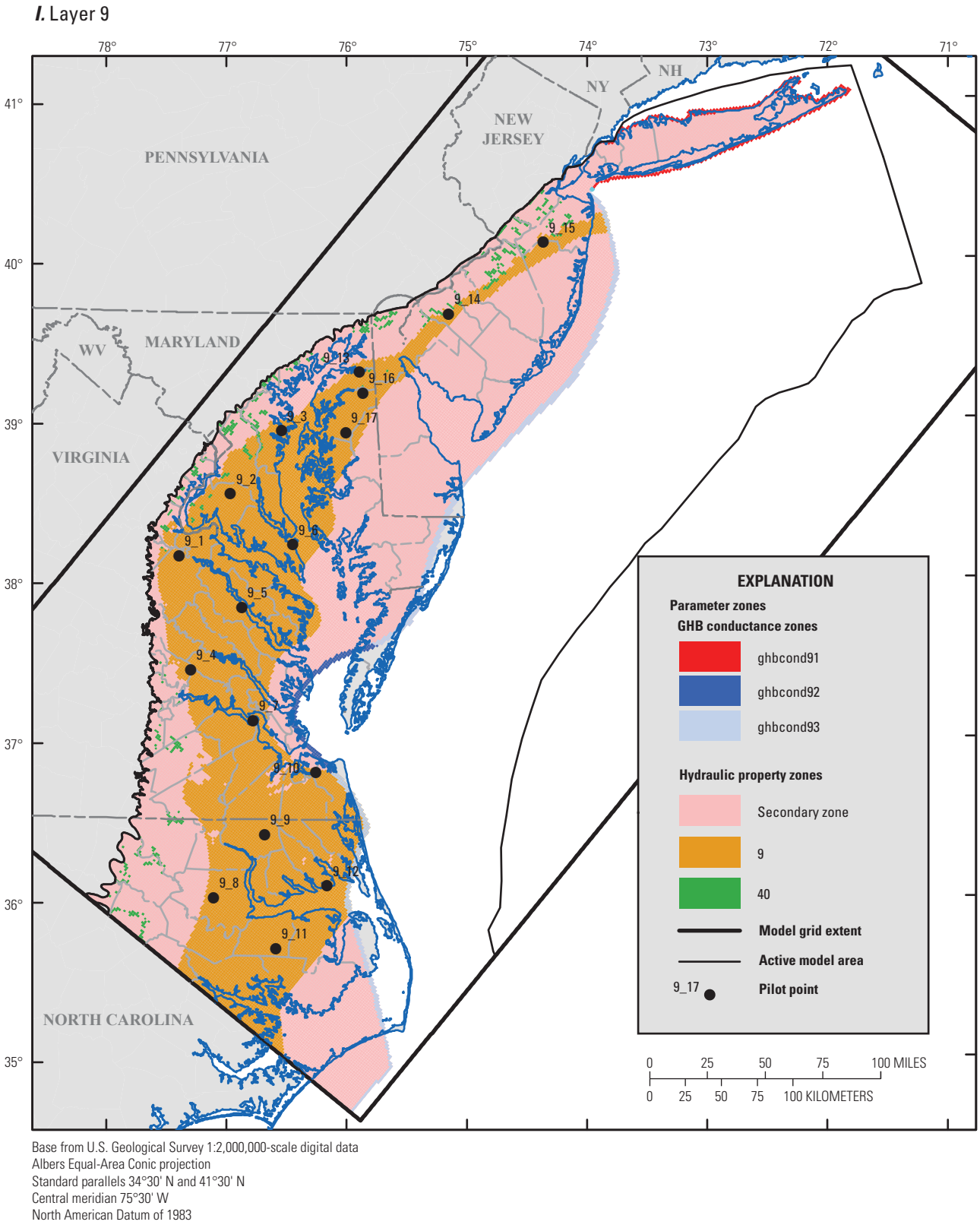

Base from U.S. Geological Survey 1:2,000,000-scale digital data
Albers Equal-Area Conic projection
Standard parallels 34°30' N and 41°30' N
Central meridian 75°30' W
North American Datum of 1983

Figure 7. Distribution of pilot points and zones used to parameterize general-head boundary (GHB) conductance, hydraulic conductivity, and specific storage in the Northern Atlantic Coastal Plain aquifer system for *A*, model layer 1 through *S*, model layer 19.—Continued

J. Layer 10

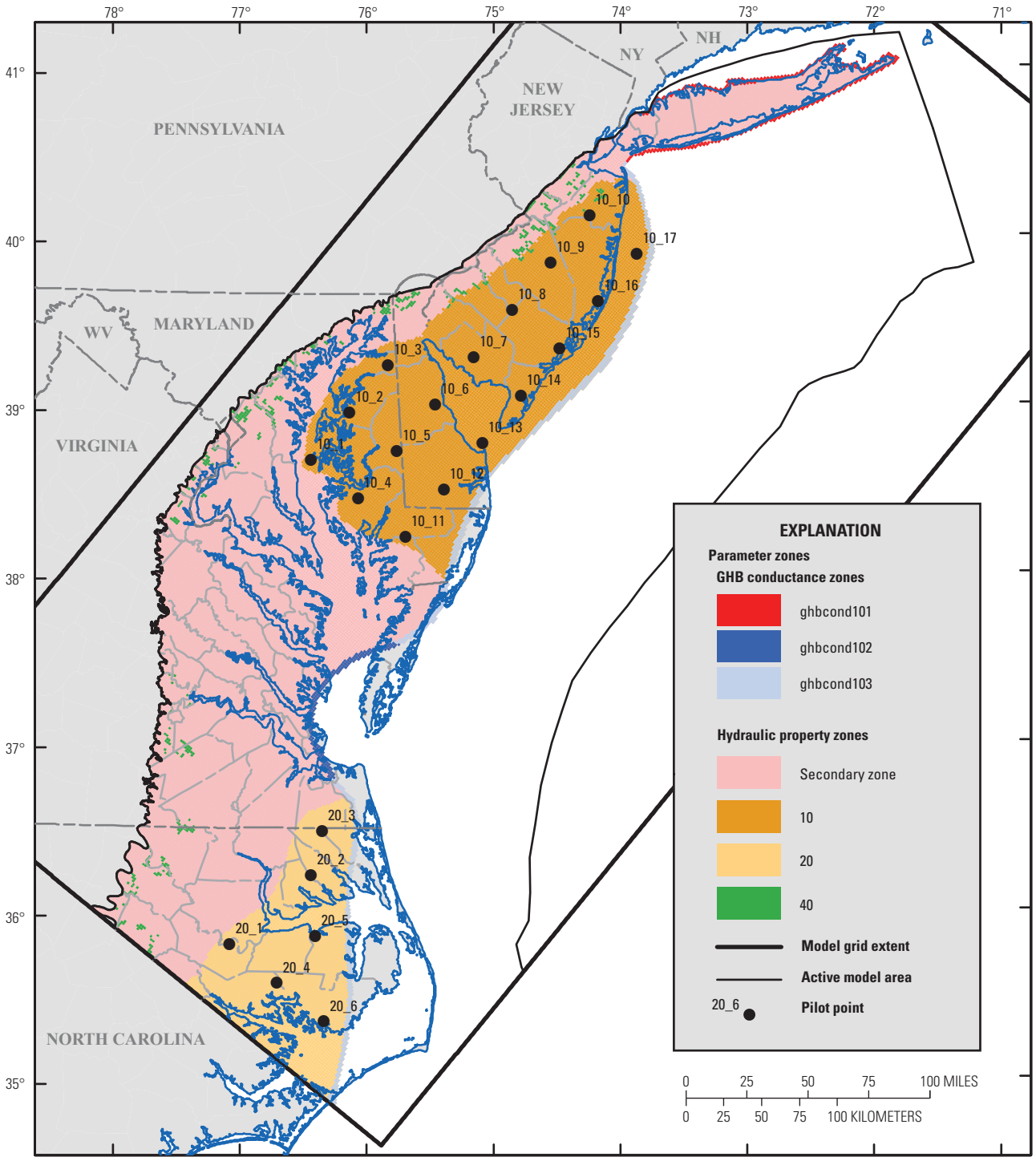

Base from U.S. Geological Survey 1:2,000,000-scale digital data
Albers Equal-Area Conic projection
Standard parallels 34°30' N and 41°30' N
Central meridian 75°30' W
North American Datum of 1983

Figure 7. Distribution of pilot points and zones used to parameterize general-head boundary (GHB) conductance, hydraulic conductivity, and specific storage in the Northern Atlantic Coastal Plain aquifer system for *A*, model layer 1 through *S*, model layer 19.—Continued

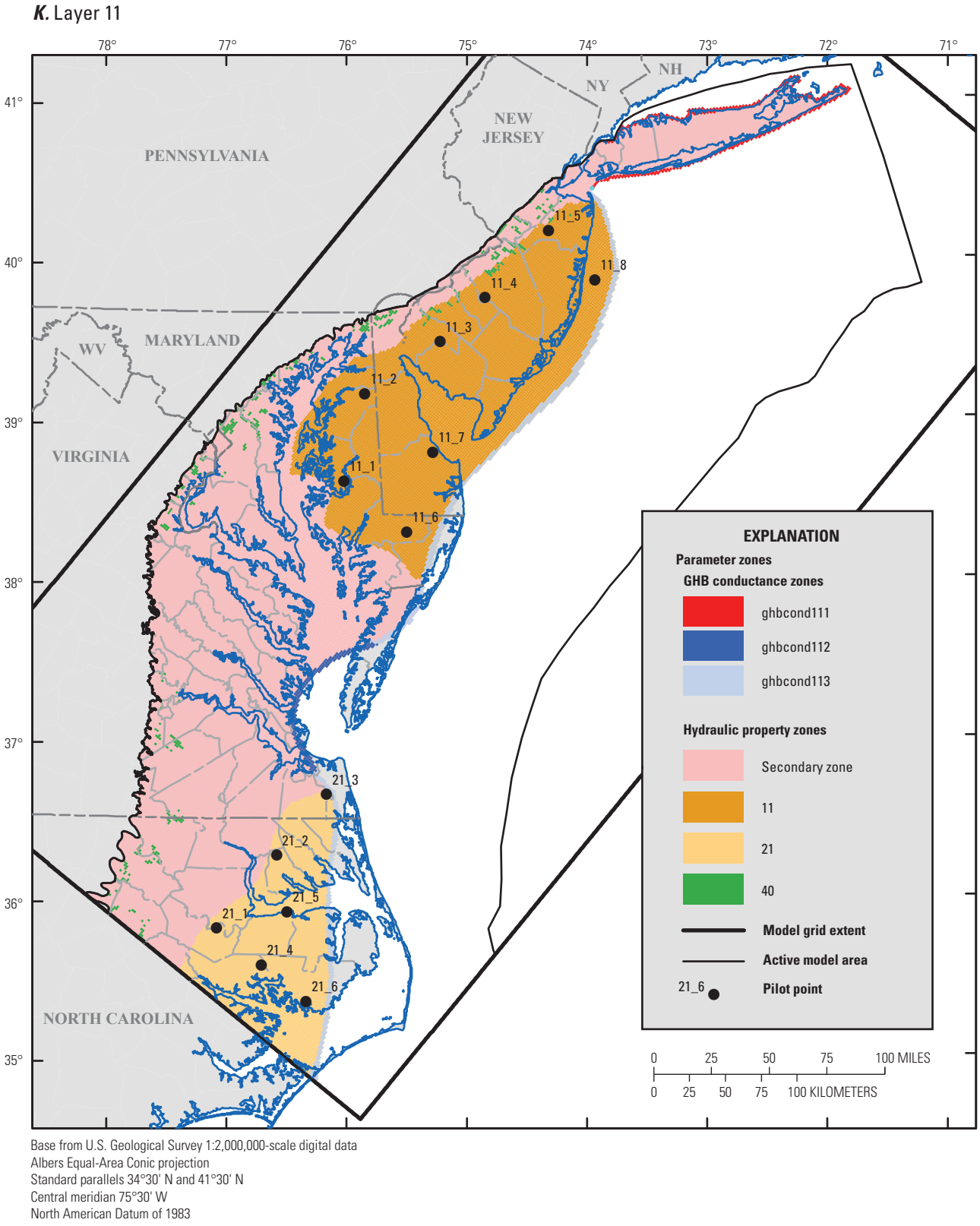

Figure 7. Distribution of pilot points and zones used to parameterize general-head boundary (GHB) conductance, hydraulic conductivity, and specific storage in the Northern Atlantic Coastal Plain aquifer system for *A*, model layer 1 through *S*, model layer 19.—Continued

L. Layer 12

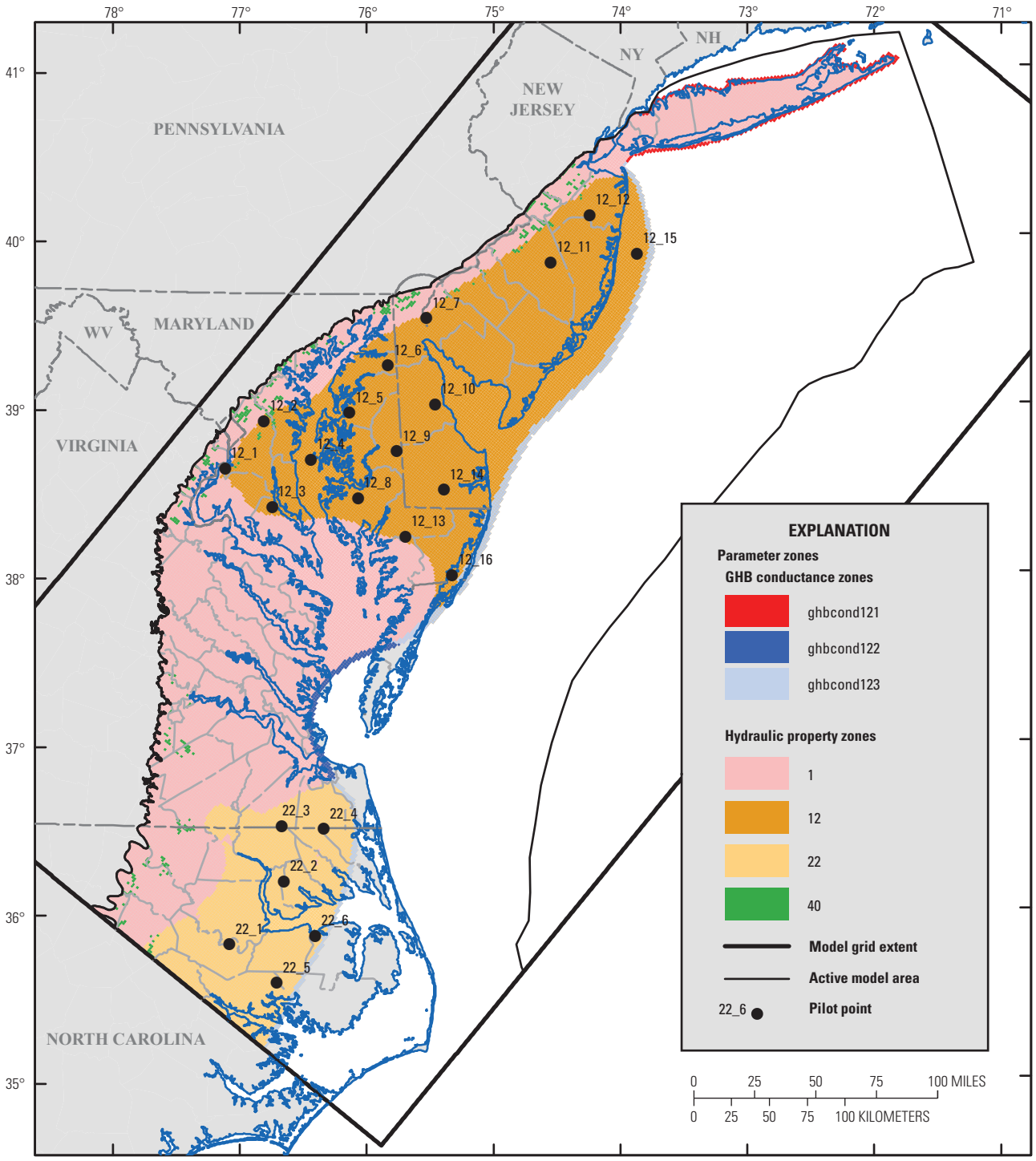

Base from U.S. Geological Survey 1:2,000,000-scale digital data
Albers Equal-Area Conic projection
Standard parallels 34°30' N and 41°30' N
Central meridian 75°30' W
North American Datum of 1983

Figure 7. Distribution of pilot points and zones used to parameterize general-head boundary (GHB) conductance, hydraulic conductivity, and specific storage in the Northern Atlantic Coastal Plain aquifer system for *A*, model layer 1 through *S*, model layer 19.—Continued

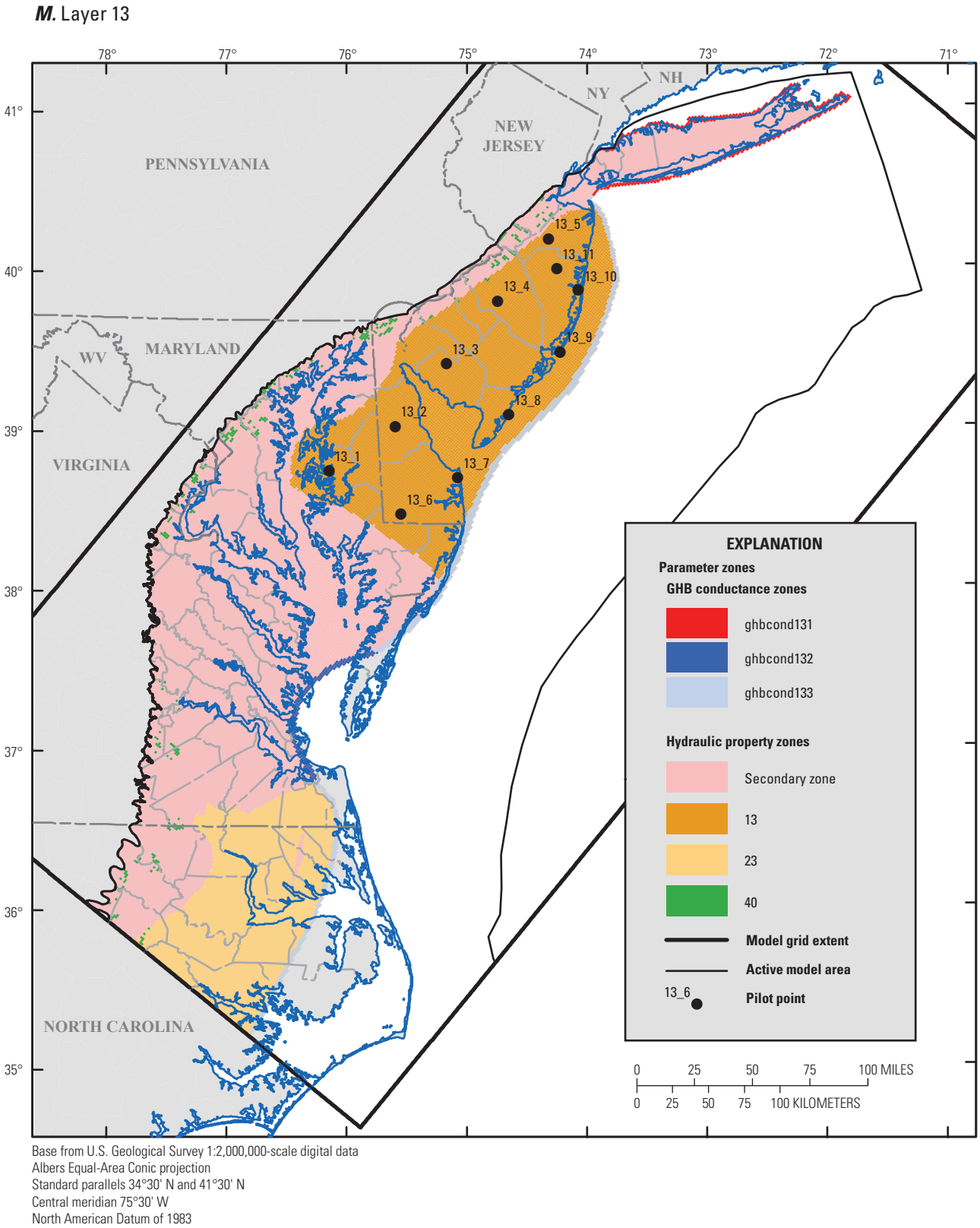

Figure 7. Distribution of pilot points and zones used to parameterize general-head boundary (GHB) conductance, hydraulic conductivity, and specific storage in the Northern Atlantic Coastal Plain aquifer system for *A*, model layer 1 through *S*, model layer 19.—Continued

N. Layer 14

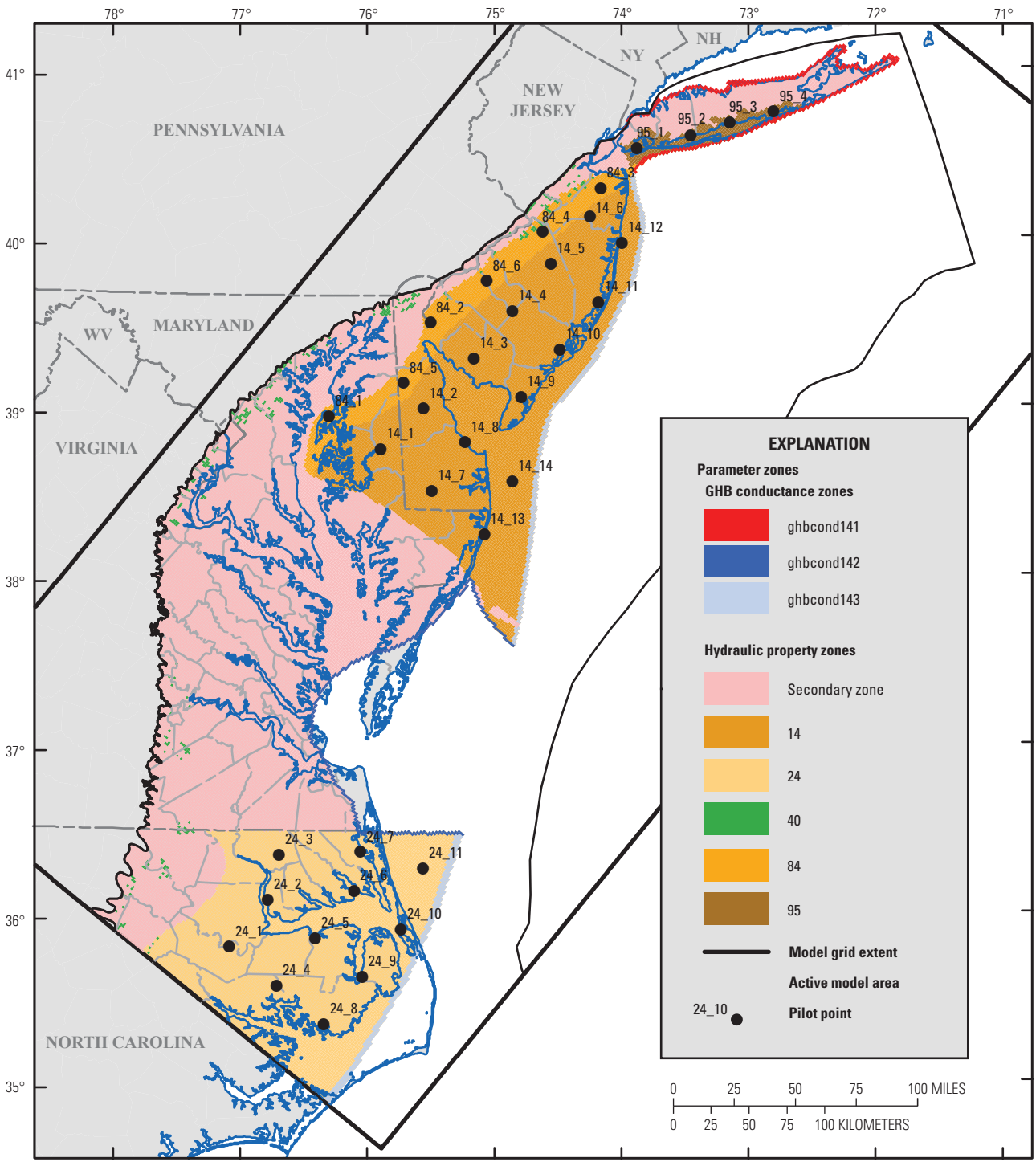

Base from U.S. Geological Survey 1:2,000,000-scale digital data
Albers Equal-Area Conic projection
Standard parallels 34°30' N and 41°30' N
Central meridian 75°30' W
North American Datum of 1983

Figure 7. Distribution of pilot points and zones used to parameterize general-head boundary (GHB) conductance, hydraulic conductivity, and specific storage in the Northern Atlantic Coastal Plain aquifer system for *A*, model layer 1 through *S*, model layer 19.—Continued

O. Layer 15

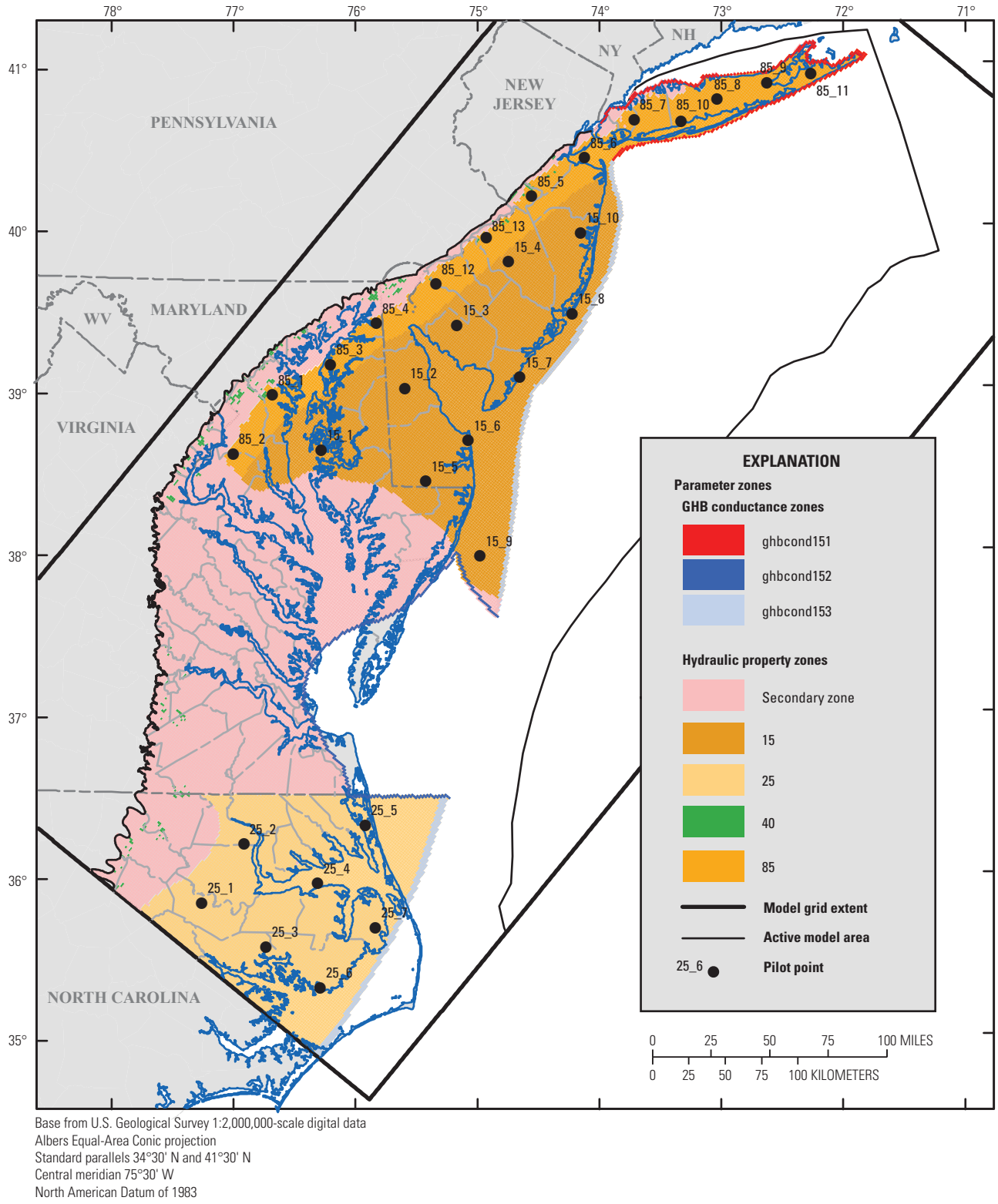

Base from U.S. Geological Survey 1:2,000,000-scale digital data
Albers Equal-Area Conic projection
Standard parallels 34°30' N and 41°30' N
Central meridian 75°30' W
North American Datum of 1983

Figure 7. Distribution of pilot points and zones used to parameterize general-head boundary (GHB) conductance, hydraulic conductivity, and specific storage in the Northern Atlantic Coastal Plain aquifer system for *A*, model layer 1 through *S*, model layer 19.—Continued

P. Layer 16

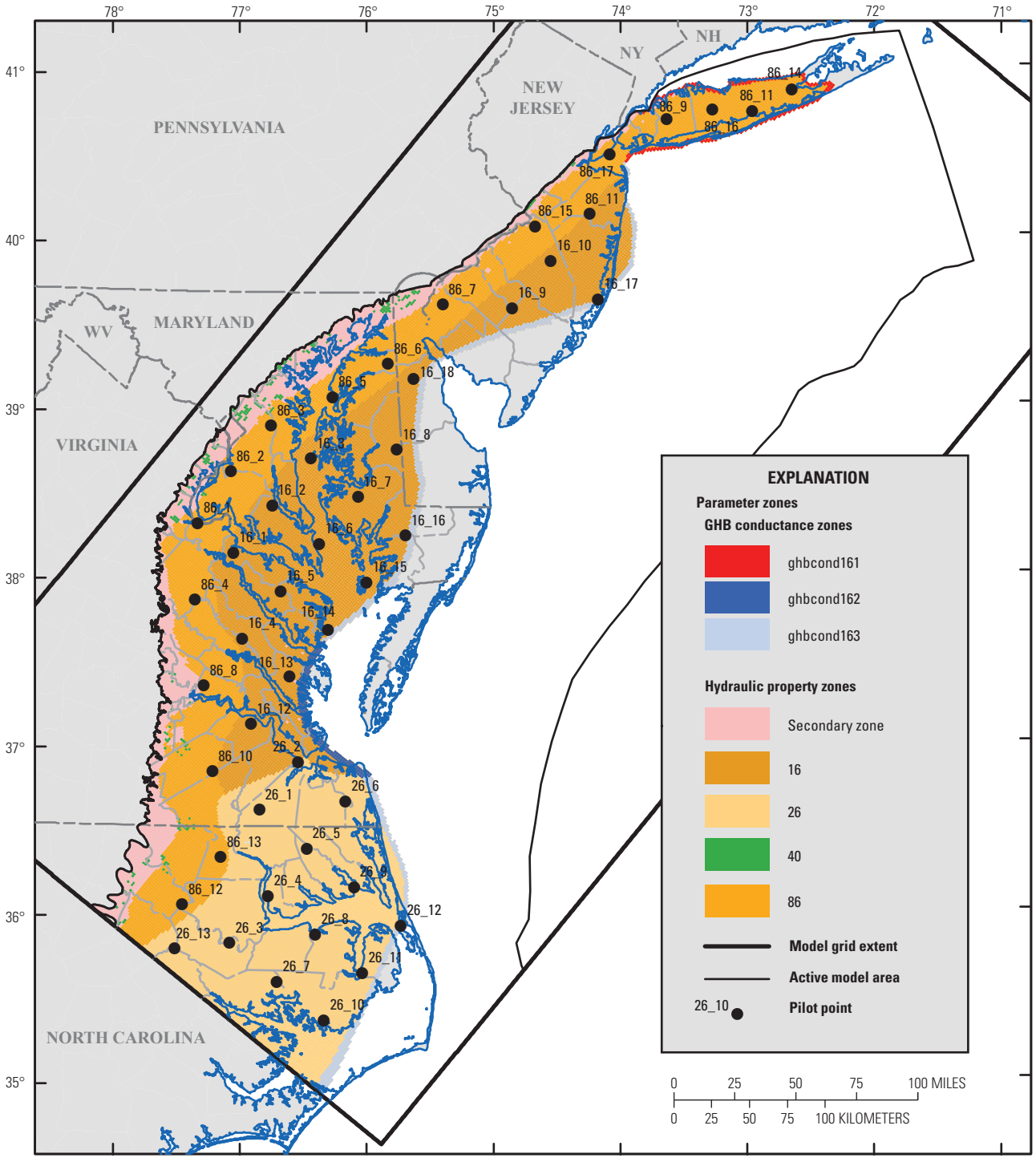

Figure 7. Distribution of pilot points and zones used to parameterize general-head boundary (GHB) conductance, hydraulic conductivity, and specific storage in the Northern Atlantic Coastal Plain aquifer system for *A*, model layer 1 through *S*, model layer 19.—Continued

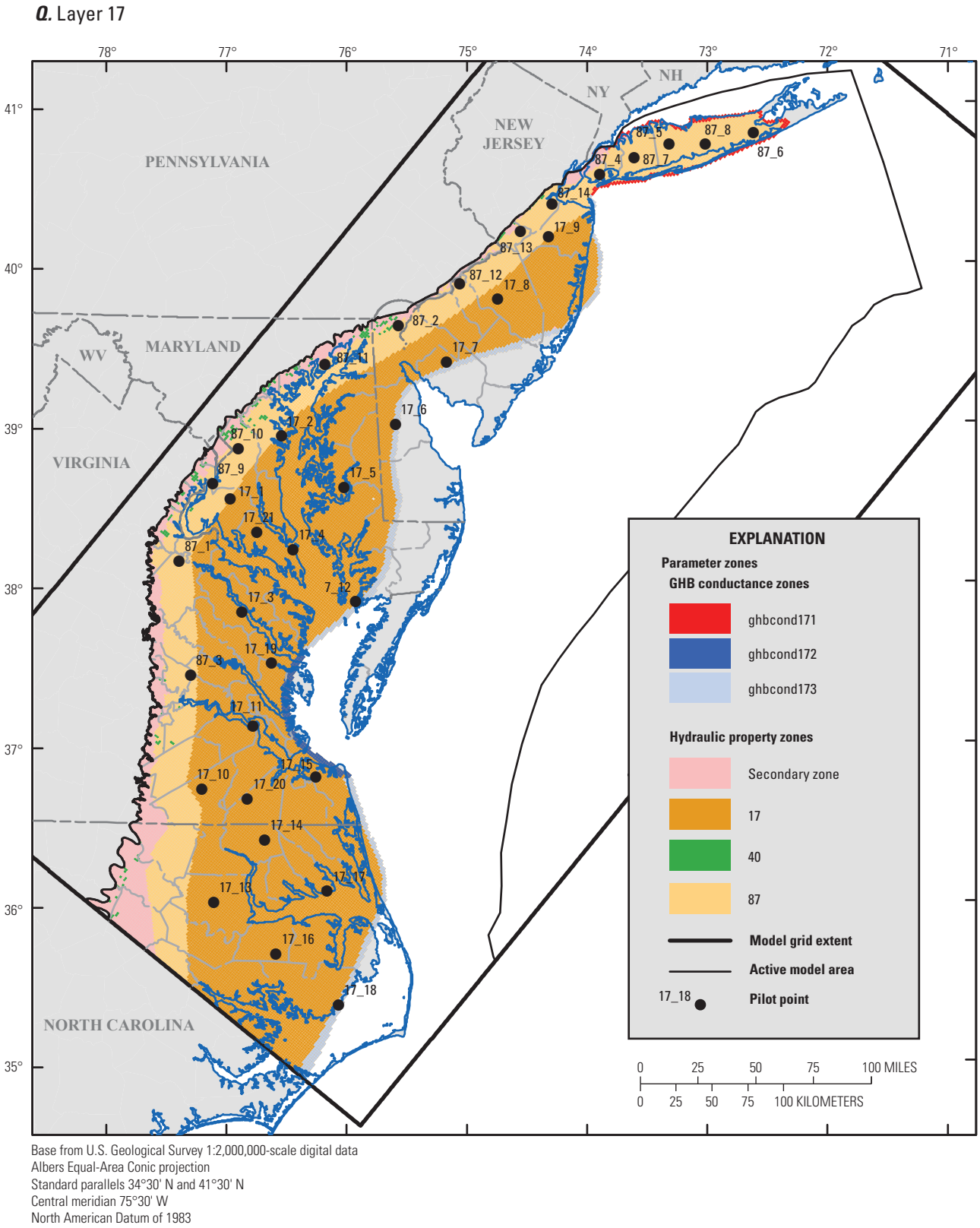

Figure 7. Distribution of pilot points and zones used to parameterize general-head boundary (GHB) conductance, hydraulic conductivity, and specific storage in the Northern Atlantic Coastal Plain aquifer system for *A*, model layer 1 through *S*, model layer 19.—Continued

R. Layer 18

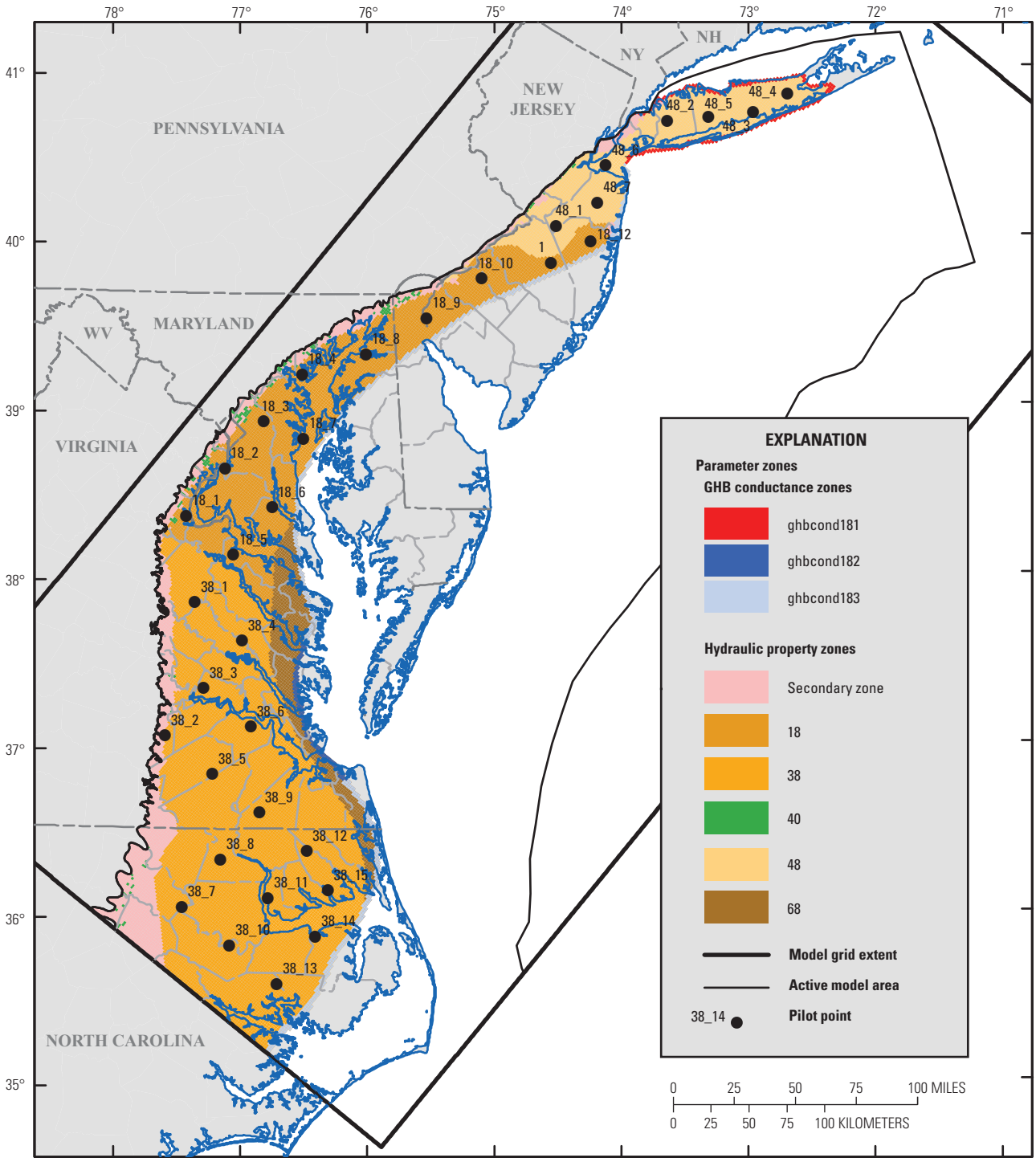

Base from U.S. Geological Survey 1:2,000,000-scale digital data
Albers Equal-Area Conic projection
Standard parallels 34°30' N and 41°30' N
Central meridian 75°30' W
North American Datum of 1983

Figure 7. Distribution of pilot points and zones used to parameterize general-head boundary (GHB) conductance, hydraulic conductivity, and specific storage in the Northern Atlantic Coastal Plain aquifer system for *A*, model layer 1 through *S*, model layer 19.—Continued

S. Layer 19

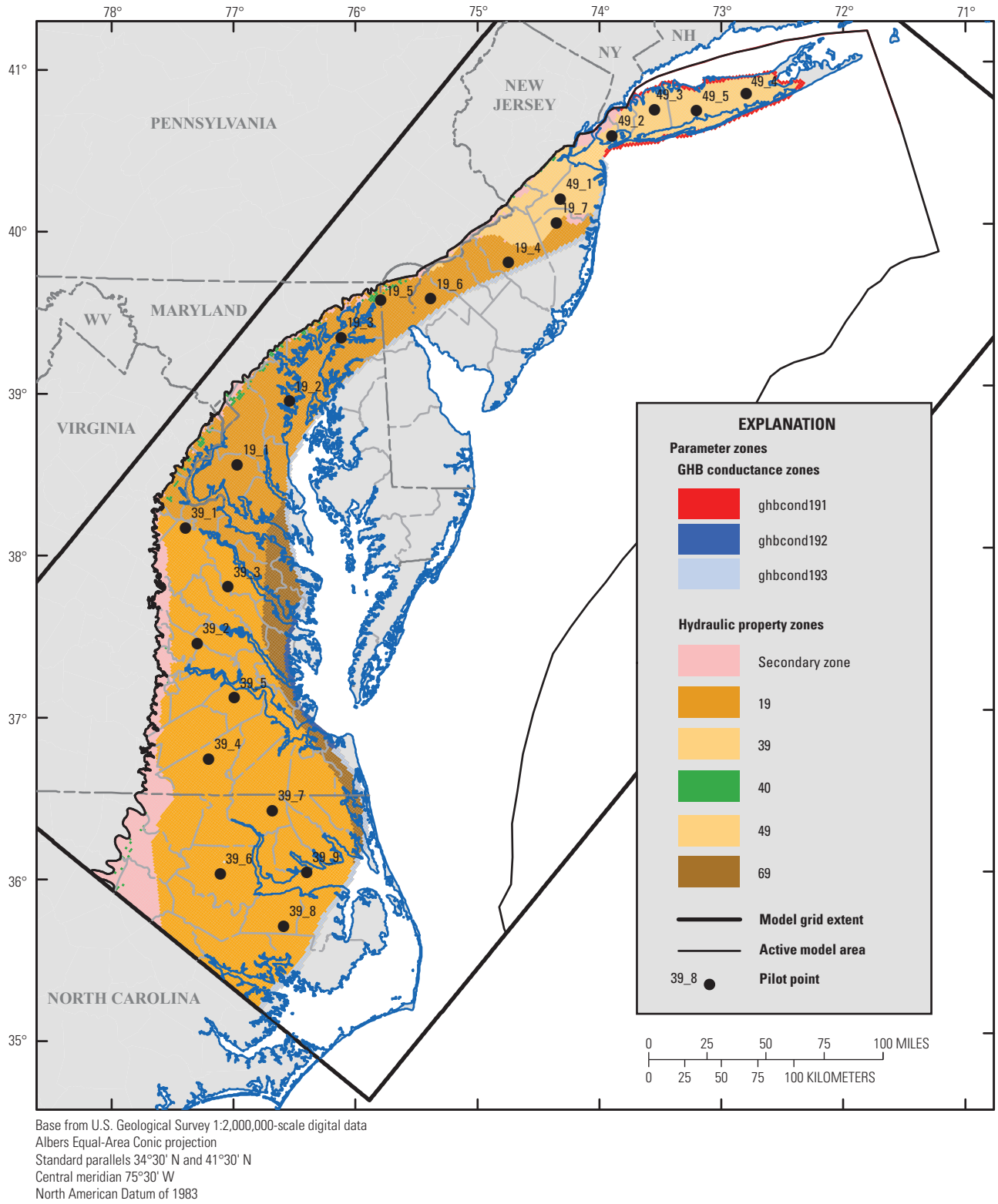

Base from U.S. Geological Survey 1:2,000,000-scale digital data
Albers Equal-Area Conic projection
Standard parallels 34°30' N and 41°30' N
Central meridian 75°30' W
North American Datum of 1983

Figure 7. Distribution of pilot points and zones used to parameterize general-head boundary (GHB) conductance, hydraulic conductivity, and specific storage in the Northern Atlantic Coastal Plain aquifer system for *A*, model layer 1 through *S*, model layer 19.—Continued

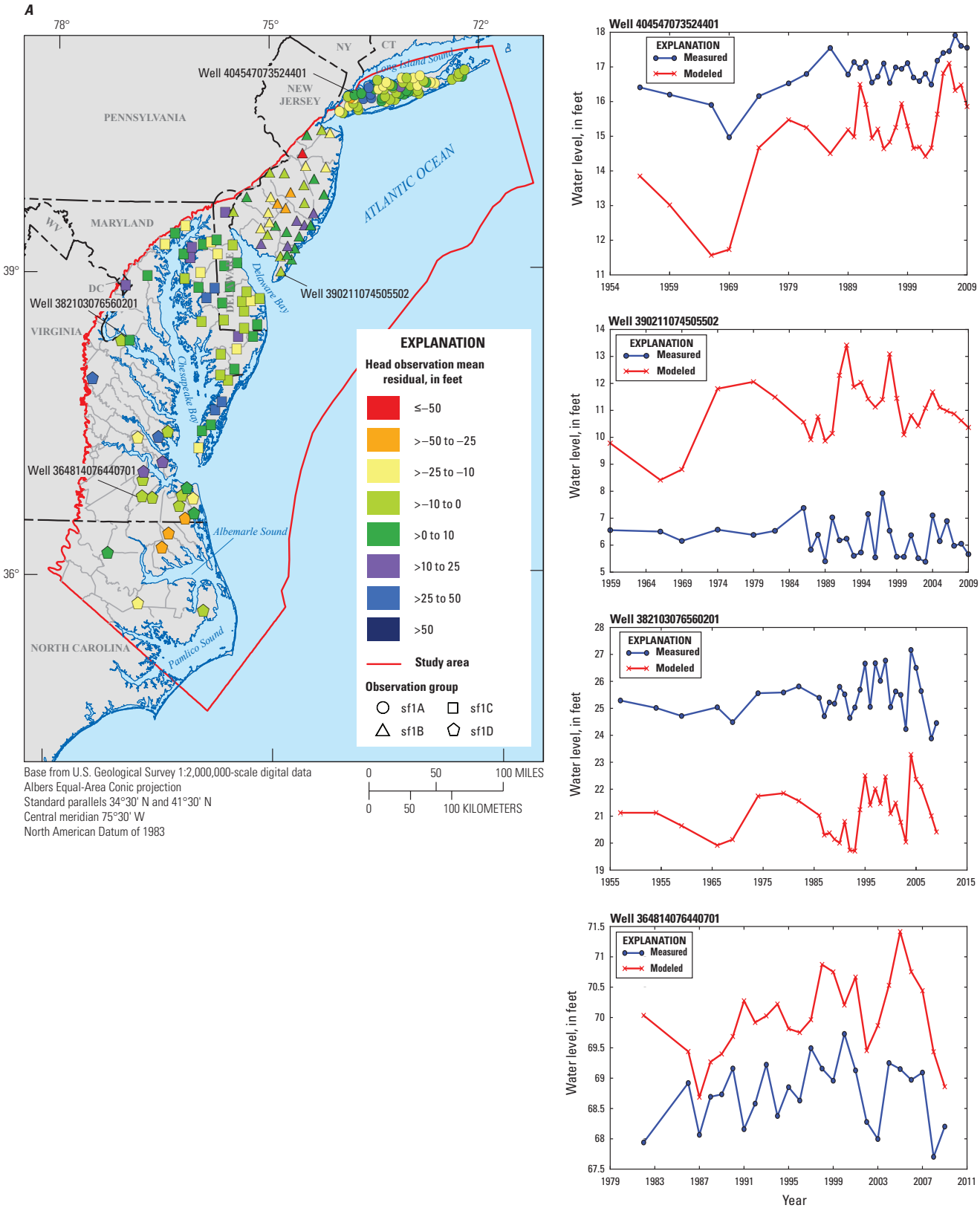

Figure 8. Location of observation groups and selected hydrographs of measured and model-calculated water levels for the *A*, surficial, *B*, Upper Chesapeake, *C*, Lower Chesapeake, *D*, Piney Point, *E*, Aquia, *F*, Monmouth-Mount Laurel, *G*, Matawan, *H*, Magothy, *I*, Potomac-Patapsco, and *J*, Potomac-Patuxent regional aquifers of the Northern Atlantic Coastal Plain aquifer system. Calibration groups are listed in table 5. All water levels are in units of feet relative to the National Geodetic Vertical Datum of 1929. ≤, less than or equal to; >, greater than.

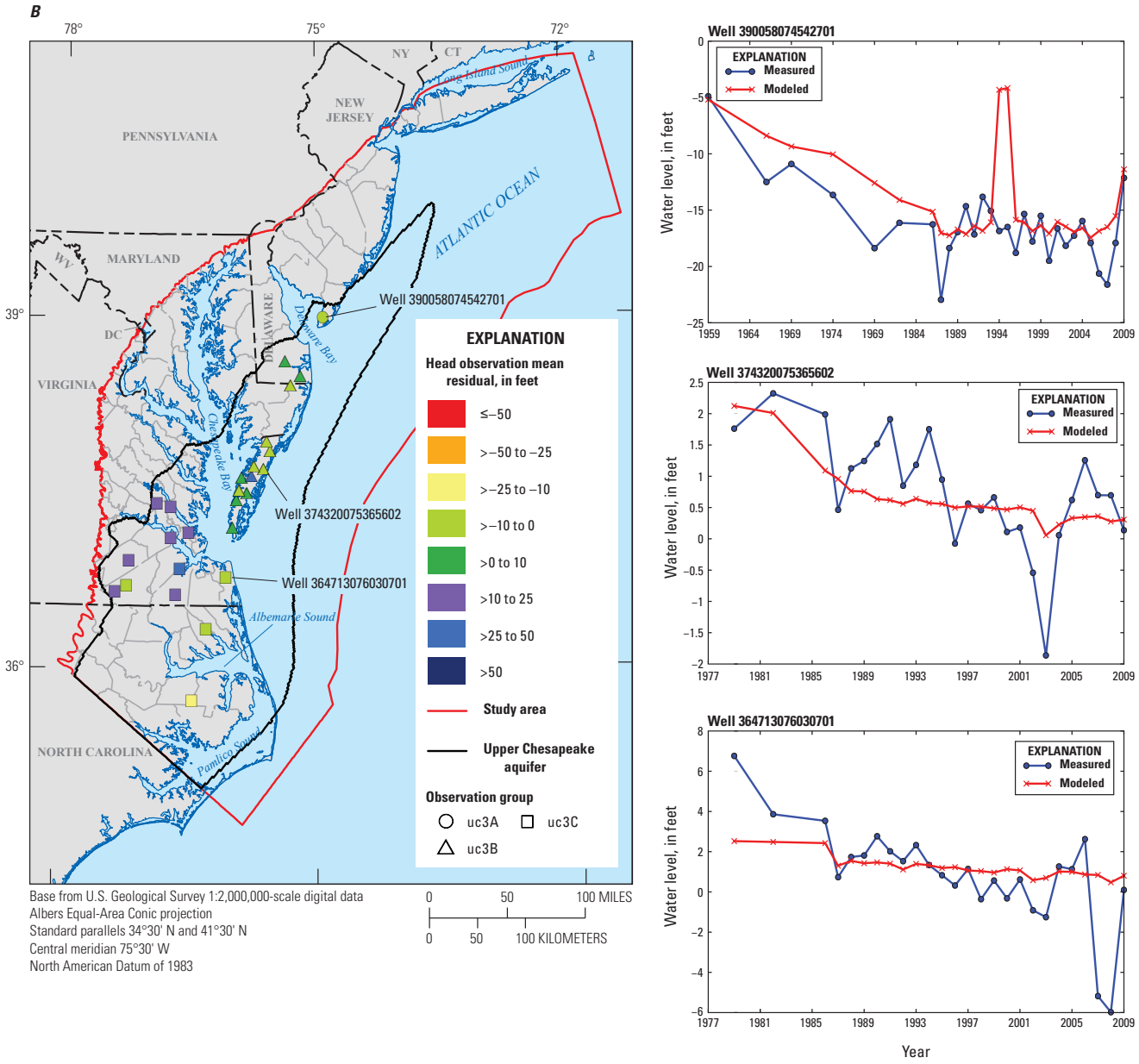

Figure 8. Location of observation groups and selected hydrographs of measured and model-calculated water levels for the *A*, surficial, *B*, Upper Chesapeake, *C*, Lower Chesapeake, *D*, Piney Point, *E*, Aquia, *F*, Monmouth-Mount Laurel, *G*, Matawan, *H*, Magothy, *I*, Potomac-Patapsco, and *J*, Potomac-Patuxent regional aquifers of the Northern Atlantic Coastal Plain aquifer system. Calibration groups are listed in table 5. All water levels are in units of feet relative to the National Geodetic Vertical Datum of 1929. ≤, less than or equal to; >, greater than.—Continued

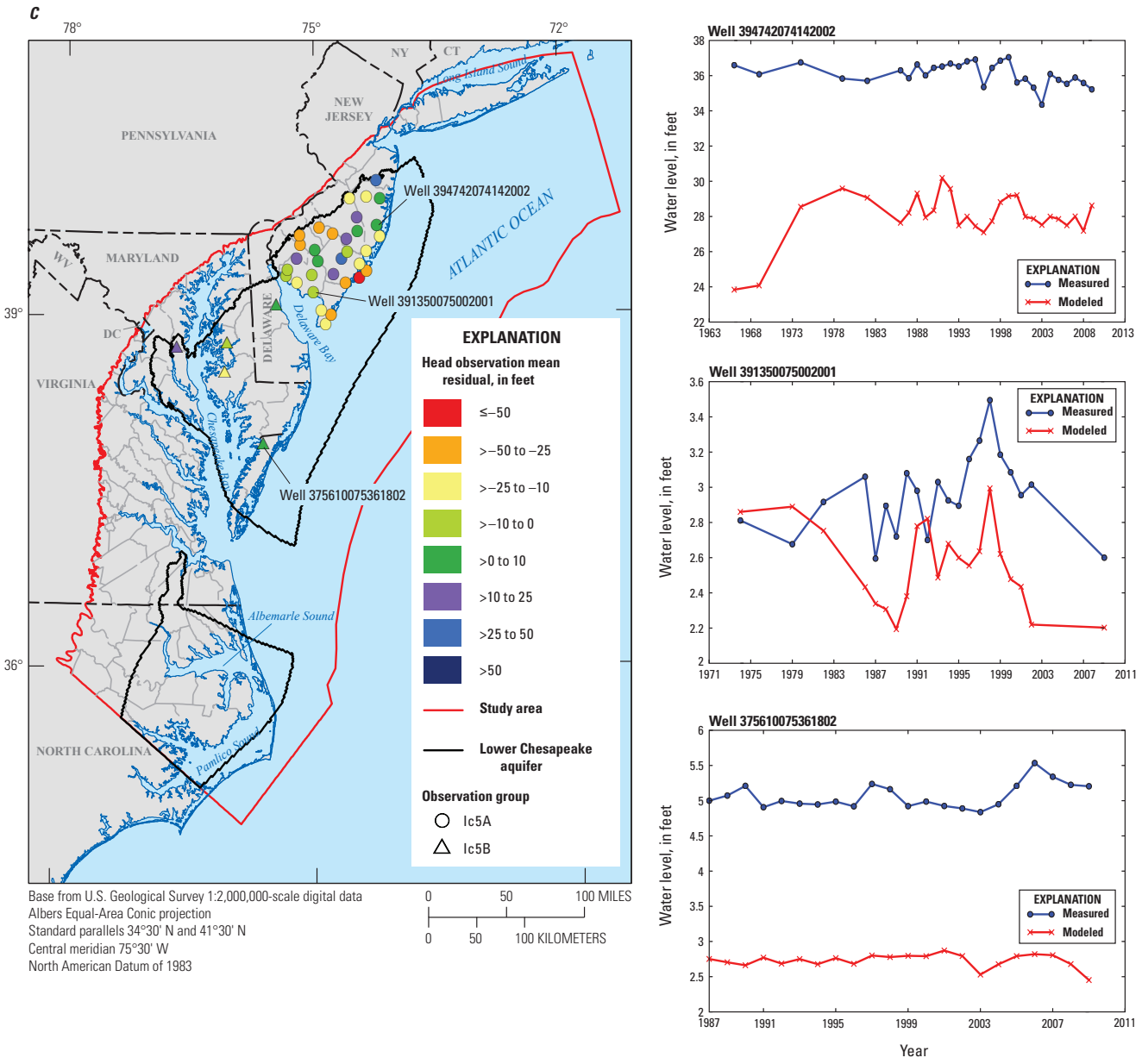

Figure 8. Location of observation groups and selected hydrographs of measured and model-calculated water levels for the *A*, surficial, *B*, Upper Chesapeake, *C*, Lower Chesapeake, *D*, Piney Point, *E*, Aquia, *F*, Monmouth-Mount Laurel, *G*, Matawan, *H*, Magothy, *I*, Potomac-Patapsco, and *J*, Potomac-Patuxent regional aquifers of the Northern Atlantic Coastal Plain aquifer system. Calibration groups are listed in table 5. All water levels are in units of feet relative to the National Geodetic Vertical Datum of 1929. ≤, less than or equal to; >, greater than.—Continued

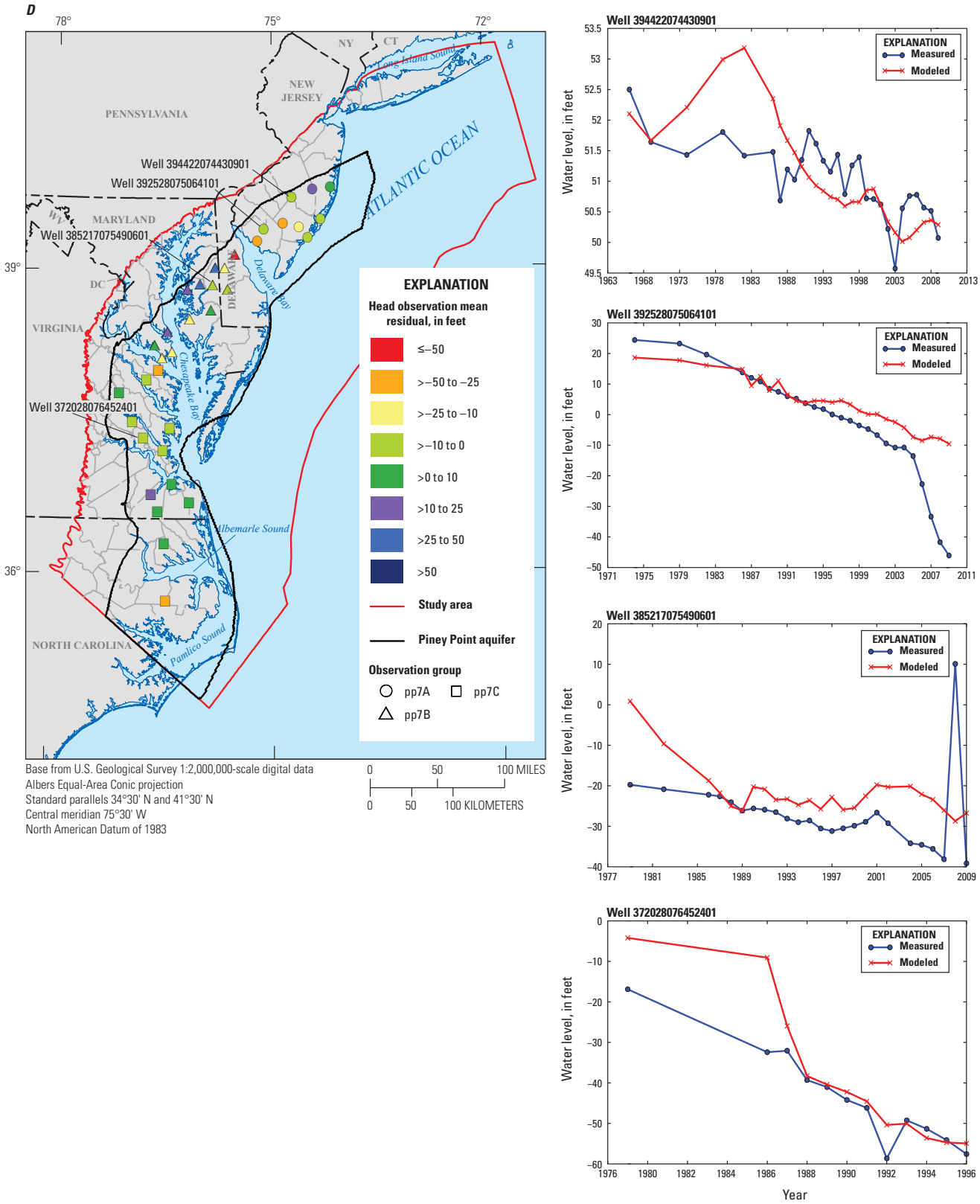

Figure 8. Location of observation groups and selected hydrographs of measured and model-calculated water levels for the *A*, surficial, *B*, Upper Chesapeake, *C*, Lower Chesapeake, *D*, Piney Point, *E*, Aquia, *F*, Monmouth-Mount Laurel, *G*, Matawan, *H*, Magothy, *I*, Potomac-Patapsco, and *J*, Potomac-Patuxent regional aquifers of the Northern Atlantic Coastal Plain aquifer system. Calibration groups are listed in table 5. All water levels are in units of feet relative to the National Geodetic Vertical Datum of 1929. ≤, less than or equal to; >, greater than.—Continued

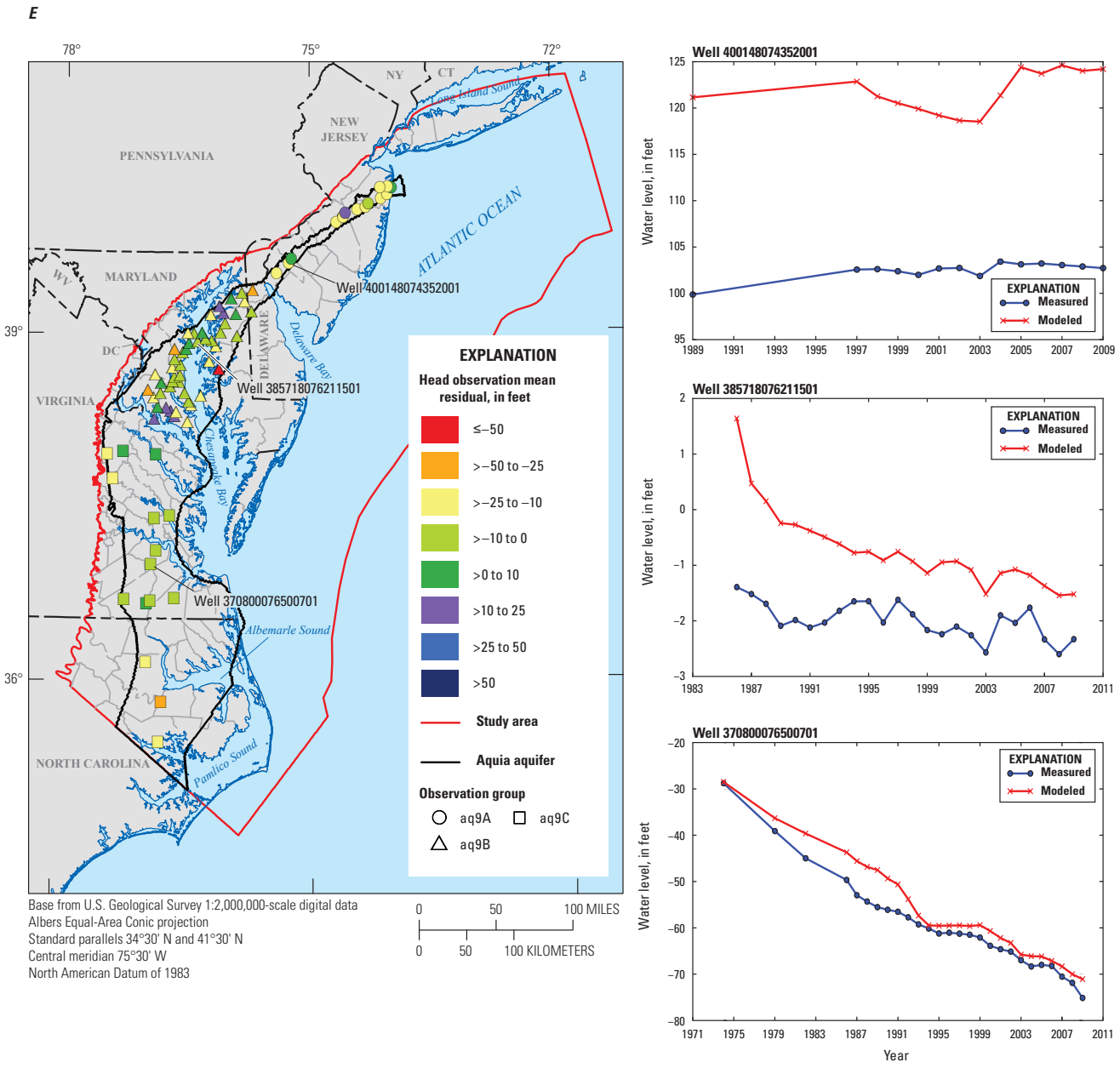

Figure 8. Location of observation groups and selected hydrographs of measured and model-calculated water levels for the *A*, surficial, *B*, Upper Chesapeake, *C*, Lower Chesapeake, *D*, Piney Point, *E*, Aquia, *F*, Monmouth-Mount Laurel, *G*, Matawan, *H*, Magothy, *I*, Potomac-Patapsco, and *J*, Potomac-Patuxent regional aquifers of the Northern Atlantic Coastal Plain aquifer system. Calibration groups are listed in table 5. All water levels are in units of feet relative to the National Geodetic Vertical Datum of 1929. ≤, less than or equal to; >, greater than.—Continued

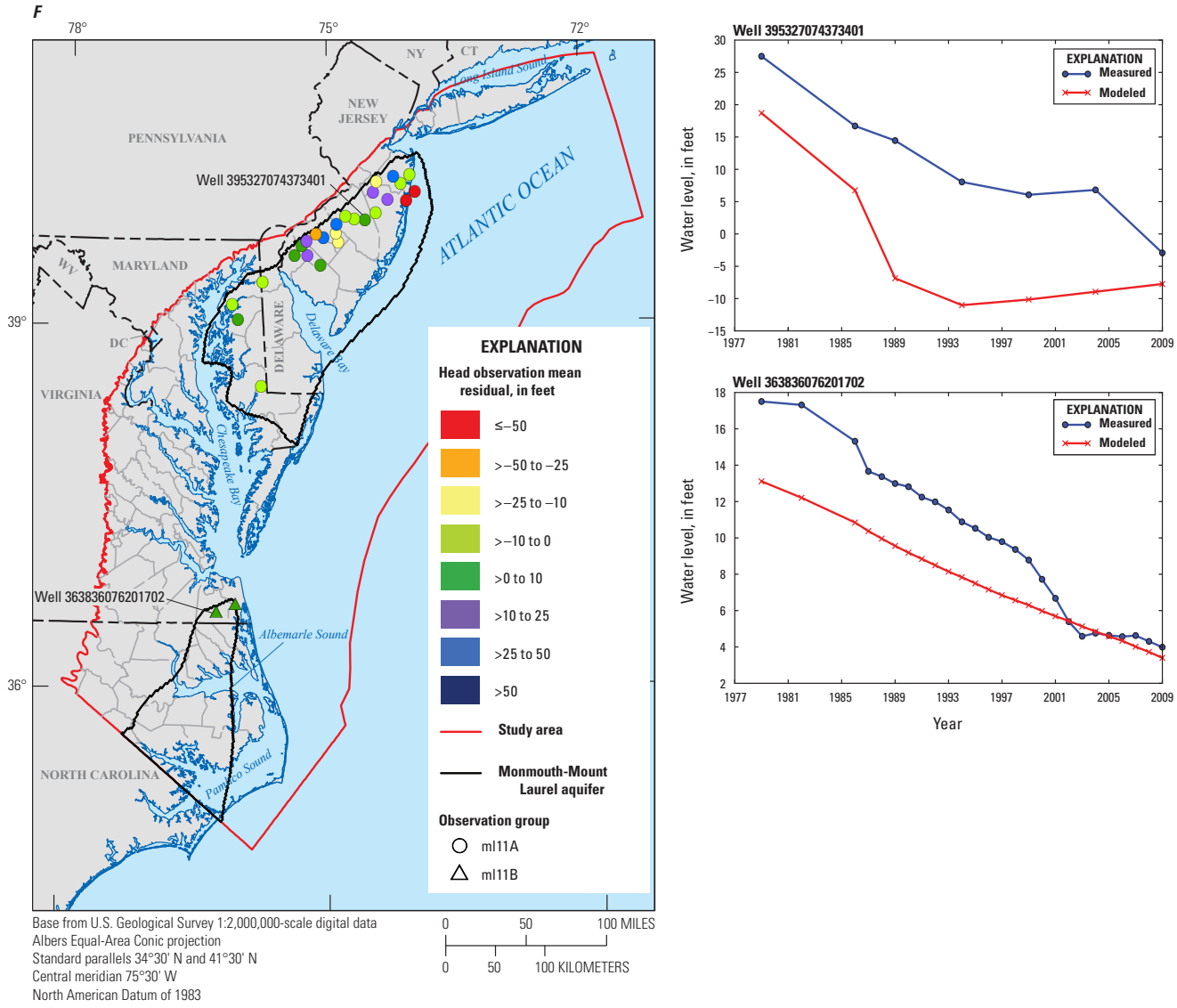

Figure 8. Location of observation groups and selected hydrographs of measured and model-calculated water levels for the *A*, surficial, *B*, Upper Chesapeake, *C*, Lower Chesapeake, *D*, Piney Point, *E*, Aquia, *F*, Monmouth-Mount Laurel, *G*, Matawan, *H*, Magothy, *I*, Potomac-Patapsco, and *J*, Potomac-Patuxent regional aquifers of the Northern Atlantic Coastal Plain aquifer system. Calibration groups are listed in table 5. All water levels are in units of feet relative to the National Geodetic Vertical Datum of 1929. ≤, less than or equal to; >, greater than.—Continued

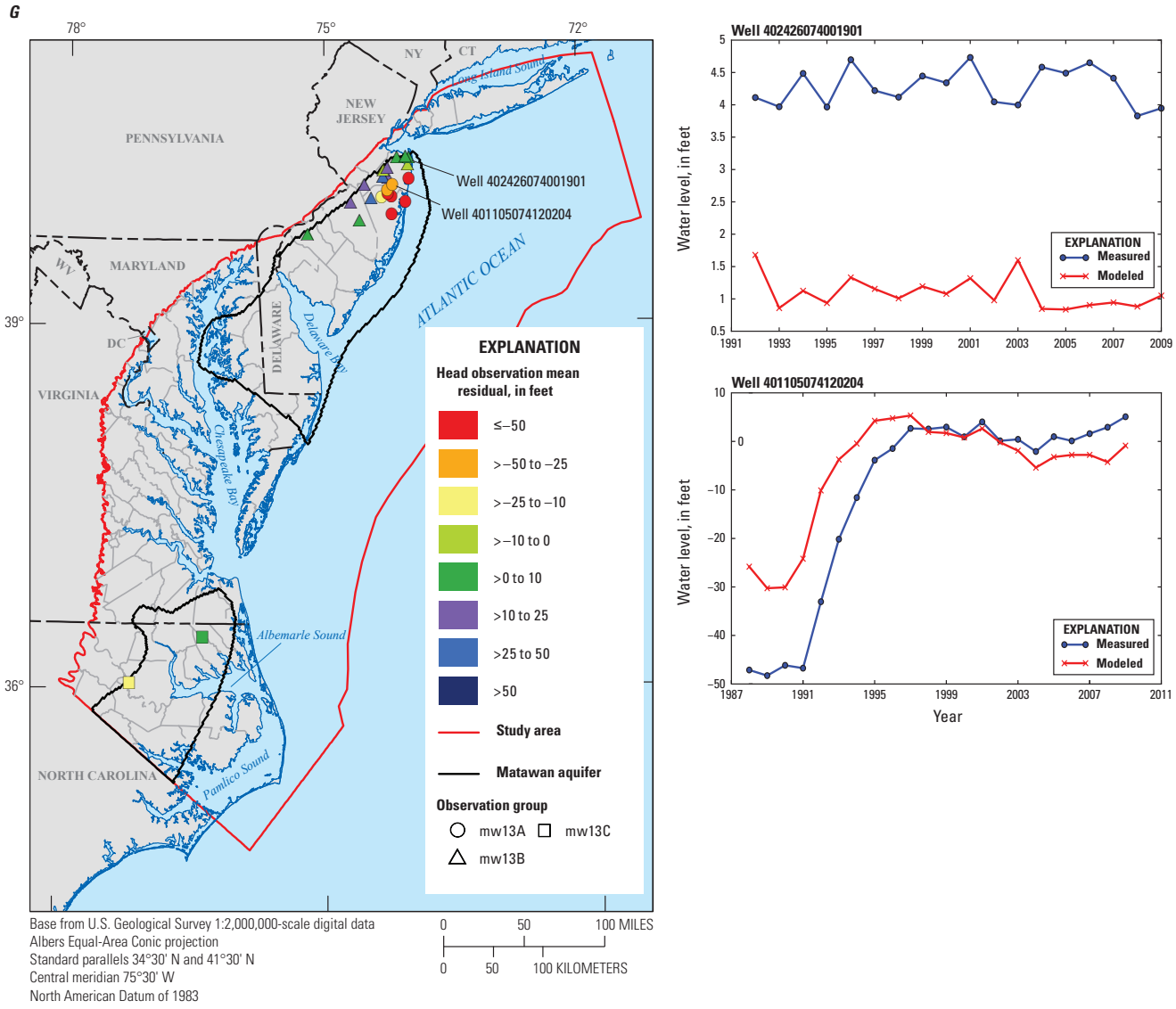

Figure 8. Location of observation groups and selected hydrographs of measured and model-calculated water levels for the *A*, surficial, *B*, Upper Chesapeake, *C*, Lower Chesapeake, *D*, Piney Point, *E*, Aquia, *F*, Monmouth-Mount Laurel, *G*, Matawan, *H*, Magothy, *I*, Potomac-Patapsco, and *J*, Potomac-Patuxent regional aquifers of the Northern Atlantic Coastal Plain aquifer system. Calibration groups are listed in table 5. All water levels are in units of feet relative to the National Geodetic Vertical Datum of 1929. ≤, less than or equal to; >, greater than.—Continued

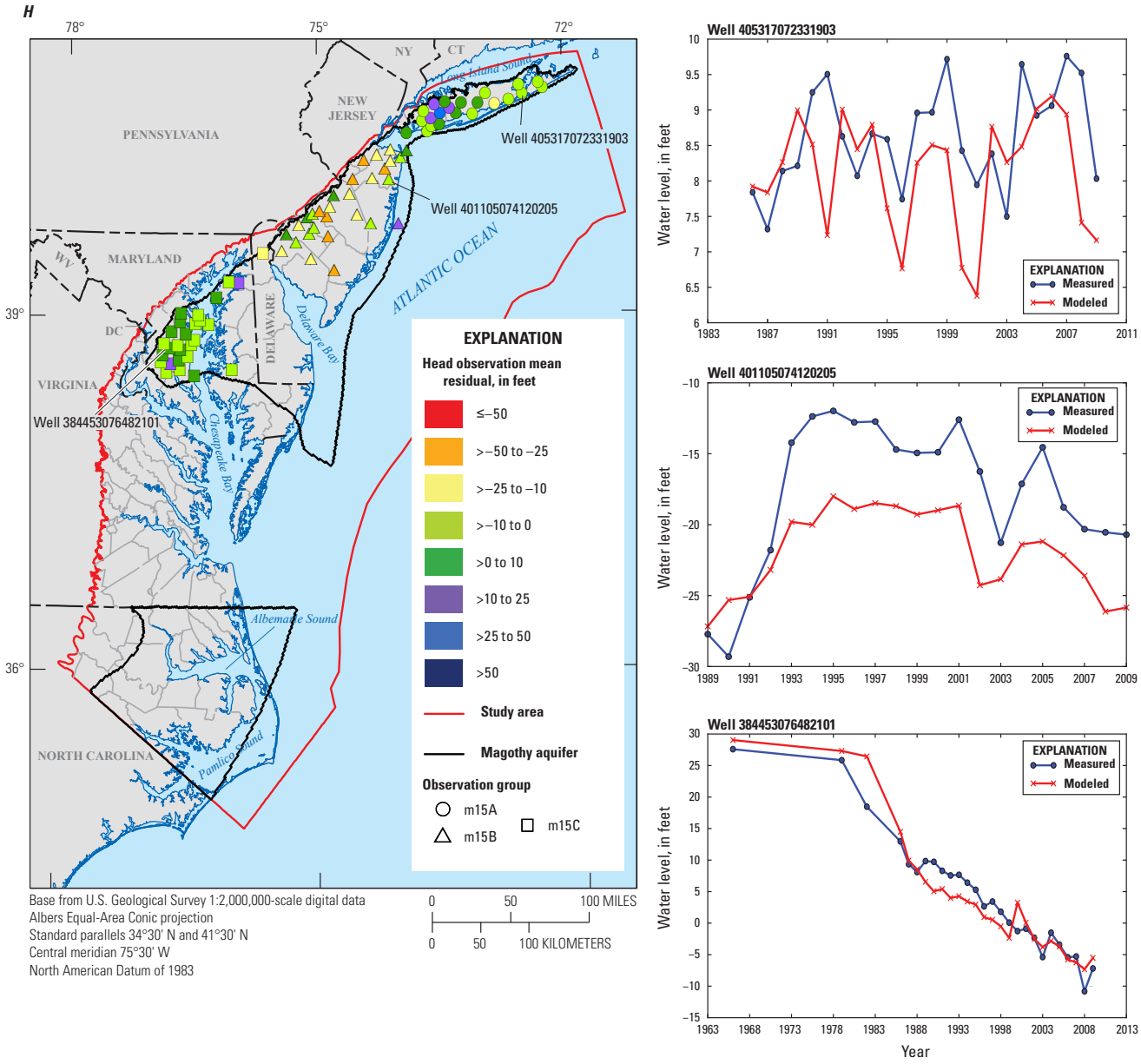

Figure 8. Location of observation groups and selected hydrographs of measured and model-calculated water levels for the *A*, surficial, *B*, Upper Chesapeake, *C*, Lower Chesapeake, *D*, Piney Point, *E*, Aquia, *F*, Monmouth-Mount Laurel, *G*, Matawan, *H*, Magothy, *I*, Potomac-Patapsco, and *J*, Potomac-Patuxent regional aquifers of the Northern Atlantic Coastal Plain aquifer system. Calibration groups are listed in table 5. All water levels are in units of feet relative to the National Geodetic Vertical Datum of 1929. ≤, less than or equal to; >, greater than.—Continued

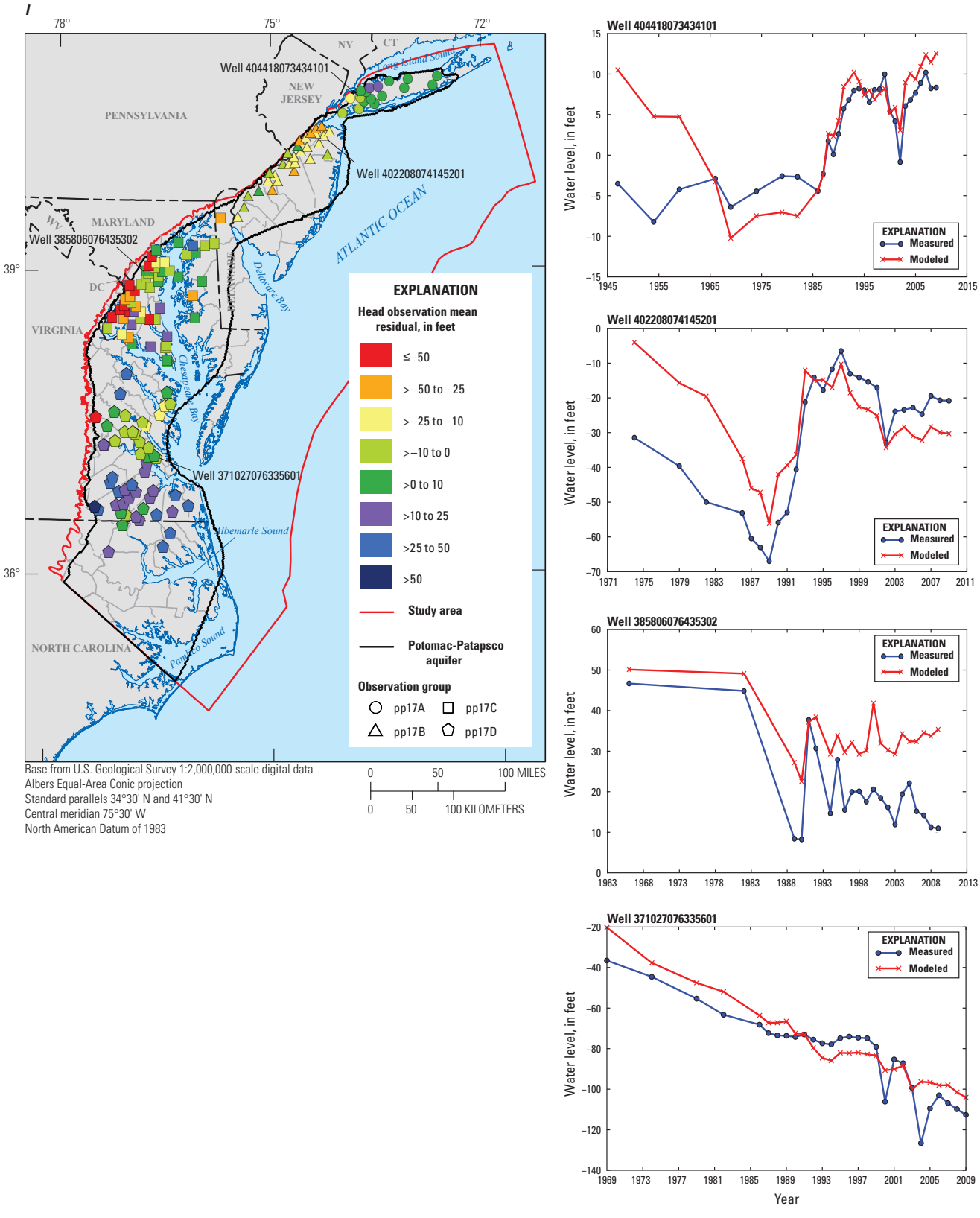

Figure 8. Location of observation groups and selected hydrographs of measured and model-calculated water levels for the *A*, surficial, *B*, Upper Chesapeake, *C*, Lower Chesapeake, *D*, Piney Point, *E*, Aquia, *F*, Monmouth-Mount Laurel, *G*, Matawan, *H*, Magothy, *I*, Potomac-Patapsco, and *J*, Potomac-Patuxent regional aquifers of the Northern Atlantic Coastal Plain aquifer system. Calibration groups are listed in table 5. All water levels are in units of feet relative to the National Geodetic Vertical Datum of 1929. ≤, less than or equal to; >, greater than.—Continued

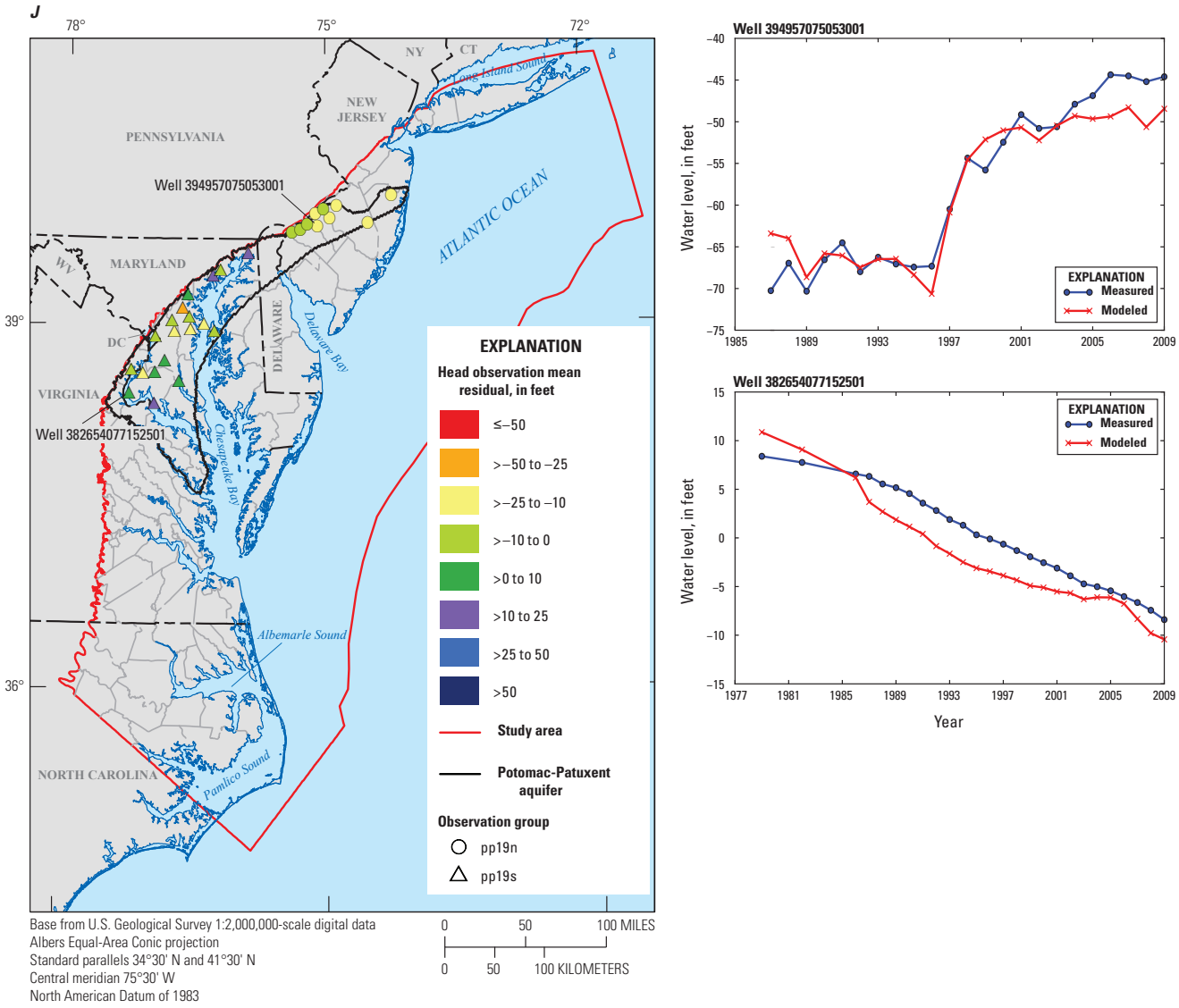

Figure 8. Location of observation groups and selected hydrographs of measured and model-calculated water levels for the *A*, surficial, *B*, Upper Chesapeake, *C*, Lower Chesapeake, *D*, Piney Point, *E*, Aquia, *F*, Monmouth-Mount Laurel, *G*, Matawan, *H*, Magothy, *I*, Potomac-Patapsco, and *J*, Potomac-Patuxent regional aquifers of the Northern Atlantic Coastal Plain aquifer system. Calibration groups are listed in table 5. All water levels are in units of feet relative to the National Geodetic Vertical Datum of 1929. ≤, less than or equal to; >, greater than.—Continued

Prepared by the USGS Science Publishing Network
Edited by Anna Glover
Pembroke Publishing Service Center
Layout by Ann Marie Squillacci
Pembroke Publishing Service Center
Illustrations by James E. Banton and Mark Bonito
Lafayette and Pembroke Publishing Service Centers

For more information concerning this report, please contact:

Water Availability and Use Science Program
U.S. Geological Survey
150 National Center
12201 Sunrise Valley Drive
Reston, VA 20192
http://water.usgs.gov/wausp/

ISSN 2328-0328 (online)
http://dx.doi.org/10.3133/sir20165076